SUPPLEMENTO
AL VOLUME XIX, SERIE X, DEL
NUOVO CIMENTO
A CURA DELLA SOCIETÀ ITALIANA DI FISICA

1961 1° Trimestre N. 1

A Device for Dip-Angle Measurement of Tracks in Nuclear Emulsions.

B. ANTOLKOVIĆ
Institute Rudjer Bošković - Zagreb

(ricevuto il 1° Agosto 1960)

Summary. — A device is described by which the dip angle of tracks in photonuclear plates can be measured. The device is an additional part of the microscope but does not require the modification of the microscope itself.

To make measurements of dip angles in nuclear emulsions more accurate, a device added to the microscope stage has been constructed. It tilts the plane of the nuclear plate, so that any track previously oblique comes into the horizontal plane. The apparatus differs from the one described by BARBOUR [1], as it does not require a modification of the stage of the microscope.

The arrangement is shown in Fig. 1. The frame (1) of the apparatus, fastened by the clips to the stage of the microscope, carries the axis of the sliding plate (2). The nuclear plate is held and fixed by a spring (3). Another spring (4) re-

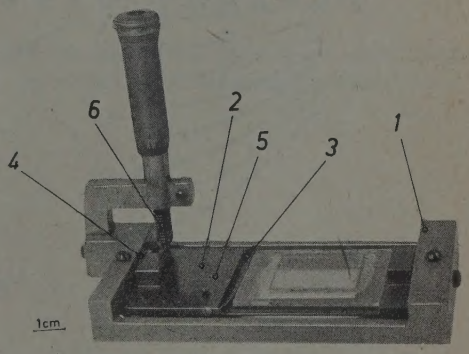

Fig. 1.

[1] I. BARBOUR: *Rev. Sci. Instr.*, **20**, 530 (1949).

moves the sliding plate in the horizontal position after the dip angle has been measured. In the hole (5) a metal plate (not shown in the picture) is screwed in to fasten the glass plate. The nuclear plate has to be moved by a micrometer (6) until the track comes in a horizontal plane. From the displacement $(h - h_0)$ of the micrometer screw, h_0 corresponding to the horizontal position of the plate, the dip angle β can be read directly by means of a calibration diagram.

The apparatus has been designed for measuring the dip angles of low energy recoil proton tracks (down to 0.5 MeV) induced by neutrons, of which the curvature, caused by the multiple Coulomb scattering, does not allow to find the dip angle from the difference in the depth of two distant points of the track. The smallest difference in angle which can be measured by means of this instrument is less than 10′. If the straight portion at the beginning of the track is short (less than 10 μm), it is in the focus of the microscope for a fairly large interval of tilting angle. The error of measurement of the dip angle of such tracks then amounts to 30′. The C-2 nuclear plates were analysed by means of this device using a Leitz ×100 immersion objective and a condenser of such a focal length, that the illumination is very near the optimum, and no altering of separation power occurs in spite of lifting the nuclear plate by a few millimeters.

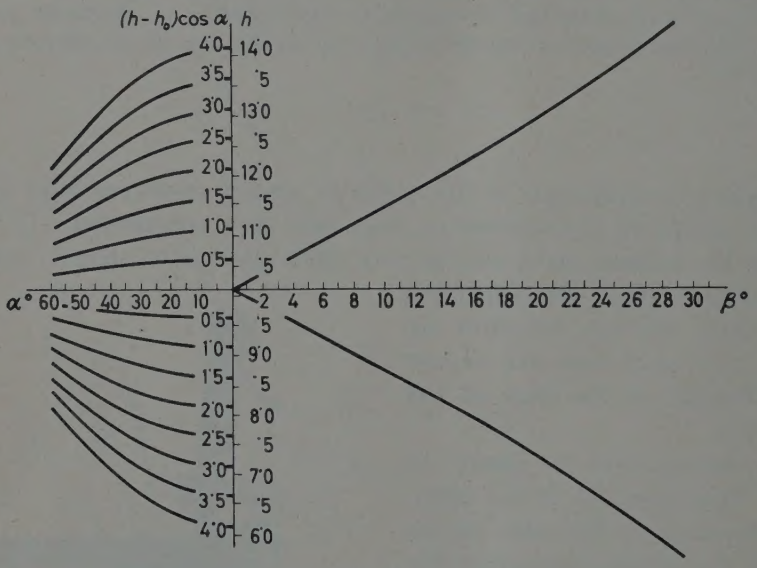

Fig 2.

When a Leitz ×100 immersion objective is used, its small focal length does not allow a greater tilting of the plate than 11°. Thus in emulsions having a shrinkage factor 2.5, only tracks less steep than $\beta = 27°$ can be measured

by means of this device. The range of measurement becomes even smaller for tracks making an angle α to the perpendicular on the tilting axis. It is easy to see that

$$\beta_{\max} = \operatorname{arctg} \frac{s \cdot (h - h_0)_{\max}}{L} \cos \alpha ,$$

(s, shrinkage factor; L, distance from the tilting axis to the point where the micrometer touches the plate), hence for a track having $\alpha = 45°$ the maximum dip angle that can be measured is 20°.

The calibration diagram is shown in Fig. 2. On the right side of the diagram the angle β (for $\alpha = 0°$) is plotted against the reading h of the micrometer screw. If the track is not perpendicular to the tilting axis, the vertical displacement $(h - h_0)$ of the screw has to be multiplied by $\cos \alpha$. These values can be obtained from the left side of the diagram, where $(h - h_0) \cos \alpha$ is plotted against the angle α. The corresponding dip angle β is read on the right hand curve. Example: *a*) $h = 11.6$ mm, or $h - h_0 = 1.5$ mm, $\alpha = 30°$; $(h - h_0) \cdot \cos \alpha = 1.3$ mm, $\beta = 9° 20'$; *b*) $h = 10.9$ mm, or $h - h_0 = 0.8$ mm, $\alpha = 30°$ by interpolation: $(h - h_0) \cos \alpha = 0.7$ mm, $\beta = 5°$.

* * *

The author wishes to thank Professor M. Paić for helpful suggestions.

RIASSUNTO (*)

Si descrive un apparecchio col quale si può misurare il dip delle tracce nelle lastre fotonucleari. L'apparecchio è un accessorio da applicare al microscopio senza richiedere modificazioni del microscopio stesso.

(*) *Traduzione a cura della Redazione.*

SUPPLEMENTO AL VOLUME XIX, SERIE X
DEL NUOVO CIMENTO

N. 1, 1961
1° Trimestre

Effective Neutron Activation Cross-Sections of Some Chlorine and Sulphur Reactions in NRX.

R. W. DURHAM and F. GIRARDI (*)

Chalk River - Ontario

(ricevuto l'8 Settembre 1960)

Summary. — Reaction rates have been measured in the lattice and reflector of NRX for those neutron activation reactions of chlorine and sulphur that lead to the production of ^{38}Cl, ^{32}P and ^{35}S. The effective cross-sections of these reactions for reactor neutrons have been calculated from cobalt monitors enclosed with the irradiated samples.

1. – Introduction.

During an attempt to use neutron activation analysis to identify hair from a particular person's head (1), it was found that the major activities produced were ^{38}Cl, ^{35}S and ^{32}P. These nuclides were identified by measurements of half-life and of β-particle absorption in aluminum using a gas-flow proportional counter with a thin window. The major constituents of hair, other than carbon, hydrogen and oxygen, are chlorine and sulphur with concentrations (2) of about 2% and 4% by weight of fresh hair, respectively. These elements will produce the observed activities by reactor neutron irradiation. Thus in order to determine the original Cl and S concentrations in the irradiated hair, it is necessary to establish the reaction rates in the particular irradiation positions in NRX used. The objective of this work has been to obtain these reaction rates and also to evaluate effective cross-sections for the reactions.

(*) Now at C.N.E.N. Radioelements laboratories, Ispra.
(1) PR-CM-16, p. 28 (1958).
(2) *Handbook of Biological Data*, W. S. SPECTOR editor (1956), p. 77.

Effective cross-sections for these reactions have been calculated from the reaction rates by dividing by the conventional flux measured simultaneously. In a well thermalized reactor such as NRX, these can be transformed into 2 200 m/s cross-sections by using Westcott's convention ([5]) after a cadmium-ratio measurement. Such values, obtained with as high a precision as is possible with present-day techniques and knowledge of nuclear constants, are valuable for comparison with theoretical cross-section calculations. Literature values show large variations and are often results of early work when no strict convention for expressing neutron flux was available. One reaction in particular for which the 2 200 m/s cross-section is uncertain is $^{35}Cl(n, p)^{35}S$. Although this is a threshold reaction in which the outgoing particle has a Coulomb barrier to surmount, the reaction appears to have its highest cross-section at thermal neutron energies. An accurate measurement of this cross-section is necessary to correlate this effect with similar behaviour in lighter nuclei.

The high-energy part of the reactor neutron spectrum may induce threshold reactions in the matrix element and thus interfere with neutron-activation analysis. An example of this is the production of ^{60}Co, during the irradiation of nickel, by the $^{60}Ni(n, p)^{60}Co$ reaction. As a large number of these reactions have been investigated in unmoderated fission-spectrum fluxes, a relationship between the high-energy fraction of the reactor flux and the 2 200 m/s flux would enable the amount of such interference to be estimated.

« Effective fission fluxes » for the two irradiation positions used in NRX for these experiments have been calculated from the $^{32}S(n, p)^{32}P$ « effective cross-section » and a published value of the cross-section in an unmoderated fission flux.

2. – Experimental.

Milligram quantities of high-purity KCl and K_2SO_4 were irradiated in the lattice of the NRX reactor using the pneumatic carrier facility (33) and in the reflector using the self-serve position S-9-4. This latter position is 7.5 in. into the graphite reflector which surrounds the vessel containing the heavy water of the reactor core. The irradiated material was dissolved in 5 ml water containing 0.5 mg KH_2PO_4 and 0.5 mg K_2SO_4 as carrier in the case of KCl and 0.5 mg KH_2PO_4 alone in the case of K_2SO_4. Two millilitres of the solution were then passed through a column of Dowex 50 (100-200 mesh) 0.5 cm in diameter and 5 cm long at a rate of 2 ml per hour in order to remove ^{42}K. The column was then washed with 2 ml water, the eluate plus washings were just neutralized with NaOH solution, and the volume made up to 5 ml. Aliquots of the solution were then pipetted onto aluminum counting trays for

counting in a gas-flow proportional counter having a 1 mg/cm² window. The aliquots taken were normally 10 μl but 1 ml was required to determine the ^{32}P activity in irradiated Cl. Self-absorption of β-particles from ^{35}S in the source was corrected for by making up a series of solutions of KCl and K_2SO_4 covering the range of concentrations used. These were spiked with a standardized carrier-free ^{35}S solution. Sources of 100 μl of each of these solutions were then counted to obtain a curve of counter efficiency against weight of material on the source. The efficiency of the counter for ^{32}P was obtained using a standardized ^{32}P solution and this efficiency $((26 \pm 1)\%)$ was also used for ^{38}Cl measurements.

No loss of ^{35}S and ^{32}P occurred on the column as the activity of the original solution after the ^{42}K had decayed was identical with that which had passed through the column after correcting for dilution.

The two sources which were used for ^{38}Cl measurements were counted at two-minute intervals for about three ^{38}Cl half-lives. The decay curves gave a half-life of 37.8 ± 0.5 minutes. After the ^{38}Cl had decayed the sources were counted daily for several weeks with and without an aluminum absorber of about 40 mg/cm². The absorber stopped all β-particles from ^{35}S and a fraction of those from ^{32}P. This fraction was evaluated by counting a source of ^{32}P, prepared by a short irradiation of red phosphorus, with and without the absorber. The short irradiation of phosphorus in a low-flux position of the reactor ensured freedom of the source from ^{33}P ([3]). The absorber was found to transmit 81% of the ^{32}P β-particles. Semi-log plots of counting rate versus time were made and curves with half-lives of 14.3 days for ^{32}P and 87 days for ^{35}S were drawn through the points to give the best visual fit. The scatter of points about the curves was about $\pm$ 5%.

The neutron flux during the irradiations was measured by enclosing a 0.005 in. cobalt-wire monitor in each irradiation capsule and measuring the activity produced in an ion chamber calibrated with ^{60}Co ([4]). The flux has been calculated as nv_0, the total neutron density multiplied by 2200 metres per second after the manner of Westcott ([5]). Self-shielding corrections for 0.005 in. cobalt wire were applied using the results Eastwood obtained from a comparison with a dilute alloy of cobalt in aluminum ([6]). These correction factors are 1.06 for the thermal contribution and 1.64 for the epi-thermal contribution to the total ^{60}Co activity. The epithermal contribution was obtained during the irradiations under cadmium.

([3]) E. N. Jensen, R. T. Nichols, J. Clement and A. Pohm: *Phys. Rev.*, **85**, 112 (1952).

([4]) R. E. Jervis: CRDC-730 (1957).

([5]) C. H. Westcott, W. H. Walker and T. K. Alexander: *A/Conf.*, 15/p/202 (1958).

([6]) T. A. Eastwood and R. D. Werner: to be published.

The details of the irradiations are listed in Table I. The numbers in the column headed « Reactor Cycle » merely refer to the normal operating periods of the reactor between shut-downs for load changes. These were noted to determine if the fast flux varied appreciably from cycle to cycle.

TABLE I. – *Details of irradiations.*

Exp.	Reactor position	Reactor cycle	Wt. of KCl (mg)	Wt. of K_2SO_4 (mg)	Duration (s)
A	Lattice	1	0.752	—	$2.70 \cdot 10^3$
B	Lattice	1	2.227	14.07	$2.70 \cdot 10^3$
C	Lattice (0.020 in. Cd cover)	1	3.962	—	$5.94 \cdot 10^4$
D	Reflector	1	1.355	8.824	$1.30 \cdot 10^5$
E	Reflector	2	12.65	17.25	$1.73 \cdot 10^5$
F	Lattice	3	—	16.37	$1.08 \cdot 10^4$
G	Lattice (0.020 in. Cd cover)	3	—	26.94	$1.08 \cdot 10^4$

3. – Results.

3·1. *Neutron flux determination.* – From the weight of the cobalt monitor its activity and the time of irradiation, the reaction rate at equilibrium, R, in dps/atom Co can be calculated. The convention due to Westcott states

$$R = (nv_0)\hat{\sigma} \,, \tag{1}$$

where $\hat{\sigma}$ is the effective cross-section for a reactor neutron spectrum having a Maxwellian distribution at thermal energies and a dE/E epithermal distribution. Furthermore, this effective cross-section is related to the 2 200 m/s cross-section by

$$\hat{\sigma} = \sigma_0(g + rs) \,, \tag{2}$$

where g and s describe the departure of the cross-section from the $1/v$ law and r is related to the epithermal contribution to the flux. For cobalt, g can be taken as unity [5]. The quantity s is temperature dependent and as the neutron temperature during an irradiation is not normally known, $s\sqrt{T_0/T}$ is evaluated from

$$s\sqrt{T_0/T} = \frac{2}{\sqrt{\pi}} \frac{\sum'}{\sigma_0} \,, \tag{3}$$

where Σ' is the resonance integral of the detector with the $1/v$ part subtracted. A new value for Σ' has recently been determined for Co by EASTWOOD (6), who obtained (57.1 ± 4.0) barns from a comparison of dilute Co-Al alloy with dilute Au-Al alloy.

Eq. (2) now becomes

$$\hat{\sigma} = \sigma_0 \left\{ 1 + r\sqrt{T/T_0} \left(\frac{2}{\sqrt{\pi}} \frac{\Sigma'}{\sigma_0} \right) \right\} . \tag{4}$$

The epithermal contribution to the neutron flux is now represented by $r\sqrt{T/T_0}$ which is still a useful quantity for defining the flux distribution during an irradiation. It is evaluated from the cadmium ratio R_{Cd}, *i.e.* the ratio of reaction rate of the detector uncovered to that covered with cadmium. Transposing eq. (11*a*) in reference (5), and multiplying by $\sqrt{T/T_0}$

$$r\sqrt{T/T_0} = \frac{1}{R_{Cd}(s\sqrt{T_0/T} + 1/K) - s\sqrt{T_0/T}} . \tag{5}$$

The coefficient K corrects for the variation in Cd cross-section with energy and the thickness of the cadmium cover. Values of this coefficient for different thicknesses of Cd have been calculated by WESTCOTT and are tabulated in reference (5). For 0.020 in. Cd and isotropic incidence of neutrons on one side of the Cd foil the values of K is 2.073. In these experiments, the cadmium ratio for cobalt was obtained by irradiating a bare Co wire monitor for a short period immediately after the sample with a Co monitor had been irradiated under cadmium. After calculating $r\sqrt{T/T_0}$ it was then possible to determine $\hat{\sigma}$ using Eastwood's data which are self-consistent. Putting these data in eq. (4)

$$\hat{\sigma} = 36.4(1 + 1.77\, r\sqrt{T/T_0}) . \tag{6}$$

This effective cross-section was then used with the measured reaction rate to calculate the neutron flux (nv_0) from eq. (1).

3·2. *Reaction rates and effective cross-sections.* – Nuclide activities were calculated from the decay curves by extrapolating back to the end of the irradiations.

$$^{32}\text{P(dps)} = \frac{\text{(cps on source with absorber)(dilution factor)}}{\text{(transmission coefficient)(counter efficiency } ^{32}\text{P)}} , \tag{7}$$

$$^{35}\text{S(dps)} = \frac{\left[\begin{matrix}\text{(total cps)} \\ \text{(on source)}\end{matrix} - \begin{matrix}(1.26 \times \text{cps}) \\ \text{(through absorber)}\end{matrix}\right] \text{(dilution factor)}}{\text{(counter efficiency } ^{35}\text{S)(self-absorption)}} . \tag{8}$$

Reaction rates at equilibrium were determined from

$$R = \frac{\text{(dps product nuclide)}}{\text{(No. of atoms of reacting isotope)}(1 - \exp[-\lambda t])} \tag{9}$$

where t is the irradiation time and λ the disintegration constant of the product nuclide.

The reaction rates of the threshold reactions have also been divided by the conventional 2 200 m/s flux (nv_0) to give an effective cross-section and Westcott's symbol $\hat{\sigma}$ has been used for this also. Although the neutron density above about 1 MeV has little effect on the value of nv_0, this is a readily obtainable parameter for normalizing the reaction rates. By comparing $\hat{\sigma}$ for a particular threshold reaction with the mean cross-section for the same reaction in a pure fission spectrum, a fraction of nv_0 representing an « effective fission flux » can be obtained. This quantity can in turn be used to predict the reaction rates in NRX of other threshold reactions from published fission-spectrum cross-sections.

It is assumed that the fission-neutron spectrum above its maximum (0.5 to 1 MeV) is not distorted in the reactor and that the threshold reactions have negligible rates below this. If these conditions do not hold, then resonance neutrons will increase the effective cross-section in the reactor. The pure-fission-spectrum cross-section is given by

$$\sigma_{f.s.} = \frac{\int_{E_T}^{\infty} \sigma(v) n(v) v \, dE}{\int_{0}^{\infty} n(v) v \, dE} . \tag{10}$$

The neutron distribution is that given by WATT [7] for pure-fission neutrons

$$n(E)\,dE = \exp[-E] \sinh \sqrt{2E}\, dE . \tag{11}$$

The effective cross-section for reactor neutrons derived in our experiments is

$$\hat{\sigma} = \frac{\int_{E_T}^{\infty} \sigma(v) n(v) v \, dE}{v_0 \int_{0}^{\infty} n(v) \, dE} . \tag{12}$$

The reactor neutron spectrum which appears in the denominator of eq. (12)

---

[7] B. E. WATT: *Phys. Rev.*, **87**, 1037 (1952).

is assumed, Westcott's convention, to have a Maxwellian thermal distribution and a dE/E resonance distribution going out to infinity. It has been found by Roy [32] however, from a study of (n, 2n) reactions in NRX, that the neutron distribution falls off in a similar manner to pure fission neutrons above 6 MeV. We assume that the dE/E distribution changes tothat of pure fission neutrons at about 1 MeV, the maximum in the unmoderated fission spectrum. It is this part of the neutron spectrum of the reactor that gives rise to the reaction rate given by the numerator of eq. (12).

This assumption has negligible effect on the 2 200 m/s flux which becomes nv_0, but as long as the threshold energy of the particular reaction is above the energy at which the unmoderated fission spectrum becomes distorted in the reactor, the numerators of eq. (10) and (12) are identical. Then,

$$\frac{\hat{\sigma}}{\sigma_{f.s.}} = \frac{\text{« effective fission flux »}}{nv_0}. \tag{13}$$

Tables II and III list the results obtained for the reaction rates, and effective cross-sections for reactor neutrons, of Cl and S. The value of $r\sqrt{T/T_0}$ shown for the reflector irradiations was obtained from short irradiations of a dilute Au-Al alloy, bare and under cadmium, in the « J-rod annulus » using the pneumatic carrier. As position S-9-4 is at the inner edge of the J-rod annulus the value of $r\sqrt{T/T_0}$ there should be approximately the same. In any case the evaluation of nv_0 would hardly be affected as it is insensitive to $r\sqrt{T/T_0}$ when cobalt is used as a monitor.

The reaction rates and nv_0 values have been calculated to three figures in order to determine the precision of the effective cross-section measurements. The standard deviations of these measurements are given in Table IV. The high value for the standard deviation of the $^{35}Cl(n, \alpha)^{32}P$ cross-section in the

Table II. – *Reaction rates and effective cross-sections of* Cl *in* NRX.

Experiment	Reaction rates (dps/atom)			nv_0 n/cm^2 s	$\hat{\sigma} = R/nv_0$ millibarns			
	$^{35}Cl(n, p)$	$^{35}Cl(n, \alpha)$	$^{35}Cl(n, \gamma)$		^{35}Cl (n, p)	^{35}Cl (n, α)	^{37}Cl (n, γ)	$r\sqrt{T/T_0}$
A	$3.70 \cdot 10^{-11}$	$3.95 \cdot 10^{-14}$	$2.70 \cdot 10^{-11}$	$6.50 \cdot 10^{13}$	570	0.607	415	0.021
B	$3.84 \cdot 10^{-11}$	$3.80 \cdot 10^{-14}$	$2.36 \cdot 10^{-11}$	$6.41 \cdot 10^{13}$	600	0.593	368	0.021
C (0.02 in. Cd cover)	$9.42 \cdot 10^{-13}$	$3.31 \cdot 10^{-14}$	—	$6.42 \cdot 10^{13}$	14.7	0.516	—	0.021
D	$5.80 \cdot 10^{-12}$	$3.46 \cdot 10^{-15}$	—	$1.00 \cdot 10^{13}$	580	0.346	—	0.015
E	$6.26 \cdot 10^{-12}$	$3.00 \cdot 10^{-15}$	—	$1.04 \cdot 10^{13}$	600	0.288	—	0.015

TABLE III. – *Reaction rates and effective cross-sections of* S *in* NRX.

Experiment	Reaction rates (dps/atom)		nv_0 n/cm^2 s	$\hat{\sigma} = R/nv_0$ millibarns		$r\sqrt{T/T_0}$
	$^{32}S(n, p)$	$^{34}S(n, \gamma)$		$^{32}S(n, p)$	$^{34}S(n, \gamma)$	
B	$1.10 \cdot 10^{-13}$	$1.93 \cdot 10^{-11}$	$6.41 \cdot 10^{13}$	1.72	300	0.021
F	$9.60 \cdot 10^{-14}$	$1.76 \cdot 10^{-11}$	$6.36 \cdot 10^{13}$	1.51	277	0.023
G (0.02 in. Cd cover)	$9.90 \cdot 10^{-14}$	—	$6.36 \cdot 10^{13}$	1.56	—	0.023
D	$7.63 \cdot 10^{-15}$	$2.37 \cdot 10^{-12}$	$1.00 \cdot 10^{13}$	0.763	237	0.015
E	$6.88 \cdot 10^{-15}$	$2.94 \cdot 10^{-12}$	$1.04 \cdot 10^{13}$	0.662	282	0.015

reflector compared with that in the lattice shows that this is probably not a statistical variation but is due to a variation in the fast component of the flux between reactor cycles. This reasoning also applies to the $^{32}S(n, p)^{32}P$ measurements in the reflector, as the Cl and S irradiations were carried out simultaneously. It is not so obvious from the standard deviations of the S cross-sections as their precision appears to be poorer than those of Cl.

TABLE IV. – *Precision of cross-section measurements.*

Reaction		Mean value of $\hat{\sigma}$ millibarns	Std. deviation per cent
$^{35}Cl(n, p)^{35}S$		587	$\pm$ 2.6
$^{35}Cl(n, \alpha)^{32}P$	(Lattice)	0.600	$\pm$ 1.7
	(Reflector)	0.317	$\pm$13
$^{37}Cl(n, \gamma)^{38}Cl$		392	$\pm$ 8.6
$^{32}S(n, p)^{32}P$	(Lattice)	1.60	+ 6.9
	(Reflector)	0.712	$\pm$10
$^{34}S(n, \gamma)^{35}$		274	$\pm$ 9.7

The standard deviations given in Table IV would only apply to measurements made with the same equipment as was used in these experiments. The absolute error in the effective cross-section will be about $\pm 15\%$ due to probable systematic errors in the counter calibration and to the nuclear data used.

4. – Discussion.

Although the deuterium-moderated NRX is considered a « well thermalized » reactor there is a relatively high flux of neutrons with energies in excess

of 1 MeV. This « fast flux » has been found by EASTWOOD and ROY ([31]) to produce measurable rates even in neutron reactions in which three neutrons are evaporated from the compound nucleus. Even though the threshold reactions of Cl are exoergic, sufficient energy must be supplied to allow appreciable penetration of the Coulomb barrier by the emitted particle. For Cl and S this barrier height is about 5 MeV for protons and 9 MeV for α-particles. Because of this barrier the large decrease in rate of the $^{35}Cl(n, p)^{35}S$ reaction when covered by cadmium is rather remarkable. A possible reason why this reaction goes mainly with thermal neutrons is given later. Literature values of the cross-sections of the reactions studied are listed in Table V for both thermal neutrons and unmoderated fission neutrons together with the reaction energies (Q-values) of the threshold reactions. The Q-values are taken from the compilation of BROMLEY and RUTLEDGE ([8]) and the binding-energy tables of WAPSTRA ([9]). These cross-sections are reviewed for individual reactions for comparison with the effective cross-sections obtained in this work.

$^{35}Cl(n, p)^{35}S$. – In 1941 KAMEN showed that this reaction was more sensitive to thermal neutrons than to those of higher energy ([10]). The rate of production of ^{35}S in CCl_4 irradiated with cyclotron-produced neutrons decreased by a factor of six when the CCl_4 was wrapped with cadmium. In 1944 GIBERT, ROGGEN and ROSSEL ([11]) measured the ratio of the rate of this reaction to that of $^{14}N(n, p)^{14}C$ using neutrons produced by the D(d, n) reaction slowed to thermal by a paraffin block. Chlorine and nitrogen were used in an ionization chamber and the emitted protons were counted. The measured ratio was 0.19 ± 0.04, and using 1.8 barns for the $^{14}N(n, p)^{14}C$ reaction, their $^{35}Cl(n, p)^{35}S$ cross-section was (340 ± 70) millibarns. Also in 1944, the first measurements using reactor neutrons were made in the Argonne reactor thermal column. LANGSDORF irradiated sodium chloride and measured the activity of the ^{35}S. He found the $^{35}Cl(n, p)^{35}S$ thermal cross-section to be 320 millibarns with a cadmium ratio of 17.4 ([12]). In the compilation of cross-section, AECD-2274 ([13]), a value of (460 ± 60) millibarns is credited to HUGHES but the original work referred to contains no mention of this reaction. It should be noted here that the 1955 edition of Hughes' compilation of cross-sections, BNL-325,([14]), gives most weight to the activation value obtained by SEREN and co-workers, namely

([8]) D. A. BROMLEY and A. R. RUTLEDGE, CRP-789.
([9]) A. H. WAPSTRA: *Handb. d. Phys.*, vol. 38/1, S. FLÜGGE editor (1958), p. 7.
([10]) M. D. KAMEN: *Phys. Rev.*, **60**, 537 (1941).
([11]) A. GIBERT, F. ROGGEN and J. ROSSEL: *Helv. Phys. Acta.*, **17**, 97 (1944).
([12]) A. LANGSDORF: CP 2638 (1944).
([13]) K. WAY and G. HAINES: AECD 2274 (1947).
([14]) D. J. HUGHES and J. A. HARVEY: BNL 325 (1955).

(169 ± 34) millibarns ([15]), measured in the Argonne reactor also in 1944. In 1949 MAURER obtained (290 ± 70) millibarns ([16]) by using Be(d, n) neutrons slowed down in paraffin and measuring the ^{35}S activity produced. BERTHET and ROSSEL ([17]) in 1954 measured the cross-section using a nuclear-emulsion technique. Plates of known chlorine and nitrogen content were irradiated in the Harwell and Chatillon reactors and the proton tracks measured. The protons from nitrogen were used to calibrate the flux and a cross-section for the $^{35}Cl(n, p)^{35}S$ reaction of (300 ± 10) millibarns was found. The most recent value for the thermal cross-section by activation is given by HUGHES in the 1958 edition of NBL 325 ([18]) as (190 ± 50) millibarns, and appears to come from unpublished work at Hanford. The value of 16 millibarns for the effective cross-section using pure-fission neutrons by irradiation inside an uranium slug ([19]) emphasizes the fact that this reaction goes with thermal neutrons.

The reason for the high thermal cross-section of this reaction is the possible existence of a « negative energy » resonance in ^{35}Cl, postulated by HIBDON and MUEHLHAUSE ([20]). The total cross-section at 0.025 eV is 44 barns and is essentially all due to neutron capture which is unusual for a light nucleus but is characteristic of a strong resonance. The negative value of the resonance is due to a level in ^{36}Cl lying just below neutron binding but which is wide enough to affect the thermal cross-section. BRUGGER and co-workers ([21]) calculate the energy of this resonance to be — 140 eV by fitting a Breit-Wigner single-level curve to their neutron absorption cross-section data.

A value of (590 ± 90) millibarns has been obtained in this work for the effective cross-section of this reaction in NRX. The high cadmium ratio and insensitivity to reactor position show this to be a thermal cross-section. Although this value is appreciably higher than other published values, no systematic error which would make it smaller is apparent. Insufficient correction for self-absorption of the soft β-particle from ^{35}S would be the most suspect source of error, but if this were increased, the cross-section would also be increased.

$^{32}S(n, p)^{32}P$. – When $\hat{\sigma}$ for this reaction is divided by the mean cross-section in an unmoderated fission flux, the « effective fission flux », as a fraction of nv_0, is obtained since the threshold energy is about 1 MeV. There is some

([15]) L. SEREN, H. N. FRIEDLANDER and S. H. TURKEL: *Phys. Rev.*, **72**, 888 (1947).
([16]) W. MAURER: *Zeits. f. Naturf.*, **4 A**, 150 (1949).
([17]) H. BERTHET and J. ROSSEL: *Helv. Phys. Acta.*, **27**, 159 (1954).
([18]) D. J. HUGHES and R. B. SCHWARTZ: BNL 325 (1958).
([19]) D. J. HUGHES: *Pile Neutron Research* (Cambridge, Mass., 1953), p. 100.
([20]) C. T. HIBDON and C. O. MUELHAUSE: *Phys. Rev.*, **79**, 44 (1950).
([21]) R. M. BRUGGER, J. E. EVANS, E. J. JOKI and R. S. SHANKLAND: *Phys. Rev.*, **104**, 1054 (1956).

doubt, however, as to which of the published values for the fission neutron cross-section to use. Table V shows the wide spread of reported values. The value of 154 millibarns is based on the work of STAFFORD and STEIN [22] who in 1953 found a value of 11 millibarns for the $^{54}Fe(n, p)^{54}Mn$ reaction in the Harwell reactor (BEPO). They stated that the ^{32}P in 1 g of sulphur irradiated simultaneously with the iron gave a cross-section for the $^{32}S(n, p)^{32}P$ reaction 14 times that of $^{54}Fe(n, p)^{54}Mn$. MELLISH, PAYNE and OTLET [23] however measured the ratio of the same two cross-sections at a later date in the same reactor and found a ratio of 1.3. The 154 millibarn value would appear to be high.

TABLE V. – *Cross-section of neutron reactions of* Cl *and* S.

Reaction	Cross-section in millibarns			Q value MeV
	Thermal	Fission spectrum	Reference	
$^{35}Cl(n, p)^{35}S$	190 ± 50		[18]	
	169 ± 34		[15]	
	290 ± 70		[16]	
	460 ± 60		[13]	+0.615
	320		[12]	
	340 ± 70		[11]	
	300 ± 10		[17]	
		6	[19]	
$^{35}Cl(n, \alpha)^{32}P$	< 0.05		[18]	
		4.1	[24]	+1.071
		3	[19]	
$^{37}Cl(n, \gamma)^{38}Cl$	560 ± 110		[15]	
$^{32}S(n, p)^{32}P$		154	[22]	−0.927
		59.9 ± 2.5	[25]	
		30	[19]	
		21	[24]	
$^{33}S(n, p)^{33}P$	2.3		[28]	+0.534
$^{34}S(n, \gamma)^{35}S$	260 ± 50		[15]	

The value of 30 millibarns for the fission-neutron cross-section was obtained by HUGHES, SPATZ and GOLDSTEIN [19] by irradiation inside an uranium fuel rod in the Argonne reactor. The fission flux was standardized against that

(22) G. H. STAFFORD and L. H. STEIN: *Nature*, **172**, 1103 (1953).
(23) C. E. MELLISH, J. A. PAYNE and R. L. OTLET: AERE I/R 2630 (1958).

obtained from a slab of uranium placed in a beam of thermal neutrons with known geometry. ROCHLIN ([24]) reports that SAELAND and SAMSAHL obtained the value of 21 millibarns from irradiations in the Norwegian heavy-water reactor using 19 millibarns for the fission-neutron cross-section of the reaction $^{31}P(n, p)^{31}Si$. This latter cross-section is due to HUGHES and co-workers also. The Norwegian value for the $^{32}S(n, p)^{32}P$ reaction is in reasonable agreement with that of HUGHES, suggesting that the fission-neutron spectrum is not badly distorted in the reactor lattice. GLOVER and MADDOCKS ([25]) and PHILLIPS ([26]) have reported a value of 60 millibarns which they attribute to RICHMOND and PHILLIPS (1957) but which has not yet appeared in the literature. The fission-neutron cross-section was also calculated by GLOVER and MADDOCKS to be 66.2 millibarns. This was done by numerically integrating the product of points 0.5 MeV apart on the excitation curve for the $^{32}S(n, p)^{32}P$ reaction published by ALLEN and co-workers ([27]) and on the fission-neutron distribution curve.

It would appear that there is some basis for weighting the 30 millibarn cross-section of HUGHES more than the 60 millibarn value from Harwell, as the latter work has not yet been published and the method of flux measurement not known.

Using Hughes' value, the « effective fission flux » in NRX lattice during these experiments was 0.053 times nv_0. In the reflector at position S-9-4 the average value was 0.024 times nv_0.

$^{35}Cl(n, \alpha)^{32}P$. – The negative-energy resonance in ^{35}Cl makes little contribution to the effective cross-section of this reaction. Even though the α-particle is emitted with an energy of about 1 MeV its penetrability of the compound nucleus is small as the Coulomb barrier is about 9 MeV. Subtracting the effective cross-section under cadmium from the average of the two values without cadmium gives an approximate thermal cross-section of 0.08 millibarns. The only literature value for this appears to be the previously unpublished figure given in BNL-325 (1958) of < 0.05 millibarns. Because this reaction is exoergic and both thermal and resonance neutrons appear to contribute to the reaction rate, no meaningful relationship between the effective cross-section and the fission-neutron cross-section can be obtained.

$^{33}S(n, p)^{33}P$. – Though the abundance of ^{33}S is only 0.75% of natural sulphur, this reaction has been included in Table II because ^{33}P with a half-life

([24]) R. S. ROCHLIN: *Nucleonics*, no. 1, 54 (1959).
([25]) R. N. GLOVER and K. MADDOCKS: AERE R/R 2687 (1958).
([26]) J. A. PHILLIPS: AERE R/R 2366 (1957).
([27]) L. ALLEN, W. A. BIGGERS ,R. J. PRESTWOOD and R. K. SMITH: *Phys. Rev.*, **107**, 1363 (1957).

of 24 days has been found in old samples of ^{32}P prepared by irradiating sulphur. The low energy of its β-particle (0.25 MeV) is comparable with that of ^{35}S (0.167 MeV) and, if it were present in a mixture of ^{32}P (1.71 MeV) and ^{35}S, it would be indistinguishable from the ^{35}S by aluminum-absorption measurements. It would be detected only by following the decay of the mixed activities for a long period. The reaction has been found by WESTERMARK ([28]) to occur at thermal-neutron energies with a cross-section of 2.3 millibarns. NICHOLS and JENSEN ([29]) irradiated sulphur enriched in ^{33}S in NRX and estimated the effective cross-section of this reaction to be about 2.6 times that of the $^{32}S(n, p)^{32}P$ reaction. This was a lattice irradiation but was done before the re-contruction of NRX in 1953. However for calculating the rate of production of ^{33}P in these experiments the ratio should be close enough. Using 1.6 millibarns for the effective cross-section of the $^{32}S(n, p)^{32}P$ reaction the ^{33}P activity at the end of the lattice irradiations would be about 2% of the ^{32}P. As the ^{35}S and ^{32}P activities were similar in these irradiations it means that about 2% of the observed ^{35}S activity from the irradiated K_2SO_4 would have been due to ^{33}P. This amount is too small to be detectable on the decay curves. In the reflector the cross-section ratio of the two reactions would be expected to be higher as the $^{33}S(n, p)^{33}P$ reaction is exoergic. As no ^{33}P was detected it is probable that this increase was cancelled by the increased ^{35}S-to-^{32}P activity ratio.

$^{37}Cl(n, \gamma)^{38}Cl$. – The effective cross-section for this reaction in NRX lattice of 390 millibarns (average of two measurements) is appreciably lower than the thermal value of (560 ± 110) millibarns obtained by SEREN and co-workers in 1947. These authors calibrated their counter with UX_2 and RaE, while in this work ^{32}P was used. With this particular counter it has been found that, using a high-geometry position, the efficiency is constant above about 1 MeV ([30]) so that ^{32}P (1.7 MeV) and ^{38}Cl (4.8; 2.8; 1.1 MeV β-particles) should have the same efficiency. The ^{38}Cl γ-rays are counted with about 1% of the efficiency of the β-particles. It is reasonable to assume that the cross-section of this reaction approximates the $1/v$ law so that (390 ± 60) millibarns may be considered as the thermal cross-section.

$^{34}S(n, \gamma)^{35}S$. – This reaction has been investigated in both the lattice and reflector of NXR and the effective cross-section of (270 ± 40) millibarns is in

([28]) T. WESTERMARK: *Phys. Rev.*, **88**, 573 (1952).
([29]) R. T. NICHOLS and E. N. JENSEN: *Phys. Rev.*, **94**, 369 (1954).
([30]) L. BOGAR: private communication.
([31]) T. A. EASTWOOD and J. C. ROY: *Can. Journ. Phys.*, **37**, 815 (1959).
([32]) J. C. ROY and MRS. D. WUSCHKE: CRC 852 (1959).
([33]) E. C. TRAPP: *Sixth Hot Labs. and Equipment Conf.* (1958), pp. 306-311.

good agreement with the value of (260 ± 50) millibarns obtained by SEREN and co-workers for the thermal cross-section. This reaction is also expected to follow the $1/v$ law.

* * *

The authors wish to thank Mrs. J. S. MERRITT for supplying the standardized ^{35}S and ^{32}P solutions.

—

RIASSUNTO

Le Sezioni d'urto della reazioni di attivazione di cloro e zolfo con neutroni per produrre ^{38}Cl, ^{32}P e ^{35}S, sono state misurate nel reticolo degli elementi di combustibile e nel riflettore del reattore NRX. Le sezioni d'urto « efficace » di queste reazioni per neutroni prodotti da reattore sono state calcolate irraggiando contemporaneamente fili di cobalto come monitori di flusso.

SUPPLEMENTO AL VOLUME XIX, SERIE X
DEL NUOVO CIMENTO

N. 1, 1961
1° Trimestre

Determination of the Electric Charge of a High-Charged Nucleus of the Primary Cosmic Rays with Nuclear Emulsions.

G. ALVIAL (*)

Centro de Radiación Cósmica, Facultad de Ciencias Físicas y Matemáticas
Universidad de Chile - Santiago

(ricevuto il 25 Ottobre 1960)

Summary. — A new method is described and discussed for the study of the heavy primary component of the cosmic radiation. It allows to determine the charge Z, in nuclear emulsions, with a standard error of less than one unit. One relativistic nucleus with a Z as large as 30 was found.

1. – The existence of primary cosmic ray nuclei highly charged and their relative abundance are directly related to the origin of cosmic rays and other important astrophysical problems. One nucleus with a possible Z between 35 and 40, of low energy, was presented by BARKOW *et al.* (1). However, the particular method they have applied to determine this Z gives errors bigger than those shown by the authors. A relativistic nucleus with a Z as large as 30 is presented in this report. The charge determination was done by applying the small δ-ray method and its standard error resulted very near to one unit of electric charge.

(*) This work was done in a nuclear emulsion stack which forms part of a group of cosmic ray researches supported in part by a joint program of the Office of Naval Research and the U. S. Atomic Energy Commission, and by the National Science Foundation. This stack was turned over to this laboratory by the Department of Physics of the University of Chicago in order to continue this type of research in the University of Chile.

(1) A. G. BARKOW, B. CHAMANY and R. E. MCDANIEL: *Nuovo Cimento*, **6**, 125 (1957).

The nucleus was found in a stack of nuclear emulsions which was flown at 131000 feet during 19 hours in Minneapolis, Minn., and belonged to MARCEL SCHEIN's laboratory of The University of Chicago.

2. – The first paper on the small δ-ray method emphasized that the existence of such small δ-rays was a presumptive hypothesis only (2). Later works (3,4) confirmed this hypothesis and established the following main conclusions:

a) The density of the studied small δ-rays is proportional to the square of the electric charge associated with the measured nuclear track. It is possible to obtain this density with an experimental error which permits the determination of the electric charge with an error of less than one unit of charge.

b) In computing the density of small δ-rays, some irregular cases appear, *i.e.* some groups of little δ-rays forming compact columns of silver and located along the track. In these cases the number of δ-rays is decided by taking the mean diameter of single grains belonging to tracks of minimum ionization. The ratio between the length of the studied silver column and the mean diameter gives the number of small δ-rays for this particular group of blobs (2). If we consider the welding together of blobs by the chemical action of the developer, the deformation of the nuclear track caused during the development process and the discriminatory power of the microscope, this ratio might give an excess value for the density of small δ-rays and consequently, an excess value for the corresponding atomic number. To perform this measurement, the degree of development of the nuclear emulsion plates was studied by applying OCCHIALINI and co-workers' suggestions (5).

To check up the reliability of the above procedure, the charge determinations were made by computing the mean free path of small δ-rays, but to do this, only a length of free paths longer than 4 times the discriminatory power of the available microscope were measured. In this way, the lengths of free paths were not measured exactly on the same counted δ-rays and the charge measurements were independent of the errors due to the optical discriminatory power and the welding of the small δ-rays. The electric charges obtained, either by computing the density of small δ-rays or computing the mean free paths deduced from the lengths of free paths longer than 4 times the discriminatory

(2) G. ALVIAL, L. GRIMALDI, J. RIQUELME, E. SILVA and S. STANTIC: *Nuovo Cimento*, **15**, 25 (1960).

(3) G. ALVIAL: *Bull. Am. Phys. Soc.*, **5**, 258 (1960).

(4) G. ALVIAL: preprint, Department of Physics, The University of Chicago. This work was done by the author as Fellow of the John Simon Guggenheim Memorial, Foundation (1960).

(5) G. ALVIAL, A. BONETTI, C. DILWORTH, M. LADU, J. MORGAN and G. OCCHIALINI: *Suppl. Nuovo Cimento*, **4**, 244 (1955).

power of the microscope, resulted in agreement within an experimental error of less than one unit of charge. This result is important because of the welding together of the small δ-rays in the tracks of high ionized nuclei.

The method of determining the mean free paths of small δ-rays from the measurements of length of free paths longer than a certain pre-fixed length is similar to that of determining the mean gap-length suggested by O'CEALLAIGH ([6,7]).

c) For nuclear tracks produced by high ionized nuclei it is necessary to count small δ-rays of two or three grains attached to the tracks. In this way, it is possible to employ the Klausen micrometer directly to select those δ-rays without measuring the track profile. This selection is faster than the profile measurements by at least a factor of 10. On the other side, for low and medium ionized nuclei the profile measurements also permit the inclusion of δ-rays as small as those formed by only one grain attached to nuclear tracks. In such cases the additional time involved in making these profile measurements is compensated by the extra number of δ-rays.

d) The contribution to the « background » of the measurements indicated in *a*) and *b*) by the physical-chemical actions of the standard photographic development is irrelevant. Also no significant influence caused by the shrinkage of the emulsions has been found in these measurements for tracks whose angles of dip are less than 15°.

The analysis of the method and of the techniques used to reach the conclusions *a*), *b*), *c*), and *d*) has been reported in the above mentioned bibliography.

3. – The measurements were performed over 8 selected nuclear tracks corresponding to relativistic primary nuclei of the cosmic radiation. Two of them are unambiguous cases of fragmentation, *i.e.*, one carbon nucleus which is fragmented into three α-particles and one oxygen which is broken into four α-particles. In the determinations of the electric charges, all the measurements were related to the oxygen track by taking this track as a calibration nucleus.

The measurements were carried out in G-5 Ilford nuclear emulsions which are 600 μm thick and present a very homogeneous degree of photographic development.

Fig. 1 shows the distribution functions of the length of the free paths at least four times greater than the discriminatory power of our microscope for small δ-rays of two or three grains directly attached to the nuclear tracks for

---

([6]) C. O'CEALLAIGH: *Report of the Bagnères de Bigorre Conference* (1953), p. 73.

([7]) C. O'CEALLAIGH: *Measurements of ionization in photographic emulsions by the technique of mean gap-length*, preprint (1954).

TABLE I. – *This table gives us the total results of the experimental measurements, α_2 is the slope of the straight lines of Fig. 1 and λ indicates the corresponding mean free paths.*

Track	Angle of dip	Energy per nucleon in GeV	Number of little δ-rays per 5 μm	Range over which the density measurements were performed	Values of $\alpha_2 \cdot 10^4$ coefficients $\alpha_2 = 1/\lambda$	Range over which the mean free path was determined	Z determined from the density of little δ-rays by taking for $Z=8$ the value $n_\delta = 0.381 \pm 0.026$	Z determined from the mean free path of little δ-rays ($1/d_2$) by taking for $Z=8$ the value $\alpha_2 = (-17.82 \pm \pm 0.89) \cdot 10^{-4}$	Z attributed to the nuclei by analysing the results of the last two columns
1	4° 8′	∼10	0.228 ± 0.014	5510 μm	− 8.03 ± 0.40	3900 μm	6.2 ± 0.3	5.6 ± 0.4	6
2	0° 47′	∼ 6.5	0.381 ± 0.026	3600 μm	− 17.82 ± 0.89	4400 μm	8.0 ± 0.0 (*)	8.0 ± 0.0 (*)	8
3	4° 10′	∼10	0.821 ± 0.056	1600 μm	− 41.89 ± 2.09	1900 μm	11.7 ± 0.6	12.3 ± 0.4	12
4	6° 29′	∼15	1.125 ± 0.084	960 μm	56.30 ± 3.15	1250 μm	13.7 ± 0.7	14.2 ± 0.5	14
5	4° 34′	∼20	2.450 ± 0.113	800 μm	− 108.90 ± 5.45	950 μm	20.3 ± 0.8	19.8 ± 0.7	20
6	2° 21′	∼ 6	3.010 ± 0.176	650 μm	− 128.95 ± 6.45	845 μm	22.5 ± 1.0	22.4 ± 0.8	22
7	3° 36′	∼13	3.700 ± 0.168	600 μm	− 170.90 ± 8.55	750 μm	24.9 ± 1.0	24.8 ± 0.9	25
8	2° 0′	∼ 2	5.525 ± 0.150 (near interaction) 5.3 ± 0.3 (∼10 cm from interaction	800 μm	− 242.80 ± 12.14	600 μm	30.4 ± 1.1	29.7 ± 1.0	30

(*) Nucleus of calibration.

8 primary relativistic nuclei. In one axis is indicated, in logarithmic scale, the number of free paths equal to or greater than the number of the micrometer divisions indicated in the X axis. In this figure, 100 micrometer divisions are equal to 3.7 μm, that is, the measured free paths are much greater than the discriminatory power of our microscope. We can see that the length distribution functions of the free paths are exponentials, *i.e.*, they are represented by straight lines. As is well known, the mean free path is in each case as the inverse of the absolute value of the slope of the corresponding straight line, and consequently, as the inverse of the square of the respective electric charge. The charges indicated in Fig. 1 were obtained by relating these measurements to the mean free path of small δ-rays for the oxygen nucleus. The experimental relative errors gave a resultant of $1/\sqrt{N}$, where N is the number of counted free paths in each track.

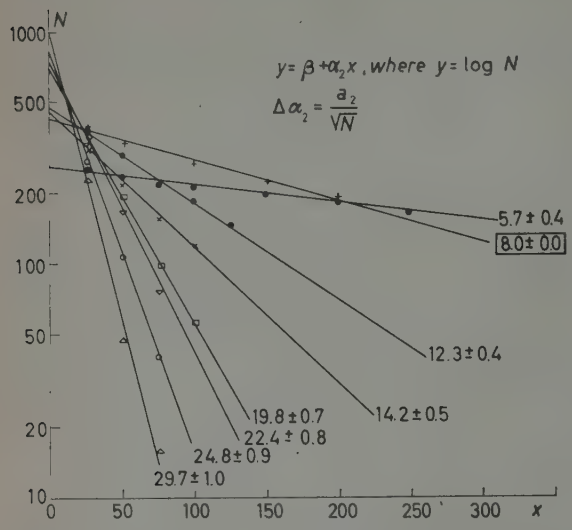

Fig. 1. – In the N axis is indicated, in logarithmic scale, the number of free paths equal or greater than the number of micrometer divisions represented in the X axis. Here α_2 indicates the absolute value of the slope of the straight lines.

In Table I the electric charge determinations deduced from the density of little δ-rays are presented. These measurements were related to the density of small δ-rays of an oxygen nucleus which was taken as a calibration track. Besides and, in order to investigate how the welding together of the small δ-rays and the optical discriminatory power influence our measurements of densities, we present a column with the charge determinations deduced from the mean free path of the small δ-rays which are independent of the discussed optical conditions and the physical-chemical action of the development process. We observe that the determined Z presented in these two columns coincides within an error of less than one unit of charge.

The energy estimation of the nuclei was done by measuring the angle of opening of the relativistic α-particles originating in the interaction of the heavy primary nucleus in the nuclear emulsions. In considering the error of this method to determine the energy and the resultant energy of nearly 2 GeV per nucleon for track 8, which is in the limit of the relativistic zone, the density

of small δ-rays was not only computed near the interaction of the heavy primary nucleus, but also at almost 10 cm from this interaction. Both densities agree within the corresponding experimental errors.

From these experimental results we conclude that it is possible to construct a charge spectrum of the heavy primary nuclei of the cosmic radiation in which the electric charges are separated and distinguished within a standard error of less than one charge unit. At the same time, the small δ-rays method is a general method to determine the relative abundance of the very heavy nuclei. These researches are now being carried out in this laboratory.

* * *

The author expresses his heartfelt gratitude to the late Professor MARCEL SCHEIN of the University of Chicago for his generous help in making available the facilities which have permitted the continuation of this work in the University of Chile.

RIASSUNTO (*)

Si descrive e si discute un nuovo metodo per lo studio della componente primaria pesante della radiazione cosmica. Permette di determinare la carica Z, nelle emulsioni nucleari, con un errore standard inferiore ad una unità. Si è trovato un nucleo relativistico con $Z = 30$.

(*) *Traduzione a cura della Redazione.*

SUPPLEMENTO AL VOLUME XIX, SERIE X
DEL NUOVO CIMENTO

N. 1, 1961
1° Trimestre

Discrimination of Tracks of Photofission Fragments with Very High Backgraund of Alpha-Particles and Electrons in Nuclear Emulsions (*).

H. G. DE CARVALHO (**) and A. G. DA SILVA (***)

Centro Brasileiro de Pesquisas Físicas - Rio de Janeiro

(ricevuto l'11 Novembre 1960)

Summary. — With common drugs used in photography such as amidol, boric acid, sodium sulfite and potassium bromide, a developing bath was prepared which permits a complete discrimination of the tracks of highly ionizing particles, such as fission fragments, in the presence of strong background radiation such as that produced by the electrons from a 2000 röntgen X-ray dose and a background of 10^{11} α-particles/cm^3.

1. – Introduction.

In order to measure the anisotropy of photofission fragments from ^{238}U [1] with nuclear emulsions Ilford D-1 and K-0 as detectors, it was considered advantageous to search for a method of developing photoplates so that only the tracks from fission fragments were clearly visible in a background produced mainly by electrons from very high X-ray doses and by α-particles.

Methods that allow discrimination between fission fragments and α-particle tracks by under-development or by erradication of the latent image are already

(*) This work is supported in part by funds provided by the Conselho Nacional de Pesquisas and Commissão Nacional de Energia Nuclear (Brazil).

(**) At present on leave of absence from the Centro Brasileiro de Pesquisas Fisicas and Brazilian Nuclear Energy Comission at the Instituto Nazionale di Fisica Nucleare - Sottosezione di Napoli.

(***) At present on leave of absence from the C.B.P.F. at the High voltage Lab. M.I.T. Mass., U.S.A..

(1) H. G. DE CARVALHO, A. G. DE SILVA and J. GOLDEMBERG: *Nuovo Cimento* **19**, 1131 (1961).

known. However, the distinction between these tracks is sometimes difficult, mainly when the number of α-particle tracks is much greater than the fission fragment tracks or when the α-particle tracks form large angles with the plane of the emulsion.

The conventional processes of development do not take full advantage of the difference in the ionizing powers of the two kinds of particles that produce the tracks. A fission fragment has on the average, an ionizing power 30 times greater than that of an α-particle; however, if a conventional development is used the resulting tracks are almost indistinguishable. A process of development, which takes advantage of the difference in ionizing power in such a way as to eliminate the development of undesirable tracks of a particle with less ionizing power, is advantageous for many reasons; in scanning it is not necessary to distinguish between numerous tracks from α-particles and from those produced by fission fragments because the only tracks visible are those from the fission fragments. Moreover, the same process which eliminates the undesirable background tracks allows the use of greater doses of X-rays, yielding a greater number of fission fragment tracks with benefit to the time of scanning.

In a nuclear fission experiment when the target nuclide loaded in the emulsion, is an α emitter such as natural uranium or thorium the experiment from the moment of the impregnation to the emulsion processing, is done as quickly as possible (in a few hours), so as to prevent the undesirable accumulation of α-particle tracks. When the technique that eliminates the α-particle tracks is used the fading of the latent image is the only limiting factor on time. The fading however can be prevented by means of a dry, low temperature, nitrogen atmosphere.

2. – Method.

In a previous paper ([2]), it has been shown which factors influence the kinetics of the development of tracks produced by charged particles and the equations that describe the rate of reaction. These equations indicate that it is pos sible to separate completely the curves grain density *vs.* development time of fission-fragment tracks from those of α-particle tracks.

The rate of development of the latent image depends on several factors, such as the nature of the photographic emulsion (including the effect of the loading), the solarization produced by intense γ radiation, the nature of the developing bath, the temperature and the ionization produced by the particle along its path.

([2]) P. Demers: *Photographie corpusculaire*, II (Montréal, 1959), p. 211.

It is possible to prepare a developing bath such that, at a given temperature, only fission tracks will be developable: α-particle tracks remaining invisible because as has been said before, fission fragments ionize much more than α-particles and thus the number and size of the latenti mages produced in the grains by fission fragments are greater than those produced by α-particles. When the developing power of the bath is so low as barely to develop the grains sensitized by a given charged particle, it is reasonable to assume a first order process for the mechanism of development; that is, dD/dt (the rate of development) is proportional to the number of sensitized grains not yet developed, $dD/dt = k(D_\infty - D)$, where k is the specific rate of the process. D_∞ represents the total number of grains that may be developed and D is the number of grains already developed at the time considered. The integrated form of this equation is the following:

$$D = D_\infty\{1 - (\exp[-k(t - t_0)])\}\,, \tag{1}$$

where t_0 is the induction period; that is, the time within which no development is observable.

Dealing with development of tracks, produced by two kinds of particles of very different ionizing powers, it is possible to adjust the time scale of the two processes so that the development induction period t_0 of the tracks of the particles with less ionization is so long that it allows time enough for tracks of the particles with greater ionization, to be fully developed.

Potassium bromide, which is usually employed to increase the induction period, was used in a relatively large quantity. It also reduces the specific rate of development. Diluting by a factor of twenty the concentration of the developing agent, keeping a sufficient quantity of sulfite and a low pH with an adequate concentration of boric acid, and carrying out the development at low temperature, it is possible to reduce considerably the specific rate of development, thus magnifying the time scale so as to obtain the desired discrimination. This developing solution diffuses in less than 2 hours in 200 μm plates, and is probably suitable for use in 600 μm films.

Since the adequate time of development for a group of plates exposed under certain conditions depends on several factors, a device was used to determine the optimum time of development. This apparatus yields plates gradually developed in such a way that in just one operation a large time interval may be studied.

The apparatus (Fig. 1), consists of a plastic holder that may hold four 1 in. × 3 in. plates, a graduated cylinder and the mechanism of an old clock. The support is dipped into the developing bath by the mechanism which is connected to several wheels of different radii, the one to be used depending on the time interval to be investigated. The clock mechanism sinks the plate

holder vertically at a uniform rate. Therefore, for each position on the plates there corresponds a particular developing time. The proper choice of time is made from a microscopic examination of the plates, choosing the region where the fission tracks are to be sharply visible in the full thickness of the emulsion and the background sufficiently weak so as to allow comfortable scanning.

The maximum tolerable γ-ray dose adequate for the ^{238}U photofission investigation was determined to begin with by exposing natural uranium loaded plates to a calibrated Ra-Be source. Keeping the source and the plates inside a block of paraffin during the exposure, one gets neutron fission tracks and a background of γ-rays that varies with the distance from the source. In this way it is possible to determine with good approximation the ideal developing conditions.

When performing the actual experiments in photofission, one or more plates are developed gradually in the apparatus described above, during a time interval that contains the optimum time obtained in the previous experience with the Ra-Be source. Once the developing time for a given temperature was established the following method was used; loaded emulsions were washed in running distilled water at 5 °C for 30 or 120 minutes (100 or 200 μm). Then the plates were kept for the optimum time previously deter-

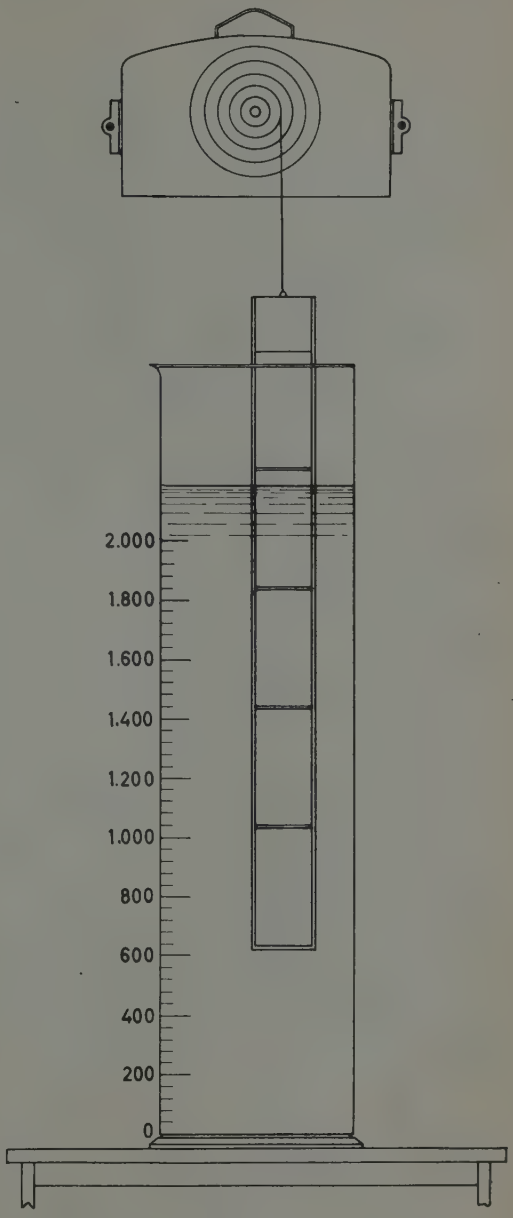

Fig. 1.

mined in the following developing bath:

Boric acid	3.5 g
Sodium sulphite	4.5 g
Potassium bromide	1.5 g
Amidol	0.45 g
Distilled water to make	2 liters

After the developing bath the plates were washed in running water at 8 °C for 60 minutes, then put in as top bath (0.7 % acetic acid solution) at 5 °C for 2 hours, washed again in running water and fixed in a 30 % hypo solution which contained some silver. Fixation is carried out at a temperature of 5 °C. The photoplates after the fixing process were washed in tap water at 8 °C, dehydrated in alcohol and dried at room temperature.

The time used for development at 10 °C for Ilford K-0 100 μm thick was between 50 to 70 minutes. For emulsions 200 μm thick, the time was 90 to 120 minutes, adjusted in each case to loading pH and X-ray doses. It was found that from batch to batch the proper time was different when the other conditions were the same. It is well known that the impregnation of uranyl salts in emulsion has a desensitization effect which is strongly affected by the pH of the solution used.

Nuclear emulsions exposed to high doses of X-rays suffer a fading of the latent image similar to the solarization in common photography and the overall effect is equivalent to a diminishing of the emulsion sensitivity ([3]). This effect depends on the rate of irradiation, on the content of water of the emulsion and on the room temperature. The solarization effect of the dose and rate of X-ray exposure and of the uranyl salt at the loading pH is such that 300 r dose given in 2 minutes exposure at 20 MeV will require 9 hours in the developing bath to render the α tracks barely visibile. With a dose of 600 r and the same rate, it was impossible to observe any α-particle track with 24 hours of development.

When the X-ray dose is not too high and the development lasts too long the fission tracks become very dark with a density of grains so high that the screw structure resulting from too many grains in the trajectory is very well observed (Fig. 2).

3. – Uses of the technique.

The method of development described above may have many different uses in problems of nuclear physics where one has production of highly ionizing particles in the presence of a strong background of radiation. For instance, using Ilford K-0 type of nuclear emulsion to study problems involving fission

Fig. 2.

fragments with high energy X-rays it is possible to use exposures up to 2 000 röntgens. This permits the study of angular anisotropy, fissionability and tripartition with emission of fragments heavier than α-particles. The method may be used to study spontaneous fission, or fission induced by very high intensity beams of neutrons or charged particles. Another possible use is the detection of heavily ionizing heavy cosmic ray primaries in exposures carried out for many hours in the Van Allen outer space belt of radiation.

* * *

The authors wish to express their appreciation to Professor J. GOLDEMBERG for the exposures to the X-ray beam of the betatron of the University of São Paulo and to Professor M. D. SOUZA SANTOS for exposures to slow neutrons in the Instituto de Energia Atomica de São Paulo.

(3) C. E. K. MEES: *The Theory of the Photographic Process*, revised edition (London 1954), p. 250.

RIASSUNTO (*)

Con i comuni prodotti usati in fotografia come l'amidolo, l'acido borico, il solfito di sodio ed il bromuro di potassio si è preparato un bagno di sviluppo che permette di fare una perfetta discriminazione delle tracce di particelle altamente ionizzanti, come i frammenti della fissione, in presenza di una forte radiazione di fondo, quale quella prodotta dagli elettroni di una dose di raggi X di 200 röntgen o da un fondo di 10^{11} particelle α/cm^2.

(*) *Traduzione a cura della Redazione.*

SUPPLEMENTO AL VOLUME XIX, SERIE X
DEL NUOVO CIMENTO

N. 1, 1961
1° Trimestre

Characteristics of Liquids for Use in a Bubble Chamber.

R. KATO

Nuclear Laboratory, Ritumeikan University - Kyoto

(ricevuto il 14 Novembre 1960)

Summary. — The sensitive regions of several liquids in a continuously sensitive bubble chamber have been determined. This sensitive regions are discussed on the saturated vapor pressure *vs.* temperature curves of the liquids which were used in the chamber. An easily operating expansion chamber has also been constructed, which works at low pressure by reducing the pressure in the liquid from pre-expansion pressure of one atmosphere. Some quantitative characteristic of it are given.

1. – Introduction.

The tests were initiated as a result of the need for quantitative experimental information on the operating conditions of continuously sensitive bubble chambers. Along this line, first, some observations were made to measure the characteristics in a continuously sensitive bubble chamber operating at atmospheric pressure which has been devised by R. H. GOOD [1].

In order to make the bubble chamber operate effectively, many important factors, which are directly or indirectly related to its operation, have been considered theoretically by many workers [2-4]. Following this theoretical knowledge, we have measured some factors, which should be essential to the working of the bubble chamber. We have also taken some numerical data from literature [5]. The values of surface tension and saturated vapor pressure of se-

[1] R. H. GOOD: *Phys. Rev.*, **107**, 1201 (1957).
[2] D. A. GLASER: *Suppl. Nuovo Cimento*, **2**, 361 (1954).
[3] F. SIETZ: *Phys. of Fluids*, **1**, 2 (1958).
[4] D. C. RAHM: *Ph. D. Thesis* (University of Michigan, 1956).
[5] *a*) LANDOLT-BÖRNSTEIN: *Physikalisch-Chemische Tabellen* (Berlin, 1927) *b*) *Physikalische Zahlenwerte und Funktionen* (Berlin, 1956).

veral organic liquids were necessary to obtain superheated states. Some values of surface tension, which were difficult for us to find in the literature, have been measured by us. We have also obtained the characteristics of several kinds of liquids used in the continuously sensitive bubble chamber. These are as follows:

1) Operating temperature in the sensitive region,

2) Depth and width of the sensitive region.

The experimental data obtained by us have been plotted and tabulated together with those from other authors. These curves have indicated that our continuously sensitive bubble chamber, in which an organic liquid containing gas, carbon dioxide for instance as in our experiment, was used, was able to operate at atmospheric pressure as that of R. H. GOOD and that the operating temperatures of the sensitive region are far below that of boiling point at atmospheric pressure of the liquid not containing the gas. In other words, the latter case shows that the equilibrium saturated vapor pressures corresponding to the operating temperature mentioned above, are lower than atmospheric pressure. For example, if normal hexane is saturated with carbon-dioxide, it can reach a highly superheated condition in the range of $(38 \div 53)$ °C and at atmospheric pressure, while, at normal pressure, the boiling point of pure normal hexane is 68.7 °C.

Considering the above results, we expected that the bubble chamber could be operated even at very low working pressure —as it were—some fraction of one atmosphere. If, thus, a bubble chamber as above could be obtained, it might be very easy to construct and be conventionally operated.

After the preliminary steps we tentatively attempted to build a new type of expansion bubble chamber which might be operated at very low pressure attained suddenly from the pre-expansion pressure of one atmosphere. The chamber after having been constructed has been operated in conditions in which highly superheated states can occur.

In most of the expansion chambers devised by many workers, expansion is achieved by a flexible rubber or metal diaphragm or a piston actuated by compressed air. Most of these chambers ([4,6-12]) are expanded to about one or more atmospheres final pressure. The final pressure of our expansion cham-

---

([6]) P. E. ARGAN and A. GIGLI: *Nuovo Cimento*, **3**, 1171 (1956).

([7]) B. HAHN: *Nuovo Cimento*, **4**, 944 (1956).

([8]) P. E. ARGAN and A. GIGLI: *Nuovo Cimento*, **4**, 953 (1956).

([9]) I. A. PRESS and R. J. PLANO: *Rev. Sci. Inst.*, **27**, 935 (1956).

([10]) B. HAHN and J. FISHER: *Rev. Sci. Inst.*, **28**, 656 (1957).

([11]) B. HAHN, G. RIEPE and A. W. KNUDSEN: *Rev. Sci. Inst.*, **30**, 645 (1959).

([12]) H. COURANT, J. E. JENSEN, R. I. LOUTTIT and J. R. SANFORD: *Rev. Sci. Inst.*, **30**, 280 (1959).

ber is only some fraction of one atmosphere. We have tried to find experimentally an optimum condition for operation of this expansion bubble chamber. We have therefore observed the ratio of expansion and the operating temperature at which the superheated states can occur.

2. – Experimental method and results.

2·1. *A continuously sensitive bubble chamber.* – As mentioned above, we have also constructed a bubble chamber, which is continuously sensitive like that of R. H. Good. This chamber employs a solution of gas, carbon dioxide, in a liquid, acetone for example. The other liquids, ethyl alcohol, hexane and etc., with carbon dioxide produce similar results. The liquids are saturated at dry-ice temperature with the carbon dioxide produced out of dry-ice by sublimation. The bottom of the chamber is placed in a dry-ice bath for cooling, while its top is heated to a suitable temperature at which bubble formation can be obtained. An uranium source inserted inside the tip of a capillary tube was brought in the chamber.

This source of unitary powder was produced by grinding uranium ore. The operating temperature of this chamber has been observed. Some experimental data and numerical values are shown in Table I. When the previously prepared uranium source was brought in the chamber, bubbles foamed in a intermediate narrow layer of the liquid and rose up to the surface of the liquid. Above the upper limit of this layer a foamy state was produced, and below the lower limit of it no bubble existed. When another capil-

Table I. - *Temperature at the sensitive region for each liquid and its equilibrium saturated vapor-pressure.*

Liquid	Upper limits of sensitive ranges		Lower limits of sensitive ranges	
	Temperature (°C)	Equilibrium saturated vapor-pressure (mm Hg)	Temperature (°C)	Equilibrium saturated vapor-pressure (mm Hg)
Acetone	53	675	38	400
n-hexane	68	735	65	675
Methyl-alcohol	52	445	42	285
Ethyl-alcohol	76	680	70	540

lary tube containing a piece of non-radioactive ore was brought in the chamber, no bubble formation was observed. Temperatures in the chamber have been measured using an alcohol thermometer, since mercury thermometers were unsuitable. Using mercury thermometers in the chamber, many background bubbles appeared from the surface of the glass envelope containing mercury. In the second and forth columns of Table I are shown the temperatures at the upper and at the lower limits, respectively, of the sensitive layers for each liquid of the first column. For example, the sensitive region of the acetone and carbon dioxide system is from 38 °C to 53 °C. The third and fifth columns indicate the numerical data of the saturated vapor-pressure corresponding to each temperature shown in the left column.

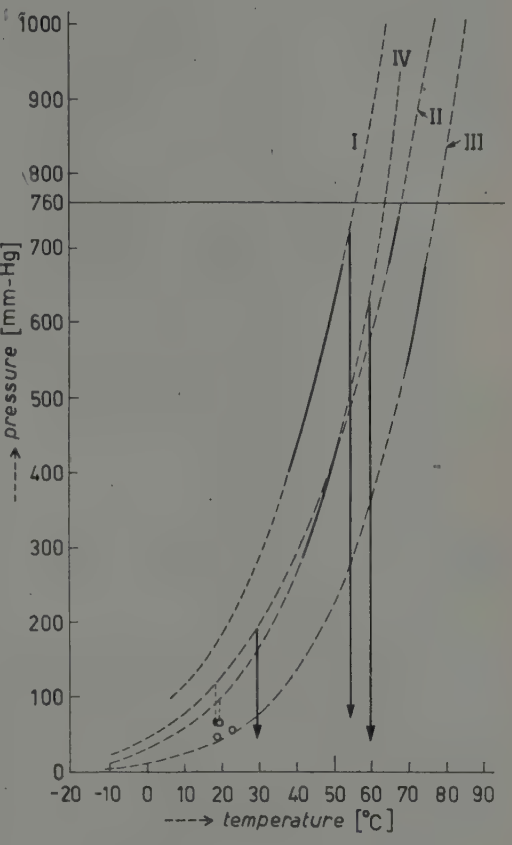

Fig. 1. – Saturated vapor pressure *vs.* temperature curves for acetone (curve I), n-hexane (curve II), ethyl alcohol (curve III), and methyl alcohol (curve IV); solid portions of the curves (I-IV) refer to sensitive regions of the continuously sensitive chamber; lengths of vertical lines with downward arrow give excess pressure drop during expansion in the expansion chamber.

TABLE II. – *Surface tension at sensitive region.*

Liquid	Surface tension (dyne/cm)	
	upper limit	lower limit
Acetone	19.0	20.1
n-hexane	13.4	13.6
Methyl-alcohol	19.6	20.6
Ethyl-alcohol	17.0	17.4

These values of the saturated vapor-pressures were obtained by interpolation from the data of literature (5). Fig. 1 shows the saturated vapor-pressure *vs.* temperature curves for each liquid. On the solid portion of each curve are plotted the values corresponding to sensitive regions of Table I. Table II shows the surface tension at the upper and lower limits of the sensitive region for each pure liquid in Table I. The values were obtained from the literature (5). The surface tension *vs.* temperature curves for each liquid are plotted in Fig. 2, and the portions of thick lines correspond to the data of Table II.

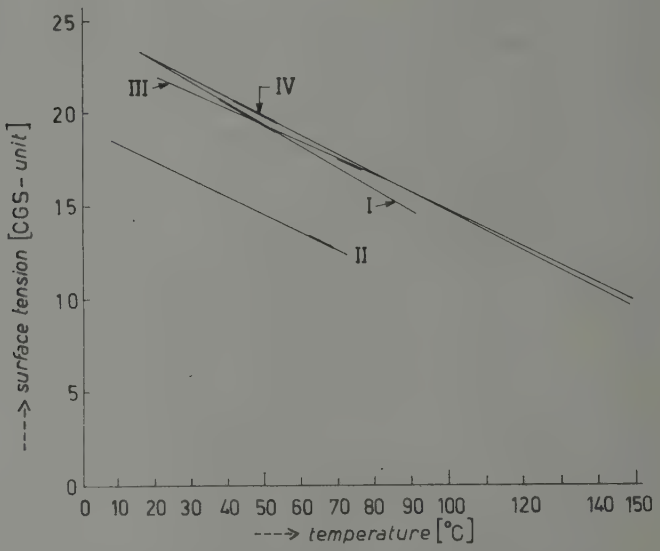

Fig. 2. – Surface tension *vs.* temperature curves for liquids; curve I: acetone; curve II: n-hexane; curve III: ethyl alcohol; curve IV: methyl alcohol. The thick portions of the lines correspond to surface tensions of the sensitive regions.

It was very difficult to determine the depths and widths of the sensitive ranges in the chamber, since the portions of the upper and lower limits were always fluctuating due to thermal diffusion of the liquids. By rough estimations, the widths of them are of the order 1 to 5 cm.

2·2. *An expansion type bubble chamber.* – After the first experiment with the continuously sensitive chamber, as already mentioned, the second step was started; *i.e.*, the second experiment was tried to find a possibility of superheating the chamber under easy operating conditions. In order to obtain more favourable experimental conditions, namely, a pre-expansion pressure lower than one atmosphere, we have undertaken a systematic search for several gas-liquid systems and for several pure organic liquids.

For this purpose, we have made an apparatus which is made of a glass chamber and a vacuum system. The apparatus is shown in Fig. 3. In Fig. 3, A is a glass chamber, which contains the sample liquid; V_1 and V_2 are vacuum tanks; T is a thermistor thermometer; P is a rotary vacuum pump; and C_1, C_2, ..., C_9 are glass vacuum valves. A and V_2 communicate through a glass tube G. V_3 is an air reservoir, and the expansion ratio in the chamber is adjusted by sending air repeatedly through V_3. The volumes of A, V_1, V_2, V_3 and other sections of the glass tubes are measured beforehand.

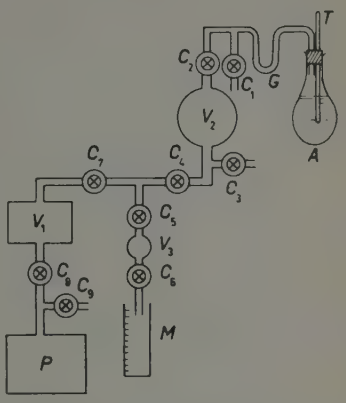

Fig. 3. – Block diagram of the whole arrangement of the expansion chamber system.

An operating cycle is as follows: namely, letting the valves C_1, C_3, C_5 be closed, and C_4 C_7, and C_8 open, then V_1 and V_2 are evacuated by the vacuum pump P. When the evacuation is finished, C_8 is closed and the sample, contained in A, is kept at a constant temperature at atmospheric pressure. After adjusting the expansion ratio by the above method, if the valve C_2 is opened, the air in the chamber expands freely, and hence, the applied pressure is suddenly reduced until the final pressure goes far below the equilibrium saturated vapor-pressure. That is, a highly superheated state can be obtained. The bubble formation, therefore, occurs.

It was expected by this process that for a given system the operating point would be found empirically by adjusting the temperature and the expansion rate until the desired sensitivity might be obtained. We have proceeded to repeat many times this cycle to determine the most favourable conditions. We have observed operating characteristics of several pure liquids and gas-liquid solutions. The results of this experiment are shown in Table III. The values given from column 3 to column 6 in Table III were measured by the present process. Column 2 shows the boiling point (t_0 °C) at atmospheric pressure; column 3 gives temperature (t_1 °C); column 4 final pressure (P mm-Hg) for obtaining sensitive condition; column 5 expansion ratio (R); and column 6 volume of the sample (V cm³) in the chamber A of Fig. 3. Moreover, in Fig. 1, the length of each vertical line gives the excess pressure drop during expansion in the chamber using a pure liquid; *i.e.*, the arrowhead of each vertical line indicates the final pressure after expansion of pure liquids. When a gas-liquid solution is used as a sample, superheat can be produced nearly above or below the saturated vapor pressure *vs.* temperature curves of pure liquid. Open circles in Fig. 1 show these points. By these empirical data, it is pointed out that the superheated condition can be produced even when the pre-

TABLE III. – *Operating characteristics of several liquids and gas-liquid solutions.*

Liquid, or solution	t_0 (°C)	t_1 (°C)	p (mm Hg)	R	V (cm³)
n-hexane (+CO_2)	57	19	69.2	11.0	250
n-hexane (pure)	68.7	30	43.6	17.4	362
Methyl alcohol (+CO_2)	32	19.5	66.0	11.7	3.0
Methyl alcohol (pure)	64.7	60	41.6	18.3	565
Acetone (pure)	56.1	55	70.1	10.8	335
Ethyl alcohol (+CO_2)	58	19	49.0	15.5	206
		22.5	51.4	14.8	180

expansion pressure is only atmospheric and when the reduced final pressure reached by expansion is only some fraction of one atmosphere. Namely, it may not be always necessary to prepare the special apparatus for applying pre-expansion pressure, because, in this case, the pre-expansion pressure is atmospheric.

As soon as the free expansion is allowed, the pressure in the chamber begins to reduce, and hence, the temperature lowers, since the evolution of vapor and the adiabatic expansion requires heat and, further, the formation of bubbles absorbs heat. The range of temperature drop is about 2 to 4 °C. The superheated state does not disappear instantly because the temperature decreases as much as this degree. Duration of the highly superheated state was about several seconds. During the duration of this state, if the liquid is imparted a mechanical shock, violent bubbles erupt in the liquid.

* * *

The author wishes to thank Prof. S. SHIMIZU of Kyoto University, Prof. Z. HASIMOTO and Prof. H. ENATSU for their advices and discussions of this and related problems.

RIASSUNTO (*)

Abbiamo determinato le zone sensibili di parecchi liquidi in una camera a bolle continuatamente sensibile. Queste zone sensibili vengono discusse basandosi sulle curve pressione di vapore saturo-temperatura dei liquidi usati nella camera. Abbiamo anche costruita una camera ad espansione di facile funzionamento, che lavora a bassa pressione riducendo la pressione nel liquido tramite una pressione di pre-espansione di una atmosfera. Esponiamo alcune sue caratteristiche quantitative.

(*) *Traduzione a cura della Redazione.*

SUPPLEMENTO AL VOLUME XIX, SERIE X
DEL NUOVO CIMENTO

N. 1, 1961
1° Trimestre

A Remark on the Detection of Events in Nuclear Emulsions.

C. J. WADDINGTON

H. H. Wills Physical Laboratory, University of Bristol - Bristol

(ricevuto il 21 Gennaio 1961)

Summary. — It is shown that the frequently used method of « rescanning » to determine the efficiency with which events have been detected in the course of a systematic search, may, under certain conditions, lead to seriously misleading conclusions.

Many experiments in cosmic ray physics involve the attempted detection of all the members of a specific class or type of event occuring in a given area or volume of nuclear emulsion. Typical examples are the number of nuclear interactions, « stars », produced in a certain volume, or the number of tracks having certain characteristics of density and length crossing a given area. The « scanning » of emulsions for such events forms the basis of all cosmic ray flux values determined with nuclear emulsions and of many of the comparisons of effects observed in different samples. Inevitably it is important to be able to determine the efficiency of this scanning, *i.e.* the probability each event has of being detected.

One suggested method of determining this probability of detection is to rescan the same area or volume, and to calculate the probability from a comparison of the results of the two scans. This method has been recently emphasized by LIM *et al.* [1] and seems to be strongly advocated by several other groups in this field. The purpose of this short note is to point out that this method can, under certain conditions, result in seriously misleading conclusions.

If *all* the events which are being considered have the same intrinsic pro-

(1) Y. K. LIM, J. E. LADY and V. D. HOPPER: *Supp. Nuovo Cimento*, **15**, 382 (1960).

bability of being detected, *i.e.* there are no systematic reasons why some should have a lower probability of detection than others, then the method of rescanning should be valid. For if there are in fact N events, each of which has a probability P of being detected in the first scan, then the number actually found, n, is

$$n = NP \tag{1}$$

and the number missed is $N - n = N(1 - P)$.

Then in a second scan, where the probability of detecting each event is P^*, the number of events detected which were missed in the first scan, $\Delta_{12}n$, will be

$$\Delta_{12}n = N(1 - P)P^* . \tag{2}$$

Similarly, the number of events found in the second scan, n^*, is

$$n^* = NP^* \tag{3}$$

and the number detected in the first scan but not in the second, $\Delta_{21}n$, is

$$\Delta_{21}n = N(1 - P^*)P . \tag{4}$$

Thus, from eq. (1)–(4)

$$P = 1 - \frac{\Delta_{12}n}{n^*} . \tag{5}$$

$$P^* = 1 - \frac{\Delta_{21}n}{n} . \tag{6}$$

Hence, in these conditions, both P, the probability of detection, and N, the true number of events can, in principle, be determined. In practice, however, the original assumption that all events have a similar probability of detection is rarely justified, and the above analysis is not valid. For example, in a scan for stars, the probability of detecting a star with many black and grey tracks is likely to be greater than that for a smaller star. Hence the events must be separated into more than one class.

Suppose there are N_1 events which have a detection probability of P_1, N_2 with P_2, etc., and that this separation cannot be made on the basis of *a priori* knowledge, then the average probability will be

$$\overline{P} = \frac{\sum_1^i N_i P_i}{\sum_1^i N_i} .$$

So the number of events actually found, v, will be

$$v = N_1P_1 + N_2P_2 + \ldots = \sum N_iP_i \tag{7}$$

and the number missed $\sum N_i - v = \sum N_i(1 - P_i)$.

Then in a second scan, where the probabilities of detection in each class of event become P_1^*, P_2^*, P_3^*, ..., the number of events detected which were missed in the first scan will be

$$\Delta_{12}v = \sum N_i(1 - P_i)P_i^* . \tag{8}$$

Similarly the number found in the second scan, v^*, will be

$$v^* = \sum N_iP_i^* \tag{9}$$

and the number found in the first scan but not in the second is

$$\Delta_{21}v = \sum N_i(1 - P_i^*)P_i . \tag{10}$$

Eq. (7)–(10) can only be solved explicitly for the values of P_i in the simplest case of two classes of events and under the assumption that P and P^* are equal.

Now experimentally, the values found by rescanning are those of v and Δv rather than of n and Δn. If these experimental values are used to calculate the probabilities from eq. (5) and (6), then this is equivalent to assuming that $\Delta_{12}n/n^*$ is equal to $\Delta_{12}v/v^*$, which is obviously false and can readily be seen to lead to an overestimate of the true probabilities. The magnitude of the error introduced depends on the specific values of N_i and P_i, but a simple numerical example will show that they can be serious. Consider a case where there are just two classes of events, and let $N_1 = N_2 = 100$, $P_1 = P_1^* = 1.0$ and $P_2 = P_2^* = 0.5$. Then $v = 150$ and $\Delta_{12}v = 25$, so P is calculated from equation (5) to be 0.833 compared with the true value, $\bar{P}$, of 0.75.

The checking of scanning efficiencies by rescanning may thus lead to serious errors, particularly since it gives an *upper* limit to the true value. In all cases where this method is used it is first necessary either to prove that there is only one class of events being considered, or to be able to separate the events into groups having unique detection probabilities. Obviously neither of these conditions are satisfied in any scan for stars. In particular it should be noted that stars cannot reasonably be separated into groups on a basis of their number of black and grey tracks. One or other of these conditions may be satisfied in scans for the tracks of particles such as α-particles or heavier nuclei, provided the data are carefully examined for the presence of any systematic losses by applying the usual tests on the length, depth and angular distributions. It should be remarked, however, that the observation of a value of

P near to 1.0 from eq. (5) in the case of a nearly, but not completely, homogeneous group is usually satisfactory as any error involved must be small. Rescanning is thus valuable if a homogeneous or nearly homogeneous sample of events is being considered and if the detection inefficiencies are small. Otherwise it may be misleading.

RIASSUNTO (*)

Si mostra che il metodo del « rescanning », usato frequentemente per determinare l'efficienza con cui gli eventi sono stati rilevati nel corso di una ricerca sistematica, può, in certe condizioni, portare a conclusioni che inducono in gravi errori.

(*) *Traduzione a cura della Redazione.*

SUPPLEMENTO AL VOLUME XIX, SERIE X
DEL NUOVO CIMENTO

N. 1, 1961
1° Trimestre

High-Velocity Range and Energy-Loss Measurements in Al, Cu, Pb, U and Emulsion.

W. H. BARKAS and S. VON FRIESEN (*)

Lawrence Radiation Laboratory, University of California - Berkeley

(ricevuto il 24 Gennaio 1961)

Summary. — Measurements were made of relative stopping powers of several materials in the proton energy intervals (750÷600) MeV, (600÷450) MeV, (450÷300) MeV and (750÷0) MeV. By collimation and magnetic analysis a « pencil beam » free of degraded particles was extracted from the 184 in. cyclotron. Using this beam in « good geometry » the stopping powers of Al, Pb, U and emulsion were measured relative to Cu. The total ranges yield the most accurate estimates of the mean excitation potentials. It is assumed that the mean excitation potential of Al is 163 eV, and that at 750 MeV substantially all the tight binding corrections required are those for the K and L shells. The mean excitation potentials in eV found with these assumptions are: copper, 323; lead, 826; uranium, 917; and emulsion, 328. The results from the differential stopping-power measurements are in general accord with these data. However, the agreement of the differential measurements with the theoretical ratios could be improved by raising the above mean excitation potentials of Al and Pb or by lowering those of copper, uranium and emulsion. This experiment confirms the general shape of the I/Z *vs* Z curve found by Bakker and Segrè, and when similarly normalized, is in reasonable absolute agreement. The status of the emulsion range-energy table is reviewed in the light of these and other relevant measurements. Incidental observations were made on the scattering, straggling and attenuation behavior of a highly collimated monoenergetic beam of protons which was brought to rest in a large block of copper.

(*) Permanent address: Department of Physics, University of Lund, Lund.

1. – Introduction.

The problem presented by the stopping of a charged particle in matter has intrinsic interest. It is also of considerable practical importance for deriving particle energies from range measurements.

Because the Bethe-Bloch theory of stopping is derived with an assumption that the particle velocity is large compared with the velocity of the atomic electrons, the approximate applicability of the theory at lower velocities is largely a matter of good fortune. At a certain low velocity, it breaks down completely. Moreover, there is no prescription for correcting the theory at the lowest velocities; at intermediate velocities only piecemeal and progressively less reliable theoretical procedures are available to correct for the tight-binding of the K shell, the L shell, the M shell, etc.

In the last few years the work of LINDHARD and SCHARFF [1] has held forth the promise of a formalism with a greater range of validity. Their theory extends the possibility of calculation to much lower velocities. It applies best to materials of high atomic number for which a statistical description of the electron density is valid. For these elements, the tenability of the Bethe-Bloch theory always has been questionable except at very high velocities. On the other hand, their formulation has not as yet the simple elegance of the Bethe-Bloch theory. A way has not been found to express the whole effect of the atom-dynamics by a single parameter such as the mean excitation potential. Accurate energy-loss calculations have not been attempted with this theory, although computations somewhat in the spirit of the Lindhard-Scharff theory have been made [2].

At relatively high velocities, the Bethe-Bloch theory, with small corrections, remains the most practical means for calculating energy-loss rates. Some of the current problems in connection with it are: *a*) how the shell corrections are to be made so that the mean excitation potential is velocity independent, and *b*) how this velocity-independent mean excitation potential depends on the atomic number.

Much of the range and energy-loss data from which the existing information is derived have been obtained at such low velocities that large tight-binding corrections are required, and the way in which these are to be made is somewhat obscure. This is especially true of the M shell and higher corrections.

---

[1] J. LINDHARD and M. SCHARFF: *Kgl. Danske Videbskab. Selskab, Mat.-fys. Medd.*, **27**, No. 15 (1953).

[2] W. BRANDT: *Energy Loss and Range of Charged Particles in Compounds*, du Pont Radiation Physics Laboratory Report (July, 1960).

[3] C. J. BAKKER and E. SEGRÈ; *Phys. Rev.*, **81**, 489 (1951).

For this reason, measurements at sufficiently high velocities for the shell effects to be small are best for defining the mean excitation potential.

Measurements by BAKKER and SEGRÈ [3] were made at a proton energy of ≈ 300 MeV, so that the shell effects were not large, and they were disregarded. Total range measurements for high proton velocities were made by MATHER and SEGRÈ [4]. The interpretation of these results has been uncertain because experiments at lower velocities [5] have tended to give higher corrected values for the mean excitation potentials than those resulting from the measurements of MATHER and SEGRÈ.

It has been suggested [6] as a possible explanation of this discrepancy that when the range is large, nuclear interaction effects become important, so that nuclear scattering as well as Coulomb scattering tends to shorten the projected range, (*i.e.*, the mean depth of penetration of charged particles which are incident normal to an absorber). When the range amounts to as much as one mean free path for a nuclear interaction, such an effect is expected already to be serious. Whereas the data of BAKKER and SEGRÈ should be relatively insensitive to this effect, it is thought that the results of MATHER and SEGRÈ are affected. They measured total ranges, and the geometry of their detector was such as to accept protons scattered through large angles. Only *relative* stopping powers were measured by BAKKER and SEGRÈ, so that raising or lowering of the mean excitation potential of Al to which their data was normalized, affects their derived excitation potentials. In addition, tight-binding effects should not be neglected altogether in calculating mean excitation potentials of heavy elements from their data.

To aid in resolving some of the existing problems regarding stopping powers, we thought it would be useful to carry out an experiment in which special care was exercised to eliminate known interfering effects. We have designed this experiment *a*) to use several proton energies all so high that shell corrections are small, *b*) to minimize scattering corrections by using a « good-geometry » experimental arrangement, *c*) to work with elements of both high and low atomic numbers, and *d*) to include materials for which absolute range-energy measurements or reliable theory exist up to high energies.

A difficulty in the employment of high particle velocities for the determination of the mean excitation potentials is that the energy-loss rate becomes insensitive to the mean excitation potential, and very good accuracy of measurement is demanded.

In this new experiment we have employed the proton beam of the 184 in.

---

(4) R. MATHER and E. SEGRÈ: *Phys. Rev.*, **84**, 191 (1951).

(5) For example H. BICHSEL, R. F. MOZLEY and W. A. ARON: *Phys. Rev.*, **105**, 1788 (1957).

(6) W. H. BARKAS: *Nuovo Cimento*, **8**, 201 (1958).

cyclotron to make measurements in « good geometry » of the relative stopping powers of Al, Cu, Pb, U and nuclear-research emulsion. The beam energy was known to be close to 750 MeV. Relative stopping powers in the energy intervals of (750÷600) MeV, (600÷450) MeV, (450÷300) MeV, and (750÷0) MeV were measured with errors that in most instances were some tenths of a percent. Emulsion was included in the experiment because in previous work (7) its absolute stopping behavior has been studied throughout this velocity interval. It was thought that it would provide a means, in addition to the range in aluminum, for absolute energy calibration, and the experiment would provide an over-all check of high-energy range curves.

2. – Apparatus.

The experiment was designed to utilize the external proton beam of the synchrocyclotron. Fig. 1 shows schematically the arrangement of the cyclotron and other pieces of equipment referred to below. The deflecting system, *D*, is of the regenerative type. The deflected beam, on reaching a cyclotron radius where the field was weak, passed through a pre-magnet collimator *C*-1,

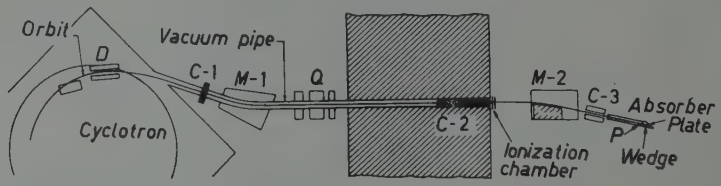

Fig. 1. – The 184 in. cyclotron proton beam. Features mentioned in the text are labeled.

and was subsequently bent by the steering magnet *M*-1 so as to be accurately parallel to the collimator *C*-2 through which it passed (with the aid of the quadrupole lens *Q*) into the experimental area beyond *C*-2.

The collimator *C*-2 was of brass 40 in. long. The aperture in it was a vertical 5/32 in. × 5/8 in. slit. From the collimator the beam emerged into the experimental area through a thin-walled ionization chamber by means of which the beam current was monitored. The beam then traverse about 3 feet of air before entering the field of an analyzing magnet, *M*-2 (magnet THOR) where it was bent through an angle of 11°. Precise adjustments of position, rotation and tilt of this magnet were necessary. The vertical clearance between the

(7) W. H. BARKAS, P. H. BARRETT, P. CÜER, H. HECKMAN, F. M. SMITH and H. K. TICHO: *Nuovo Cimento*, **8**, 91 (1958).

pole faces of magnet, M-2 was 5/32 in. The brass plate S, which filled the magnet aperture vertically, limited the beam on its low momentum side. The edge adjacent to the beam was cut in the arc of a circle. When the beam passed through the analysing magnet, the field was adjusted so that the point of maximum intensity of the beam followed a path with a radius of curvature about 1/8 in. greater than that of the edge of the brass plate. The plate therefore acted as a « scraper » which effectively eliminated degraded components of the beam which had insufficient momentum to clear it.

After the beam emerged from the analysing magnet most of its cross-section was contained in a circle of about 1/4 in. diameter, but owing to small angle scattering within the analysing magnet, a weak degraded « halo » surrounded the central core of the beam. This was eliminated by the lead collimator C-3, which was tailored to the cross-sectional structure of the beam so that none of the central core of the beam was intercepted but the « halo » was largely eliminated. The longitudinal dimension of this collimator, 15 in., was made greater than the range of the protons.

After emerging from C-3 the beam was considered to have met sufficiently stringent requirements, and was permitted to traverse absorbers, the energy losses in which were among the subjects of this investigation.

The absorbers were in the form of rectangular parallelopiped rods or bars. In cross-section they were 1 in. $\times$ 1 in. The protons traversed these bars longitudinally. This insured that if a proton were deflected through an appreciable scattering angle it would emerge from the side of the absorber and be eliminated from the beam. The emulsion absorbers were constructed by cutting out a large number of 1 in. $\times$ 1 in. squares of 600 μm Ilford G-5 emulsion which were taped into bars. At point P of Fig. 1 the beam entered a range analyser in the form of a wedge absorber with a nuclear track plate as the detector. The construction of this wedge analysing instrument is shown in Fig. 2. Except when the U wedge was used, the nuclear track plate was of 1 in. $\times$ 6 in.

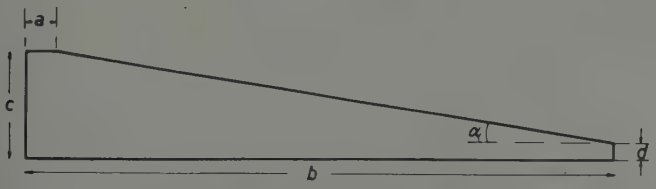

Fig. 2. – Shape of the wedge absorbers. The dimensions are given in Table I.

glass coated with Ilford C-2 emulsion, either 50 or 200 μm in thickness. With the U wedge, 1 in. $\times 1\frac{3}{8}$ in. plates were employed. Each plate was wrapped in black paper to exclude light, but care was taken to provide good contact between the emulsion coated face of the plate and the inclined surface of the

metal wedge. One end of the plate was made accurately flush with the tapered end of the wedge, as all measurements on the plate were to be taken with respect to this, the marked end of the plate.

The dimensions in millimeters of the wedges fabricated of the different metals are given in Table I.

TABLE I.

	a	*b*	*c*	*d*
Al	6.2	158.5	25.4	1.6
Cu	6.0	158.7	25.4	1.6
Pb	6.3	158.6	25.2	1.9
U	0	24.1	24.0	0.3

The lateral and vertical positioning of the wedge was established by finding the beam trajectory with no absorbers in position. The distance to the wedge, about 40 in. from the collimator *C*-3, was maintained for all exposures. This distance must be at least equal to the range of 750 MeV protons in Al (≈ 1 meter).

Absorbers I, II and III as listed in Table II were calculated to bring the proton energy down to about 300 MeV in three steps (750÷600) MeV. (600 ÷450) MeV, (450÷300) MeV. The remaining energy was to be expended in the copper wedge absorber described above. In addition the total range was

TABLE II. – *The absorbers used, the approximate energy interval they encompassed, and their measured copper equivalents in* g/cm².

Al Cu. Eq. Ratio	Pb Cu. Eq. Ratio	U Cu. Eq. Ratio	Em Cu. Eq. Ratio	Energy interval (MeV)
273.29 314.91 0.867 8	415.62 314.91 1.319 8	432.50 314.91 1.373 4		(750÷0)
79.01 89.90 0.878 9	118.73 90.20 1.316 2	121.53 89.68 1.355 2	94.644 94.20 1.002 6	I (750÷600)
71.47 81.27 0.879 4	108.71 82.32 1.320 5	111.49 82.10 1.358 0	85.831 85.26 1.006 7	II (600÷450)
61.34 69.67 0.880 4	93.67 70.76 1.323 8	94.60 68.86 1.373 8	73.346 72.61 1.010 1	III (450÷300)

found in the metals by providing absorbers plus wedges of the same material calculated to bring the particles to rest near the middle of the wedge. In

Table II these measured ranges are listed. The absorbers were supported by a light aluminum channel, and were located so that the center of each type of absorber, I, II, or III was maintained at the same position regardless of the material.

3. – Experimental procedure.

For an experiment such as this, it is important that the beam be monoenergetic, or at least that its structure be known. A preliminary investigation ([8]) was made, and it was found that the unanalysed beam coming through the collimator C-2 was complex, consisting of at least two components, B and B' emerging at a small angle with respect to each other. The mean range of B' was less than that of B by about 10%. The spread of ranges observed in B' was 2 or 3 times as large as that in B. The beams could also be resolved from each other by their time of emergence from the cyclotron. For analysing the temporal behavior of the beam, a scintillator was placed in the beam after it emerged from C-2.

While it would have been interesting to study this effect further, there was insufficient time allotted to the experiment for us to make a detailed investigation of the origin of the second beam, and we simply undertook to eliminate it.

The collimating slit C-1 is constructed so that the width and lateral position are adjustable. By reducing this slit-width to $\frac{1}{4}$ in. and varying its position, it was found that the relative intensity of beam B' was affected, and a position was found where its presence was not detected.

After the currents in quadrupole Q and, magnets M-1 and M-2 were optimized, regulating equipment maintained the fields constant to a few parts in 10^4. The currents in M-2 and Q were also personally monitored by the experimenters. The structure of the beam cross-section was studied at various points beyond where it emerged

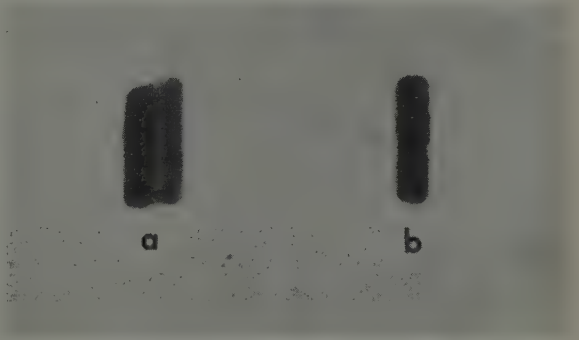

Fig. 3. – *a*) Beam structure at entrance to magnet M-2, before eliminating beam B'. *b*) Beam structure at entrance to magnet M-2, after eliminating beam B'.

([8]) S. von Friesen and W. H. Barkas: Lawrence Radiation Laboratory Report, UCID-613 (Jan., 1959).

from C-2. This was done with standard $1\frac{3}{16}$ in.$\times 1\frac{5}{8}$ in. films used in film badges for radiation monitoring. These could be exposed, developed, and fixed in a few minutes, and were very convenient for the purpose. Fig. 3*a* is the image recorded in this way of the double beam structure at the entrance to magnet M-2, and Fig. 3*b* is the image after B' was eliminated. Fig. 4*a* and 4*b* are similar prints that show the actual size of the beam at the entrance to C-3 and at the point where the beam reached the absorber.

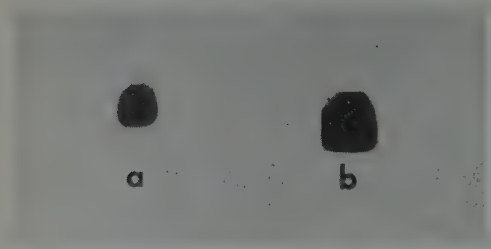

Fig. 4. – *a*) Contact print showing the actual size of the beam at the entrance to collimator C-3. *b*) Contact print showing the actual size of the beam as it entered the absorber.

As a supplement to this experiment the absorption, scattering, and straggling behavior of this highly collimated beam of protons was observed as it was stopped in a « semi-infinite » block of copper. These results are summarized in Appendix A.

Exposures were made as follows: To determine total ranges in Al, Cu, Pb, and U, absorbers and wedges of the same materials were placed in the beam. To determine relative differential stopping powers, exposures were made with these materials and emulsion absorbers successively placed in each position I, II, and III, while maintaining copper absorbers in all other positions. Each exposure was carried out twice, once with a detecting plate of 200 μm emulsion and once with a 50 μm plate. Interleaved with the other exposures, were 15 in which the absorber was copper alone. These exposures were made to give us an external measure of the beam stability and our measurement error.

The intensity of the exposure was determined by preliminary tests and an exposure of 1 minute at $4.5 \cdot 10^{-8}$ A measured at the entrance to the experimental area was adopted. This intensity turned out to be satisfactory except for the 50 μm emulsion exposure to obtain the total range in U. Only a small fraction of the beam intensity survived to this detecting plate. In 50 μm C-2 emulsion, the track segments of protons emerging from the U were badly scattered, and were very short so that only poor differentiation between beam protons and background was obtained. Fortunately, a good range spectrum was obtained from the 200 μm plates.

4. – Measurements.

The 50 μm plates were analysed at Berkeley and the independently exposed 200 μm plates were scanned in Lund. The 200 μm plates were of somewhat

better quality and were more completely analysed. The 50 μm plates were also carefully measured and served as a check on the 200 μm plates. In the final analysis double weight was assigned to the Lund plates. No serious discrepancies were found, however, so the weighting was of little importance.

The plates were examined under oil immersion with either 60× or 100× objectives. Each plates was scanned as follows: The plate was mounted on a microscope stage so that it could be translated along its longitudinal or x-axis, the amount of this translation being defined as x. It was possible to adjust the reading to be zero at the end of the plate that had been at the tapered end of the wedge. As x was increased from zero, first no tracks were seen, then a region in which protons were seen ending in the emulsion was passed. Scanning was not begun until a region of the emulsion was reached where proton endings again were not seen, but a flux of proton tracks directed generally along the x-axis was visible. The plate was then scanned by moving it so that the observer followed the tracks in the direction in which the particles were going; toward small values of x. Protons coming to rest in the emulsion were counted in each 1 mm or each ½ mm interval of x, and in a y-interval defined by limit lines in the microscope ocular. To be counted, the angle of entrance of a track into the emulsion was required to be less than 45° to the x-axis.

The tracks seen to terminate between $x = x_1$ mm and $x = x_1 + 1$ mm from the end of the plate were recorded as measuring the density of endings at $x = x_1 + \frac{1}{2}$ mm. More than one traversal of the plate was made if the intensity was low, but the scanning was confined to a narrow band along the long axis of the plate.

Because the plates were inclined at an angle, α, equal to arc $\mathrm{tg}[(c-d)/(b-a)]$, a correction was required for this inclination. The finite thickness of the emulsion and the thickness of the covering paper and tape was also included in the

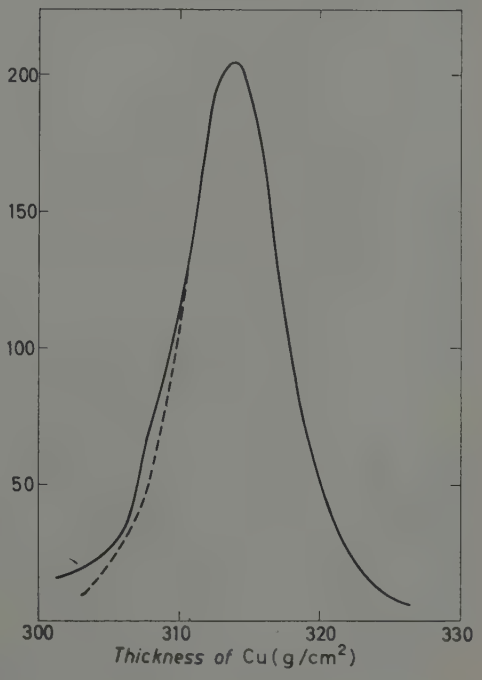

Fig. 5. – The range distribution of the beam in copper. The actual distribution is shown as a solid line. The dashed portion is symmetrical with the high energy side of the peak.

calculated stopping positions of the particles, after a mean value of x was found on each plate.

The range distribution derived from 7 exposures of 200 μm plates in which all-copper absorbers were used is shown in Fig. 5.

It will be noticed that an asymmetry exists in the peak, there being an excess of low energy particles. The « tail » is probably explainable as residue of beam B', to the presence in the beam of degraded particles from collimator scattering, and possibly to inelastic nuclear processes. Nevertheless this beam was regarded as « clean » enough for carrying out precise range measurements.

As a practical means for eliminating the effect of the low energy « tail » a preliminary range estimate was found. Then the parts of the spectrum extending beyond $\pm 2.5\%$ of this range were omitted in the final range average. As may be seen from Fig. 5 the straggling in range, arising from all causes, is hardly more than the theoretical range straggling, thus indicating that the beam energy remained constant, the scattering effects were small, and observer and instrumental errors did not seriously affect the data.

Numerous density measurements of the absorbers were made. The U absorbers were cut from pieces of density (18.848 ± 0.005) g/cm³, which was established by weighing and measuring the dimensions of pieces after their final accurate machining into the form of rectangular parallelopipeds. Measurements on the 5 pieces of lead gave densities of 11.324, 11.298, 11.305, 11.252, and 11.315 g/cm³. These differed enough so their individual densities were used. The density of the Al was determined to be (2.7852 ± 0.0017) g/cm³. The aluminum, however, was actually an alloy, # 2024, of nominal composition Al: 93.4%, Cu: 4.5%, Mn: 0.6%, and Mg: 1.5%. By chemical analysis the composition was determined to be Al: 93.62%, Cu: 4.57%, Mn: 0.44%, and Mg: 1.37%. The copper used had a density of (8.909 ± 0.001) g/cm³.

The path lengths in all the metal absorbers were measured with an accuracy an order of magnitude better than the densities could be determined and the systematic errors in the density measurements limit the ultimate accuracy obtainable. The emulsion bars, made up of 1 in. × 1 in. emulsion pellicles were carefully machined so as to have a square cross-section. The average area of 15 pellicles taken at random from the bars was $(0.9920 \pm \pm 0.001)$ square inches. The bars were also weighed, and the emulsion density was determined, by weighing in pure CCl_4 and in air, to be (3.853 ± 0.002) g/cm³. The weighing and density measurements were made immediately after use, and when in the form of bars, the emulsion was carefully taped to prevent water loss or gain by the emulsion.

5. – Scattering corrections to the measured ranges.

MATHER and SEGRÈ [4], and more recently, BICHSEL and UEHLING [9], estimated the range shortening caused by Coulomb scattering in the absorber. In the calculations of MATHER and SEGRÈ for high velocity particles, no restriction on the lateral displacement of the beam in traversing the absorber was made. As described above, to reduce the scattering correction, we limited this distance to about $\frac{1}{2}$ in. by using bars of 1 in. $\times$ 1 in square cross-section.

The beam traversed these longitudinally, and particles reaching the edge of the bar escaped so that their ranges were not measured. The particles that remained in the rod for its entire length traversed straighter paths, and the correction obviously is less for them than for particles with unrestricted paths. The geometry also insured that we need consider only small-angle Coulomb scattering. A large nuclear deflection would cause the particle to emerge from the side of the absorber. In order to get an estimate of the true range in this case, model calculations have been made by means of a Monte Carlo method. The Lund university electronic computer SMIL was used and the computations directed by Dr. C. E. FRÖBERG.

We have assumed the following model: Protons enter a square rod along its axis. The length of the rod equals the measured practical range of 750 MeV protons in the material. The cross-section of the rod is 1 in. $\times$ 1 in. We choose a scale where the length of the rods is 100 units. In the same units the widths of the different rods are:

$$\text{Al} = 2.52,\ \text{Cu} = 7.20,\ \text{Pb} = 6.96, \quad \text{and} \quad \text{U} = 11.12.$$

We divide the rods up into 102 cells of decreasing length in the following way:

Number	Length	Σ length
2	5	10
10	3	30
30	1	30
60	0.5	30
Sum 102		100

The particle which originally entered the rod on the axis and parallel to it, is deflected in the various cells and we assume in the following that it changes its direction discontinuously when passing from one cell to the next. We use

(9) H. BICHSEL and E. UEHLING: *Phys. Rev.*, **119**, 1670 (1960).

an orthogonal system of co-ordinates with the x-axis in the direction of the motion of the proton when entering the cell. According to eq. (2.17.6) in ROSSI's ([10]) book the probability of finding a particle which has travelled the distance x in the interval $(y, y+\mathrm{d}y)$ and with the direction between θ_y and $\theta_y+\mathrm{d}\theta_y$ is

$$P(x, y, \theta_y)\,\mathrm{d}y\,\mathrm{d}\theta_y = \frac{2\sqrt{3}}{\pi\theta_s^2 x^2}\exp\left[-\frac{4}{\theta_s^2}\left(\frac{\theta_y^2}{x}-\frac{3y\theta_y}{x^2}+\frac{3y^2}{x^3}\right)\right]\mathrm{d}y\,\mathrm{d}\theta_y\,.$$

One makes the change of variables (*): $x = 2\sigma^2/\theta_s^2$; $y = 2(\sigma^2/\theta_s^2)\vartheta_y$; $\theta_y = \chi_y + \frac{3}{2}\vartheta_y$, so that $\mathrm{d}y\,\mathrm{d}\theta_y = 2(\sigma^2/\theta_s^2)\,\mathrm{d}\vartheta_y\,\mathrm{d}\chi_y$. Then by direct substitution, the new distribution function is

$$Q(\sigma, \vartheta_y, \chi_y)\,\mathrm{d}\vartheta_y\,\mathrm{d}\chi_y = \frac{\exp\left[-3\vartheta_y^2/2\sigma^2\right]}{(2\pi\sigma^2/3)^{\frac{1}{2}}}\,\mathrm{d}\vartheta_y \cdot \frac{\exp\left[-2\chi_y^2/\sigma^2\right]}{(\pi\sigma^2/2)^{\frac{1}{2}}}\,\mathrm{d}\chi_y\,.$$

The variables ϑ_y and χ_y are independently normally distributed with variances of

$$\sigma_\vartheta^2 = \sigma^2/3 \qquad \text{and} \qquad \sigma_\chi^2 = \sigma^2/4\,.$$

For the different cells we choose ϑ_y and χ_y at random from normal distributions with the appropriate σ's. If we omit the index y, we get for the projection of the trajectory on the xy plane a series of values

$$\vartheta_1,\quad \chi_1,\quad \vartheta_2,\quad \chi_2,\quad \ldots.,\quad \vartheta_n,\quad \chi_n,\quad \ldots$$

From these we calculate the angle φ_n, which the projection makes with the x-axis in cell n and its direction of motion on entering cell n, given by angle ψ_n. We do the same for the projection on the xz plane. The value σ has been calculated for each cell from

$$\theta_s^2 = 16\pi N\frac{Z^2}{A}r_e^2\left(\frac{m_e c}{\beta p}\right)^2 \ln\left[196\,Z^{-\frac{1}{3}}(Z/A)^{\frac{1}{3}}\right] \quad \text{(ROSSI ([10]), 2.16.4)}.$$

We can now calculate the distance between the points where the particle enters and leaves the cell. In order to take into account the fact that the particle does not travel on a straight line but is scattered inside the cell we apply for each cell the appropriate correction α_n calculated according to MATHER and SEGRÈ ([4]).

([10]) B. ROSSI: *High-Energy Particles* (New York, 1952).

(*) We thank Dr. S. B. NILSSON, Lund, for advice in this matter.

When calculating the true range, SMIL starts in cell number one and goes along producing its own random numbers and using the corresponding values of σ_n and α_n.

As soon as a particle escapes from the rod through one of its side surfaces the calculation is broken off. The machine makes a new attempt, registering the number of the cell from which the escape took place. A supplementary condition has been that only particles, which reach the end of the rod at an angle of less than 45° to the axis shall be included. Nuclear scattering has not been taken into account. A cut-off at 3.3 standard deviations has been applied.

The results of the Monte Carlo calculations are

750 MeV *Proton range corrections.*

Element	Attempts	Successfull attempts	Ratio	Correction (%)
Al	1431	100	14.3 : 1	0.076 ± 0.003
Cu	1356	400	3.4 : 1	0.228 ± 0.005
Pb	2311	200	11.6 : 1	0.518 ± 0.013
U	983	200	4.9 : 1	0.696 ± 0.019

Fig. 6 shows the distribution of escaping particles along the copper rod, Fig. 7 shows the distribution of the individual range corrections.

Fig. 6. – Distribution of the distance from the point where the particle entered the copper rod to the point where it escaped. The distributions found for the other absorbers were similar.

In order to check the correctness of the calculations we also computed the correction for an infinitely wide copper rod and got the value $(0.458 \pm 0.013)\%$.

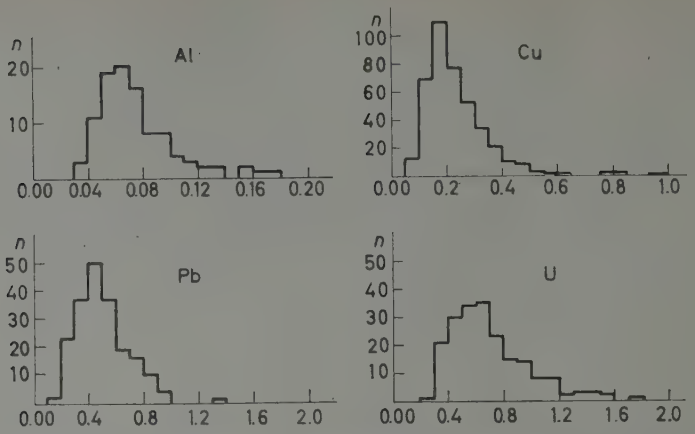

Fig. 7. – Distributions of range shortening caused by scattering. The range reduction is expressed in percent of mean range. The origin, which is labeled 100.00, is the point reached by an unscattered particle.

This agrees well with a value 0.45% obtained from Mather and Segrè's formula.

The corrected ranges measured in this experiment are given in Table II.

6. – The range straggling.

The distribution of proton endings in the plates was recorded. Owing to a small asymmetrical background, as shown in Fig. 5, the high energy side of the distribution was nearly gaussian, but the other side was slightly distorted. It was found that the straight line obtained from the high energy part of the curve when the data were plotted on « normal-distribution » graph paper gave reliable estimates of the apparent range straggling.

TABLE III. – *Range straggling effects. Standard deviations expressed in percent of mean range.*

	Al	Cu	Pb	U
Observed total	1.11	1.30	1.33	1.57
Scattering effect	0.03	.1	.2	0.25
Bohr straggling	0.95	0.99	1.06	1.08
Residue	0.58	0.83	.76	1.11

The percentage straggling is given in the first row of Table III. The second row lists what the standard deviation of the ranges would be were the sole straggling effect that caused by scattering. The third row is the Bohr straggling

as calculated by STERNHEIMER (11). The residue must be attributed to the energy dispersion of the primary beam, effects of energy losses to nuclei, inexact correction for scattering, and perhaps other unknown effects. While the statistical reliability of these data is not high, a range straggling of perhaps $(0.6 \div 0.8)\%$ could be assigned to energy dispersion of the beam. The extra straggling in uranium may have statistical significance.

In spite of the large thicknesses of matter traversed by these protons, the straggling does not show any clear influence of nuclear collisions. An interaction causing nuclear excitation generally is a catastrophic event leading to a substantial loss of energy, and one in which the particle is normally deflected out of the good-geometry beam.

7. – Stopping power results.

What we obtained in this experiment were the mass stopping powers, for several energy intervals, of Al, Pb, U and emulsion relative to copper. The total ranges in Al, Cu, Pb and U were also observed. The proton energy was known only insofar as it can be inferred from these ranges.

In Table II we have listed each absorber and its observed copper equivalent. These figures enable us to calculate the mass stopping powers relative to copper. Because we have also measured Al/Cu and emulsion/Cu ratios all our results can almost as well be related to Al or emulsion. The ranges in the aluminum alloy have been converted to range in pure aluminum using Bakker and Segrè's relative stopping powers. The emulsion absorbers have also been adjusted to the equivalent absorber of standard emulsion having a density of 3.815 g/cm³, assuming that the density change was caused by loss of moisture (7).

In Table II the measurement uncertainties are not given separately for each entry because the situation, as explained below, is rather complicated. Each measurement consisted of the determination of a range either in a pure material or in a two-component absorber. To find the statistical error in this part of the measurement, we referred to the numerous measurements of the range in pure copper that were carried out alternately with other runs. These ranges have a standard deviation of 0.09 g/cm² for a single determination.

In addition, there are small uncertainties in the density measurements, as discussed above. Probably additional errors were introduced because the geometry of the experiment could not be made precisely the same for the various absorbers. They were not all of the same size. Finally, the scattering correction is only approximate. The typical error in measurement, therefore, is perhaps ≈ 0.2 g/cm² of copper.

(11) R. STERNHEIMER: *Phys. Rev.*, **117**, 1621 (1690).

dence from the experimental data for a velocity-dependent systematic error, however.

The magnitude of the discrepancy can be illustrated by the ratios for emulsion. If emulsion is compared with Al through the ratios of Al to Cu and emulsion to Cu, we find that the emulsion mean excitation potential would have to be reduced to 304 eV for agreement. On the other hand, raising the mean excitation potential of Al to 178 eV also would bring about agreement.

The Al to emulsion ratio obtained in this way is subject to a number of errors and may represent an extreme fluctuation. It could be caused by small errors in more than one measurement that have in this case been additive.

As reported in a preliminary account of this experiment ([17]) our data generally confirm the shape of the I/Z *vs.* Z curve found by BAKKER and SEGRÈ. Their data, of course, are to be normalized to $I_{Al} = 163$ eV. Whereas $I/Z = 12.5$ for Al, we find that it falls to 11 for copper and to 10 for lead and uranium.

9. – Remarks on the emulsion standard.

Because it is much needed for measurements of reaction and disintegration energies of elementary particles, the range-energy relation in emulsion has assumed a special importance. It is the only material in which *absolute momentum* and range measurements have been made at velocities as high as those of this experiment ([7]).

Other measurements, including this one, rely on the theoretical extrapolation of low-energy measurements for an absolute standard. Particle ranges measured in emulsion, while beset with certain special problems, also have an advantage in being free of the scattering error. The range is simply the visible length of the particle path in emulsion, and is easily rectified.

This experiment relates the stopping power of emulsion to that of copper in three velocity intervals. These three ratios, which are independent of each other, do not confirm well the measurements of HEINZ ([18]) at a lower velocity. At a proton energy which we now believe to have been 336.7 MeV, he measured an emulsion/copper range ratio of $0.990 \pm .003$. On the other hand, at 208 MeV DECARVALHO and FRIEDMAN ([19]) found the ratio to be 1.005 ± 0.006, in agreement with what would be expected from our data. If we take the value 323 eV, derived above, for the mean excitation potential of copper with Walske's corrections, then our emulsion stopping power ratios to copper give for emulsion a mean excitation potential of 328 eV, in excellent agreement

([17]) S. VON FRIESEN and W. H. BARKAS: *Bull. Am. Phys. Soc.*, **4**, 369 (1959).
([18]) O. HEINZ: *Phys. Rev.*, **94**, 1728 (1954).
([19]) H. G. DE CARVALHO and J. I. FRIEDMAN: *Rev. Sci. Inst.*, **26**, 261 (1955).

with the value of 331 eV implied by the absolute range-momentum measurements ([6]).

In emulsion, a number of systematic effects can be introduced in the measurement of track-lengths. Corrections were made for them in establishing the range-energy relation ([7]). They include, for example, the track-length lost between pellicles, and the distortion caused by compression of emulsion. Such effects do not enter as corrections in this experiment. It was recommended in connection with the emulsion range table ([6]), that the method of applying corrections be the same as that used in measuring the ranges of BARKAS *et al.* ([7]). Systematic errors then are not introduced in tracing particle tracks through the emulsion. When compared with the ranges measured in this experiment, however, systematic differences still can enter. All the corrections made in ref. ([7]) were in the direction to increase their tabulated range. It is possible, if there remains a measurable systematic error, that it may be one of overcorrection; that the tabulated emulsion ranges may be too long when compared with ranges measured by the method of this experiment or by track-tracing without applying corrections.

To study this possibility, we shall review the relevant published measurements.

The ranges of meson secondaries from K-meson decay were measured in a number of researches ([20-23]). With the present best values of the masses of K, π and μ-mesons ([24]), the expected ranges are 11.86 cm and 20.96 cm, respectively, for the $K_{\pi 2}$ and $K_{\mu 2}$ modes. The weighted averages adjusted for emulsion density, but not including all the corrections employed in preparing the range table, are (11.72 ± 0.05) and (20.81 ± 0.08) cm. The correction for radiative decay, which tends to lower the measured ranges also has not been made. The differences here are 1.2 and 0.7%.

A test was made of the range tables at very high energies by FELDMAN ([25]). For pions with an energy equivalent to protons of 1600 MeV, she measured a range that was (1.005 ± 0.010) times that given by the emulsion range table.

FRIEDLANDER *et al.* ([26]) made direct comparisons of emulsion with alu-

([20]) D. M. RITSON, A. PEVSNER, C. S. FUNG, M. WIDGOFF, G. T. ZORN, S. GOLDHABER and G. GOLDHABER: *Phys. Rev.*, **101**, 1085 (1956).

([21]) R. W. BIRGE, D. H. PERKINS, J. R. PETERSON, D. H. STORK and M. N. WHITEHEAD: *Nuovo Cimento*, **4**, 834 (1956).

([22]) G. STACK COLLABORATION: *Nuovo Cimento Suppl.*, **4**, 398 (1956).

([23]) J. CRUSSARD, V. FOUCHÉ, G. KAYAS, L. LEPRINCE RINGUET, D. MORELLET, F. RENARD and J. TREMBLEY: *Nuovo Cimento Suppl.*, **3**, 373, 616 (1956).

([24]) W. H. BARKAS and A. H. ROSENFELD: *UCRL*-8030, Revised (Sept., 1960).

([25]) R. FELDMAN: Lawrence Radiation Laboratory Report, *UCRL*-3802 (1957).

([26]) M. W. FRIEDLANDER, D. KEEFER and M. G. K. MENON: *Nuovo Cimento*, **5**, 461 (1957).

minum at velocities somewhat lower than those of our experiment. For protons of nominal energy 146.5 MeV, they measured a median range of (60.13 ± 0.20) mm in emulsion of density (3.791 ± 0.004) g/cm³. When aluminum absorbers of 6.080 5 g/cm² and 11.486 4 g/cm² were successively placed in the beam the ranges in emulsion were reduced to (41.42 ± 0.17) and (25.18 ± 0.21) mm, respectively. These measurements did not include adequate scattering corrections, and total ranges are therefore subject to doubt. Differential energy loss measurements are not sensitive to them, however, and we can deduce Al/emulsion ratios as follows from their paper:

$$(146.5 \div 84.4)\ \text{MeV} \qquad .866\,9 \pm 0.006\,9\ ,$$

$$(146.5 \div 117.9)\ \text{MeV} \qquad .857 \pm 0.012\ .$$

From the shell-corrected Al ranges, and the emulsion range table, these ratios are expected to be 0.847 and 0.849, respectively. Agreement could be reached by reducing the mean excitation potential of emulsion to (307 ± 10) eV.

The mass of the Σ^+-hyperon is best determined from the reaction $\Sigma^+ \to p + \pi^0$. The range of the proton is in an interval where the range-energy relation is thought to be well known. The pion range of the alternate mode of decay $\Sigma^+ \to n + \pi^+$ has been measured ([27]). It is $(9.248\,4 \pm 0.049)$ cm. Using the mass of the Σ^+-hyperon found from the proton decay mode, the pion range is expected to be 9.317 5 cm. Again the measured range is low by about $\frac{3}{4}$ percent. The radiation correction, which has not been made, would tend to reduce the measured range below this predicted value.

Recently ZRELOV and STOLETOV ([28]) measured the range of 658 MeV protons in copper using an experimental arrangement very similar to that of MATHER and SEGRÈ. They found a range of (257.6 ± 1.2) g/cm². From this range they obtain a mean excitation potential for copper of (305 ± 10) eV. Using the same data, with Bichsel's table we obtain (309 ± 11) eV. No allowance for a density-effect correction was made in deriving this figure, although according to STERNHEIMER ([29]) a small effect exists. While they did not make the measurement in « good geometry » this appears to be an excellent measurement. It must be taken as further evidence that the mean excitation potential of copper (and emulsion which is tied to it by our measurements) is somewhat lower than our total range measurement would indicate.

([27]) J. N. DYER, W. H. BARKAS, H. H. HECKMAN, C. J. MASON, N. A. NICHOLS and F. M. SMITH: *Bull. Amer. Phys. Soc.*, **5**, 224 (1960). For more details see J. D. DYER: *UCRL*-9450.

([28]) V. P. ZRELOV and G. D. STOLETOV: *Sov. Phys. JETP*, **36** (9), 461 (1959).

([29]) R. STERNHEIMER: *Phys. Rev.*, **58**, 854 (1952).

In spite of the excellent accord we found in our total range measurements, these various pieces of evidence lead us to believe that the emulsion range table overestimates high-velocity ranges by perhaps $\frac{1}{2}$ %.

* * *

In carrying out this experiment we were aided by the helpful co-operation of the cyclotron crew under JAMES T. VALE. To Dr. C. E. FRÖBERG and Mrs. K. KJÄLLQUIST we are indebted for the SMIL calculations. Mr. J. C. WELLS helped both with microscopy and calculations, and EUGENE H. HUFFMAN made the chemical analysis of the aluminum alloy. The scanning of the emulsion that recorded the protons penetrating the large copper absorber was carried out by Mr. L. ENOS. S.v.F. would like to thank the Lawrence Radiation Laboratory for the generous hospitality shown to him and the Royal Physiographie Society of Lund for financial support. We are most grateful to Dr. H. BICHSEL for the use of his range tables.

APPENDIX

The « pencil beam » prepared for the range experiment was studied in some detail as it was brought to rest in a large copper block. Emulsion layers embedded in the copper were used as detectors so that the lateral spreading, angular distribution, and range distribution were obtained. For scanning this emulsion we are indebted to Mr. L. T. ENOS.

The observations may be summarized as follows: as the beam traversed the copper it was scattered and attenuated. The mean attenuation cross-section of the copper nucleus was found to be $7.2 \cdot 10^{-25}$ cm^2. The range on the beam axis was $(314.9 \pm .3)$ g/cm^2. The range straggling was 2.94 g/cm^2 when measured on the axis. The mean depth of penetration diminished with distance from the beam axis, apparently in a roughly linearly way so that the range 5 cm off the axis was reduced by 3.6 g/cm^2. The straggling of these off-axis protons was increased perhaps 40 % also. The spreading of the beam can be crudely described as follows: let $\varrho_{1/2}$, $\varrho_{1/10}$ and $\varrho_{1/30}$ be the distances

TABLE VI.

S (g/cm^2)	$\varrho_{\frac{1}{2}}$ (cm)	$\varrho_{1/10}$ (cm)	$\varrho_{1/30}$ (cm)
68.8	0.28	0.52	0.7
114.5	0.42	0.82	1.1
188.3	0.80	1.6	2.1
275.5	1.7	3.4	5.1

from the axis where the density of the beam is reduced respectively to $\frac{1}{2}$, $\frac{1}{10}$, and $\frac{1}{30}$ of that on the axis. Then as the beam penetrated the copper these distances increased with the depth of penetration, S, according to Table VI.

The median projected angle made by the beam particles with the axis varied linearly with the distance off the axis. It amounted to 3° per cm at a depth of penetration of 296 g/cm², where the width of the beam was near maximum. The projected angular distribution of the beam at this depth of penetration had a standard deviation of 5.0° on the beam axis and increased to 11° at a point 5 cm off the axis. It remained nearly flat for about 2 cm on either side of the axis.

The full details of these observations are too lengthy for presentation here. More information can be obtained from one of us (WHB).

RIASSUNTO (*)

Abbiamo eseguito la misura del potere relativo d'arresto di alcuni materiali entro gli intervalli di energia dei protoni (750÷600) MeV, (600÷450) MeV, (450÷300) MeV e (750÷0) MeV. Mediante collimazione ed analisi magnetica, abbiamo estratto dal ciclotrone di 184 in. un « pennello » privo di particelle degradate. Usando questo fascio in « buona geometria », abbiamo misurato il potere d'arresto dell'Al, del Pb, dell'U e dell'emulsione, relativamente al Cu. I percorsi totali forniscono le stime più accurate dei potenziali medi di eccitazione. Si suppone che il potenziale medio di eccitazione dell'Al sia 163 eV, e che a 750 MeV tutte le richieste correzioni di legame stretto siano sostanzialmente quelle per gli strati K ed L. I potenziali medi di eccitazione in eV, trovati in base a queste supposizioni, sono: rame, 323; piombo, 826; uranio, 917; emulsione, 328. I risultati, dedotti dalle misure del potere d'arresto differenziale, sono generalmente in accordo con questi dati. Comunque l'accordo fra le misure differenziali ed i rapporti teorici può essere migliorato elevando i suddetti potenziali medi di eccitazione dell'Al e del Pb od abbassando quelli del rame, dell'uranio e dell'emulsione. Questo esperimento conferma la forma complessiva della curva I/Z in funzione di Z trovata da Bakker e Segrè, che, analogamente normalizzata, concorda in modo ragionevolmente assoluto. Alla luce di queste e di altre importanti misure abbiamo riveduto la composizione della tabella percorso-energia. Incidentalmente abbiamo eseguito delle osservazioni su comportamento di scattering, straggling ed attenuazione di un fascio monoenergetico di protoni, fortemente collimato, che venne fatto arrestare in un grosso blocco di rame.

(*) *Traduzione a cura della Redazione.*

SUPPLEMENTO AL VOLUME XIX, SERIE X
DEL NUOVO CIMENTO

N. 1, 1961
I° Trimestre

Camera di ionizzazione a pareti spesse per misurazione di intensità di radiazioni γ di energia fino a 100 MeV.

G. BUSSETTI

Istituto di Fisica dell'Università - Torino
Istituto Nazionale di Fisica Nucleare - Sezione di Torino

(ricevuto il 23 Febbraio 1961)

Riassunto. — Si descrive una camera di ionizzazione a pareti spesse in alluminio adatta per la misurazione dell'intensità della radiazione γ di un sincrotrone fino a 100 MeV. Si dà l'intensità della radiazione γ di data frequenza in funzione dell'intensità di corrente della camera. Il calcolo tiene conto degli effetti dei fotoni primari del fascio incidente e dei fotoni Compton secondari prodottisi nelle pareti (1).

1. – Schematicamente la nostra camera di ionizzazione si compone (Fig. 1) di un cilindro di alluminio di raggio $b = 5$ cm. Sull'asse, alla profondità X, vi è una piccola cavità contenente un elettrodo. Il fascio di raggi γ di cui si vuol misurare l'intensità incide sulla faccia frontale CC' di area πb^2. Misurando la corrente i fra l'elettrodo ed il corpo della camera si risale alla potenza incidente $I_0(k_0)\cdot\pi b^2$ mediante le relazioni date più avanti. Si suppone che il fascio di fotoni monocromatici di energia $k_0 = h\nu_0$ sia uniforme in tutta la sua sezione ed abbia intensità $I_0(k_0)$.

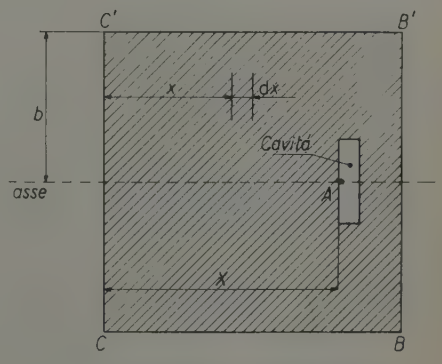

Fig. 1. – Sezione della camera.

Chiamiamo $w = w(k_0, b, X)$ la potenza di ionizzazione per unità di volume,

(1) Una camera abbastanza simile alla nostra ma adatta per misurazioni soltanto fino a 25 MeV è stata costruita da B. H. FLOWERS, J. D. LAWSON e E. B. FOSSEY: *Phys. Soc.*, B **65**, 286 (1952).

cioè l'energia che fu assorbita dal fascio per unità di tempo e di volume per ionizzare entro l'alluminio. Poniamo

$$I_0(k_0)\cdot\pi b^2\cdot S_0(k_0, b, X) = w(k_0, b, X) \tag{1}$$

e chiamiamo $S_0(k_0, b, X)$ sensitività della camera per i fotoni $k_0 = h\nu_0$.

Abbiamo calcolato S_0 in funzione di k_0 fino a $k_0 = 100$ MeV, per $X = 7$ cm, ed $X = 10$ cm, ($b = 5$ cm).

Però w viene misurato nell'aria, nella piccola cavità di volume V, anzichè nell'alluminio, ma com'è noto si ha [2]

$$\frac{w_{\text{Al}}}{w_{\text{aria}}} = \frac{(\mathrm{d}T/\mathrm{d}s)^{(\text{ionizz})}_{\text{Al}}}{(\mathrm{d}T/\mathrm{d}s)^{(\text{ionizz})}_{\text{aria}}}, \tag{2}$$

dove $(\mathrm{d}T/\mathrm{d}s)^{(\text{ionizz})}$ è la perdita di energia per unità di lunghezza subita da un elettrone per ionizzare [3]. Nel calcolo del secondo membro della (2) si sono presi degli opportuni valori medi per tener conto che gli elettroni prodotti da un fotone k_0 hanno diverse energie. Supposto che l'energia necessaria per formare una coppia di ioni nell'aria sia 35 eV, abbiamo ottenuto

$$\pi b^2\cdot I_0(k_0) = \frac{1}{S_0(k_0)}\left[\frac{(\mathrm{d}T/\mathrm{d}s)^{(\text{ion})}_{\text{Al}}}{(\mathrm{d}T/\mathrm{d}s)^{(\text{ion})}_{\text{aria}}}\right]_{\text{medio}}\cdot 2{,}185\cdot 10^{14}\cdot\frac{i}{V}, \tag{3}$$

se si misura la potenza incidente $\pi b^2\cdot I_0$ in $\mathrm{MeV}\cdot\mathrm{s}^{-1}$, la corrente i in ampere, e il volume della cavità V in cm^4. Dovendosi determinare la potenza totale $\int I_0(k)\,\mathrm{d}k$ di tutto lo spettro $\psi(k)$ della radiazione di rallentamento emessa da un sincrotrone, si prenderà il valor medio di S_0

$$\bar{S}_0 = \frac{\int\psi(k)\cdot S_0(k)\,\mathrm{d}k}{\int\psi(k)\,\mathrm{d}k}. \tag{4}$$

Abbiamo calcolato $S_0(k_0, b, X)$ tenendo conto della geometria della camera e ponendo $S_0 = S_1 + S_2$, essendo S_1 e S_2 i contributi alla sensitività rispettivamente dei fotoni primari del fascio collimato e di quelli Compton generati dai primari.

([2]) Vedi R. D. Evans: *The Atomic Nucleus* (New York, 1955), p. 723.

([3]) Vedere la formula (52) nell'articolo H. A. Bethe e J. Ashkin, in E. Segrè: *Experimental Nuclear Physics*, vol. 1 (New York, 1953).

([4]) R. R. Wilson: *Phys. Rev.*, **84**, 100 (1951); vedere anche a p. 268 dell'opera citata nella nota precedente.

([5]) R. M. Sternheimer: *Phys. Rev.*, **103**, 511 (1956).

Le Fig. 2 e 3 riportano la sensibilità $S_0(k_0)$ ed il rapporto S_1/S_2 in funzione dell'energia k_0 dei fotoni incidenti.

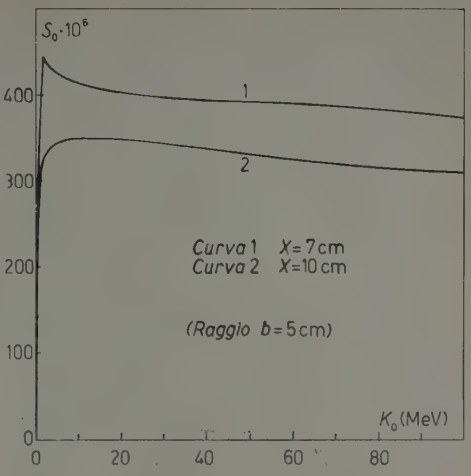

Fig. 2. – Sensitività totale moltiplicata per 10^6.

Una camera di ionizzazione dello stesso tipo ma con cavità grande, avente sezione uguale a quella del fascio incidente, è stata costruita e tarata da J. S. PRUITT e S. R. DOMEN (6). Tale Dural Chamber ha il convertitore antecedente la cavità spesso circa 9.4 cm. Con uno spettro di bremsstrahlung avente l'energia massima di 100 MeV, la risposta è circa $4.36 \cdot 10^{-19}$ coulomb/MeV.

Per un confronto grossolano, abbiamo calcolato la risposta della nostra camera supponendo che la cavità avesse le dimensioni di quelle della Dural Chamber, utilizzando i nostri risultati per $X = 10$ cm, usando la (5) con uno spettro di bremsstrahlung calcolato per un bersaglio di platino di un sincro-

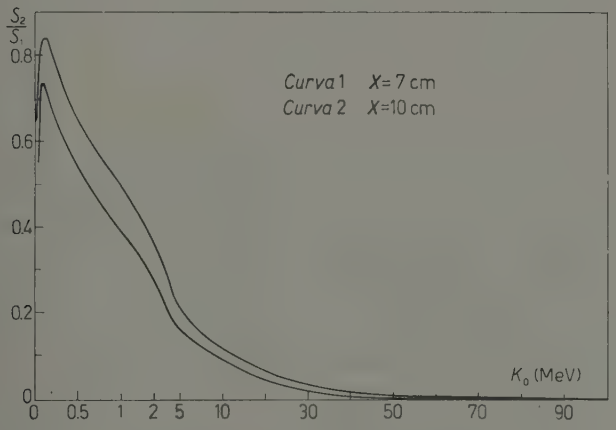

Fig. 3. – Rapporto fra le sensitività prima e seconda.

trone operante a 100 MeV, ed abbiamo trovato che la analoga risposta vale $3.41 \cdot 10^{-19}$ coulomb/MeV. La differenza fra i due valori è accettabile consi-

(6) J. S. PRUITT and S. R. DOMEN: N. B. S. Report no. 6218 (Washington, 1958).

cioè l'energia che fu assorbita dal fascio per unità di tempo e di volume per ionizzare entro l'alluminio. Poniamo

$$I_0(k_0)\cdot\pi b^2\cdot S_0(k_0, b, X) = w(k_0, b, X) \tag{1}$$

e chiamiamo $S_0(k_0, b, X)$ sensitività della camera per i fotoni $k_0 = h\nu_0$.

Abbiamo calcolato S_0 in funzione di k_0 fino a $k_0 = 100$ MeV, per $X = 7$ cm, ed $X = 10$ cm, ($b = 5$ cm).

Però w viene misurato nell'aria, nella piccola cavità di volume V, anzichè nell'alluminio, ma com'è noto si ha [2]

$$\frac{w_{\text{Al}}}{w_{\text{aria}}} = \frac{(\mathrm{d}T/\mathrm{d}s)^{(\text{ionizz})}_{\text{Al}}}{(\mathrm{d}T/\mathrm{d}s)^{(\text{ionizz})}_{\text{aria}}}, \tag{2}$$

dove $(\mathrm{d}T/\mathrm{d}s)^{(\text{ionizz})}$ è la perdita di energia per unità di lunghezza subita da un elettrone per ionizzare [3]. Nel calcolo del secondo membro della (2) si sono presi degli opportuni valori medi per tener conto che gli elettroni prodotti da un fotone k_0 hanno diverse energie. Supposto che l'energia necessaria per formare una coppia di ioni nell'aria sia 35 eV, abbiamo ottenuto

$$\pi b^2\cdot I_0(k_0) = \frac{1}{S_0(k_0)}\left[\frac{(\mathrm{d}T/\mathrm{d}s)^{(\text{ion})}_{\text{Al}}}{(\mathrm{d}T/\mathrm{d}s)^{(\text{ion})}_{\text{aria}}}\right]_{\text{medio}}\cdot 2{,}185\cdot 10^{14}\cdot\frac{i}{V}, \tag{3}$$

se si misura la potenza incidente $\pi b^2\cdot I_0$ in $\mathrm{MeV}\cdot\mathrm{s}^{-1}$, la corrente i in ampere, e il volume della cavità V in cm^4. Dovendosi determinare la potenza totale $\int I_0(k)\,\mathrm{d}k$ di tutto lo spettro $\psi(k)$ della radiazione di rallentamento emessa da un sincrotrone, si prenderà il valor medio di S_0

$$\bar{S}_0 = \frac{\int\psi(k)\cdot S_0(k)\,\mathrm{d}k}{\int\psi(k)\,\mathrm{d}k}. \tag{4}$$

Abbiamo calcolato $S_0(k_0, b, X)$ tenendo conto della geometria della camera e ponendo $S_0 = S_1 + S_2$, essendo S_1 e S_2 i contributi alla sensitività rispettivamente dei fotoni primari del fascio collimato e di quelli Compton generati dai primari.

([2]) Vedi R. D. Evans: *The Atomic Nucleus* (New York, 1955), p. 723.

([3]) Vedere la formula (52) nell'articolo H. A. Bethe e J. Ashkin, in E. Segrè: *Experimental Nuclear Physics*, vol. **1** (New York, 1953).

([4]) R. R. Wilson: *Phys. Rev.*, **84**, 100 (1951); vedere anche a p. 268 dell'opera citata nella nota precedente.

([5]) R. M. Sternheimer: *Phys. Rev.*, **103**, 511 (1956).

Le Fig. 2 e 3 riportano la sensibilità $S_0(k_0)$ ed il rapporto S_1/S_2 in funzione dell'energia k_0 dei fotoni incidenti.

Una camera di ionizzazione dello stesso tipo ma con cavità grande, avente sezione uguale a quella del fascio incidente, è stata costruita e tarata da J. S. PRUITT e S. R. DOMEN [6]. Tale Dural Chamber ha il convertitore antecedente la cavità spesso circa 9.4 cm. Con uno spettro di bremsstrahlung avente l'energia massima di 100 MeV, la risposta è circa $4.36 \cdot 10^{-19}$ coulomb/MeV.

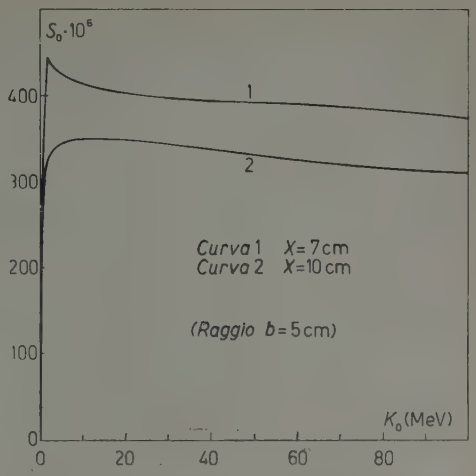

Fig. 2. – Sensitività totale moltiplicata per 10^6.

Per un confronto grossolano, abbiamo calcolato la risposta della nostra camera supponendo che la cavità avesse le dimensioni di quelle della Dural Chamber, utilizzando i nostri risultati per $X = 10$ cm, usando la (5) con uno spettro di bremsstrahlung calcolato per un bersaglio di platino di un sincro-

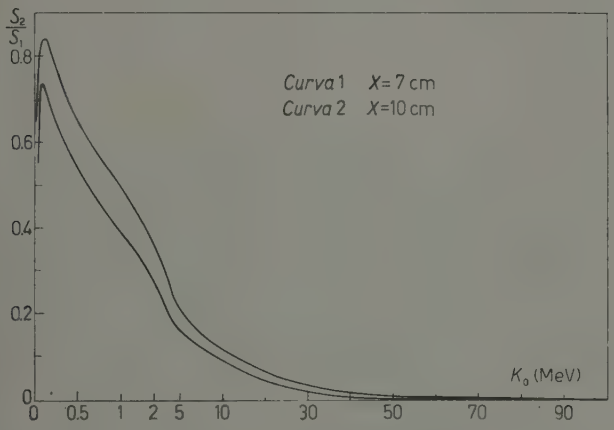

Fig. 3. – Rapporto fra le sensitività prima e seconda.

trone operante a 100 MeV, ed abbiamo trovato che la analoga risposta vale $3.41 \cdot 10^{-19}$ coulomb/MeV. La differenza fra i due valori è accettabile consi-

(6) J. S. PRUITT and S. R. DOMEN: N. B. S. Report no. 6218 (Washington, 1958).

derando la diversa geometria e tenendo conto dei vari effetti secondari non considerati nelle formule, e dell'approssimazione contenuta nelle relazioni utilizzate per i calcoli numerici relativi ai vari fenomeni entranti in guioco.

* * *

Ringrazio il prof. R. Malvano per le discussioni sull'argomento.

SUMMARY

An aluminium thick-walled ionisation chamber suitable for measuring the radiation intensity from syncrotrons and betatrons operating at energies up to 100 MeV is described. Curves giving the chamber sensitivity for γ-radiation of given frequency as function of the current in the chamber are reported. In the calculation the effects of the secondary Compton photons produced in the walls from the incident beam have been considered.

SUPPLEMENTO AL VOLUME XIX, SERIE X
DEL NUOVO CIMENTO

N. 1, 1961
1° Trimestre

Some Notes on Thermonuclear Reactors.

G. MARTELLI (*)

Physics Department, The University of Birmingham - Birmingham

(ricevuto il 27 Febbraio 1961)

Summary. — This article is based on the second part of a series of lectures for postgraduate students in this University, and assumes a knowledge of the elementary principles of plasma physics. It is aimed to give both a description of the present achievements in this field and some critical discussion of the principles involved in the various types of machines. Constructional details of the devices mentioned in the article can be found in the references.

I. – Introduction.

1. – Any thermonuclear reactor with a net power gain, using magnetic confinement, must satisfy certain general requirements. First, the rate of energy release, which is proportional to $n^2v\sigma$ (where n is the number of ionized particles, v their velocity and σ the effective nuclear cross-section) must exceed the rate of energy loss from the plasma. The main process which causes such a loss, is the bremsstrahlung from electrons colliding with ions, which is also proportional to n^2 and increases with temperature as $T^{\frac{1}{2}}$. Therefore a critical temperature exists below which the bremsstrahlung predominates and a thermonuclear reaction with a net energy release becomes impossible. For the deuterium-tritium mixture this temperature is 4 keV ($\sim 4 \cdot 10^7$ °C) and for pure deuterium 35 keV [1]. Another important limitation to the permis-

(*) On leave of absence from the University of Pisa (Italy).

[1] D. N. ZUBARIEV and V. N. KLIMOV: *Plasma Physics and the Problem of Controlled Thermonuclear Reactions*, edited by M. A. LEONTOVICH, English translation (London and New York, 1959-60), vol. 1, p. 302.

sible range of temperatures is imposed by the so-called « magnetic radiation » of the electrons in a magnetic field (²). The rate of magnetic radiation is proportional to nTH^2 or, allowing that $nT = H^2/8\pi$, to n^2T^2. According to the original calculations of B. A. TRUBNIKOV, the presence of such radiation limits the use of the deuterium-tritium mixture to the temperature range from 7 to 45 keV (for $T_e = T_i$ and $H = 10$ kG), whilst the reaction in pure deuterium turns out not to be self-sustaining, unless special precautions are taken for the self-absorption of the magnetic radiation in the plasma. The losses due to magnetic radiation can also be decreased by the use of cusped geometry, or by the so-called « picket-fence » system, where the magnetic field inside the plasma volume is kept small. Recently R. DRUMMOND and M. ROSENBLUTH found errors in Trubnikov's calculations which lead to overestimating of losses (³) (*).

There is obviously a large number of additional processes which lead to energy loss from plasma. They are, for instance, radiation of exited atoms and ions of impurities having high Z values, acceleration of considerable numbers of plasma ions and electrons by electric field up to energies exceeding the plasma temperature, etc. These additional losses impose further limitation on the useful range of plasma temperatures.

2. – There are two main methods of obtaining a hot plasma. The first one consists in ionizing a cold gas and then raising its temperature to the thermonuclear range. It is doubtful, however, whether Joule heating can create temperatures higher than a million degrees or so, for plasma resistance decreases rapidly with increasing temperature. Nevertheless, some other ways of heating are possible as, for instance, adiabatic compression, resonance heating and shock heating.

The second method consists in the accumulation of « hot » particles inside a trap, until they build up a plasma. This accumulation must be accompanied by some irreversible process, such as a change of the magnetic field during the injection, dissociation or break-up of injected particles, change of the energy of the particles, etc.

Recently J. L. TUCK has proposed the so-called « entropy-trapping » for a

---

(²) B. A. TRUBNIKOV and A. E. BAZHDANOVA: *Plasma Physics and the Problem of Controlled Thermonuclear Reactions*, edited by M. A. LEONTOVICH, English translation (London and New York, 1959-1960), vol. **3**, p. 249.

(³) J. DRUMMOND and M. ROSENBLUTH: *Physics of Fluids*, **3**, 45 (1960).

(*) The results obtained by these authors differ from those obtained by TRUBNIKOV only for one particular case ($\beta = 1$). They reach the conclusion that the method employed by TRUBNIKOV is substantially correct (see also: *Applied Atomics*, **218**, 12, where the results of these authors have been published first).

hot plasma injection into a magnetic trap [4]. If the pressure ϱv^2 of the plasma jet exceeds that of the magnetic field $H^2/8\pi$, the jet penetrates the field forming a kind of « diamagnetic » channel. Individual particles are reflected from the channel walls and, when reaching a region of weaker magnetic field, spread out across the whole volume of the trap, thus randomising the initial velocity. Hence it is impossible for a particle to escape through the magnetic field at some other place. The rate of return of particles back into the channel (if the injection lasts continuously) is not certain, but should be comparable with the rate of escape of particles from the trap in other ways. In this case the mechanism of confinement is also based on an irreversible process, *i.e.* on the increase of entropy of the system by randomising the motion of the plasma particles. Experiments have shown that the plasma is trapped in the cusped geometry with an efficiency of 10 %, provided the injection is performed through the magnetic mirror and remains confined there for a period of some hundreds of μs at least, with a density of 10^6 cm^{-4} [5].

More recently TUCK has suggested another mechanism for confining plasmas in a volume with a weak magnetic field, the boundary surface between plasma and containing field having everywhere positive curvature. The device, called Helixion, should produce a chain of regions along the axis of an open torus, where the field generated by an external helical winding is weakened by the currents induced in an internal levitating helical conductor [6].

3. – The second condition which a self-sustaining thermonuclear reactor must satisfy is that the released energy should exceed the energy supplied to produce the hot plasma:

$$\frac{1}{2} n^2 \langle \sigma v \rangle Q t \geqslant \frac{3}{2} nT \,, \tag{1}$$

where t is the period of confinement of the particles in the trap, Q is the rate of energy generation, and the angle brackets indicate averaging over the distribution of ions velocities [7].

With the help of the relation $nT = H^2/8\pi$, one finds

$$H^2 t \geqslant A \,, \tag{2}$$

where $A \sim 10^{10}$ for the d-d reaction (this figure is taken for the temperature

---

[4] J. L. TUCK: *Phys. Rev. Lett.*, **3**, 313 (1959); *Proc. of the Fourth International Conference on Ionization Phenomena in Gases* (Uppsala, 17-21 August 1959) (Amsterdam), vol. **2**, p. 926.

[5] J. L. TUCK: loc. cit.

[6] J. L. TUCK: *Nature*, **187**, 863 (1960).

[7] S. I. BRAGINSKY and V. D. SAFRANOV: *Proc. of the Second United Nations International Conference on the Peaceful Uses of Atomic Energy*, (Geneva, 1958), vol. **31** p. 45.

of 50 keV, where $T^2/\langle\sigma v\rangle$ has its minimum value); for the d-t reaction $A \sim 10^8$ (for $T = 15$ keV). It follows that the pulsed operation is hardly suitable for achieving thermonuclear reactions of economic interest, because too strong a magnetic field would be required. Because of the limits imposed by the mechanical strength of the metal, it is impossible to build up magnetic fields stronger than 10^6 G (for copper this limit is $3 \cdot 10^5$ G). Nevertheless, it is possible to get a net power gain even in unstabilised pinch discharges, where instabilities grow in times of the order of microseconds, but the magnetic field is developed by currents flowing through the plasma. On the basis of reasonable assumptions, the characteristics of such a pinch can be calculated, provided that the temperature is raised during the first compression up to 10 keV and condition (2) is satisfied with t larger than the relaxation time of the ions. Some typical figures for such a device could be: the voltage across the tube: 3 MV; the tube radius: 3 m; the tube length: 6 cm; the initial density: $2 \cdot 10^{18}$ cm^{-3}. This gives an energy imput of about 10^9 joule per unit length of pinch, equivalent to the explosion of a ton of TNT ([8]) (*).

At present there is a widespread belief that reactors of economic interest can be designed only on the basis of a steady-state or quasi-stationary device, and hence the achievement of long periods of plasma confinement in traps (as well as the suppression of instabilities) is generally considered an essential requirement for the control of thermonuclear reactors, and most laboratories have orientated their efforts on such a line of research.

However, suggestions have been made recently that if long term confinement cannot be achieved, fusion reactors where the plasma is not confined or only marginally confined, could still be operated ([9]). The mechanism in this case could be compared to that of a miniature laboratory-controlled H-bomb, where a magnetically driven plasma shell would generate the interacting plasma column and the power output would be absorbed by the laboratory apparatus (**). No experimental proof of the feasibility of this type

---

([8]) See, for instance, R. Latham and J. Nation: *Nuclear Instruments and Methods*, **4**, 261 (1959).

(*) Many figures and reactor dimensions in particular depend on the assumptions made and can be determined but very roughly. The main conclusion drawn from all the estimates is that the energy input for an economical thermonuc ear reaction should be $(10^8 \div 10^9)$ joules per unit length of discharge, which is equivalent to a heavy explosion.

([9]) J. G. Linhart: *Nuovo Cimento*, **17**, 850 (1960). On this problem see also W. M. Elsasser: *Magnetohydrodynamics*, (Edit. R. K. M. Landshoff, Stanford 1957) p. 27.

(**) The use of H-bombs for controlled production of energy has also been considered; see, for instance, E. Teller: *Proc. of the Second United Nations International Conference on the Peaceful Uses of Atomic Energy*, (Geneva, 1958), vol. **31** p. 32.

of reactor has been published, and it is not yet clear whether such an explosive reactor could be used in practice.

It should also be pointed out that in the above estimate the value $\beta = 8\pi nT/H^2$ has been assumed to be unity, while in practice conditions for hydromagnetic stability require $\beta < 1$, and this makes the requirements for the design of a thermonuclear reactor much more complicated.

Almost all thermonuclear devices now in operation are pulsed. Although they are not designed to provide a net power gain from fusion, they are used and will be used to help better understanding both of the ways of formation of hot plasmas and of the processes occurring in them.

In the following pages a brief review of the progress in different fields is given.

II. – Stabilized pinch discharges.

4. – Useful information concerning stable magnetohydrodynamic states and the mechanism of energy loss from plasma has been obtained by the study of stabilized pinch discharges.

Instabilities occurring in the ordinary pinch discharge (« sausages », kinks, corkscrews) can be suppressed by an external longitudinal magnetic field and using metal sheeting around the discharge chamber. Two mechanisms of stabilization can then occur. First, when $H_z > H_\varphi$ (where H_φ is the self-magnetic field of the discharge) the stabilizing field is not trapped by the plasma. But in this case the corkscrews instabilities with wave length $\lambda = a(H_z/H_\varphi)$, where a is the radius of the column, are not completely suppressed.

In the second case a thin sheet of electric current is formed around the plasma. Owing to the presence of the self-magnetic field, it contracts onwards, traps the longitudinal field and compresses it until a pressure balance is reached. The stability conditions can be worked out essentially on the basis of the hypothesis one can make on the shape of the current sheet. In the case of a sheet with diffused boundaries, which is of practical interest, there exists the Suydam condition [10]

$$\frac{8\pi}{H_z^2}\left(\frac{\mathrm{d}p}{\mathrm{d}r}\right) + \frac{1}{4} r \left(\frac{1}{m}\frac{\mathrm{d}m}{\mathrm{d}r}\right)^2 > 0 \,, \tag{3}$$

where $m = H_\varphi/rH_z$. This condition is necessary, but so far has not been proved to be sufficient.

([10]) B. R. SUYDAM: *Proc. of the Second United Nations International Conference on the Peaceful Uses of Atomic Energy* (Geneva, 1958), vol. **31** p. 157.

It should be pointed out that stability is affected also by the way in which a certain magnetohydrodynamic configuration is built up. The inertial forces, for instance, produced during a fast plasma column contraction, may generate oscillations of the plasma which might otherwise be in a steady state, and can even destroy stability.

The duration of the stabilizing action of the longitudinal magnetic field is determined by the time of diffusion of H_z and H_φ into the plasma. This time is of the order of $2 \cdot 10^{-7} T^{\frac{3}{2}} L^2$ s, where T is the temperature in eV and L the plasma dimensions in cm ([11]).

The image currents induced in the plasma because of the diffusion, supply additional heating. The duration of the stabilizing action of the metal sheet is to be determined in the same way.

5. – Experimental data on the stabilized pinch discharge are fairly extensive. In the Columbus *S*-4 experiment ([12]) (linear pinch discharge) the formation of the current sheet has been traced. Magnetic probe measurements have shown that the Suydam condition is not maintained here, and that 3 μs later small scale oscillations of the order of centimeters begin in the outer surface of the sheet. Macroscopic (hydrodynamic) stability has been observed in many stabilized toroidal pinch discharges. In the Perhapsatron *S*-4 experiment ([13]) the period of stability of the plasma column is estimated to be (30÷50) μs, whereas in « Zeta » it is about 100 μs. In the latter case the current sheet is absent and the current flows uniformly through the cross-section of the whole column ([14]).

Some very interesting results have been achieved in the tubular pinch experiment, where the plasma is compressed into a sheet between two concentric conducting cylinders, through which the return current flows. Such geometry can be related easily to the plane case, which is interesting for the following reasons. It is known from the theory that if the vector normal to the interface between the plasma and the vacuum (magnetic field volume) is

---

([11]) S. I. Braginsky and V. D. Safranov: *Plasma Physics and the Problem of Controlled Thermonuclear Reactions*, edited by M. A. Leontovich, English translation (London and New York, 1959-1960), vol. **2** p. 39.

([12]) L. C. Burkhard and R. N. Lovberg: *Proc. of the Second United Nations International Conference on the Peaceful Uses of Atomic Energy* (Geneva, 1958), vol. **32** p. 29; J. L. Tuck: *Proc. of the Fourth International Conference on Ionization Phenomena in Gases* (Uppsala, 17-21 August 1959), (Amsterdam), vol. **2** p. 921.

([13]) J. P. Conner *et al.*: *Proc. of the Second United Nations International Conference on the Peaceful Uses of Atomic Energy* (Geneva, 1958), vol. **32** p. 297; J. L. Tuck: *Proc. of the Fourth International Conference on Ionization Phenomena in Gases* (Uppsala, 17-21 August 1959), (Amsterdam), vol. **2** p. 920.

([14]) P. B. Butt *et al.*: *Proc. of the Second United Nations International Conference on the Peaceful Uses of Atomic Energy* (Geneva, 1958), vol. **32** p. 42.

directed outwards from the plasma (as in the case of the pinch discharge), the whole magnetic system is unstable, whereas in the opposite case (cusped geometries) the system is stable. The plane plasma sheet has neutral stability. In the Triax experiment ([15]) a stable plasma sheet is formed, which is confined between magnetic fields H_φ of opposite polarities. Inertial oscillations do not destroy the stable state and disappear within 8-10 periods. It is not excluded, however, that instabilities might subsequently occur, possibly of electrostatic nature. Such instabilities are associated with plasma oscillations and lead to neutron production. This has been proved by further work of COLGATE ([16]) who has modified tubular devices. In the hard-core pinch experiment, the current flows through concentric conductors and creates the initial field H_φ. A longitudinal magnetic field H_z can also be developed, and by adjusting the strength of these fields and the value of the discharge current, COLGATE has obtained distributions of magnetic fields and plasma which are stable from a hydrodynamic point of view. Microinstabilities observed during these experiments are not of magnetohydrodynamic nature and seem to be of electrostatic origin.

In order to reduce the influence of electrodes, some experiments have been carried out in a toroidal chamber, where the hard-core ring current is levitated by image currents (Levitron) ([17]).

6. – The temperature reached in the pinch experiments has been estimated to be $(100 \div 150)$ eV for unstabilized discharges. There are two possible ways of measuring the temperature. The electron temperature may be determined from the electrical conductivity of the discharge. The sum of the electron and ion temperatures may be found by measuring the magnetic field patterns and using the relation $H^2/8\pi = nT$. In this case the energy due to turbulence of the plasma should also be taken into account.

In stabilized discharges electron temperatures up to some tens of eV are achieved; in toroidal discharges the velocity of the mass motion of the ions corresponds to some hundreds of eV. It should be noted that a sharp in-

([15]) O. A. ANDERSON *et al.*: *Proc. of the Second United Nations International Conference on the Peaceful Uses of Atomic Energy* (Geneva, 1958), vol. **32** p. 151; for the problem of the stability in these geometries see M. ROSENBLUTH: *Proc. of the Second United Nations International Conference on the Peaceful Uses of Atomic Energy* (Geneva, 1958), vol. **31** p. 90.

([16]) D. H. BIRDSALL and S. A. COLGATE: *Proc. of the Fourth International Conference on Ionization Phenomena in Gases* (Uppsala, 17-21 August 1958), (Amsterdam), vol. 2 p. 888 and 892. See also D. H. BIRDSALL, S. A. COLGATE and H. P. FURTH: U.C.R.L. Report 5599 and 5602 (abstracted in *Nucl. Sci. Abstracts*, **13**, 22, 2685 and 2686, abstracts no. 20012 and 20013).

([17]) D. H. BIRDSALL *et al.*: *Proc. of the Fourth International Conference on Ionization Phenomena in Gases* (Uppsala, 17-21 August 1959), (Amsterdam), vol. 2 p. 893.

crease of the input energy does not result in a rise of the temperature of the particles. In the Perhapsatron *S*-4 experiment the input energy is 5 500 eV per particle, but the electron temperature does not exceed (10÷15) eV. This fact indicates that a considerable amount of energy is lost from the plasma mainly because of the escape of fast particles to the walls and electrodes (in the case of linear pinch discharges). In stabilized pinch discharges the temperature cannot be raised higher than about 50 eV. From this point of view the Triax experiment is more suitable: the absence of longitudinal magnetic fields makes it more difficult for the particles to escape to the electrodes.

The other mechanism responsible for energy losses from the plasma is the ultraviolet radiation of ions and atoms of impurities. V. D. KIRILLOV has shown that almost all the energy released in plasma during ohmic heating may be lost because of this radiation, even if impurities are of the order of some parts of a percent ([18]).

7. – In toroidal discharges the so-called runaway electrons may constitute a serious drawback ([19]). In electric fields higher than the critical value of about $10^{-13}\, n/T$ V/cm, electrons are accelerated until they escape through the confining magnetic field. COLGATE has pointed out that in some cases runaway electrons accelerated up to (3÷5) keV transfer the largest part of their energy to the walls ([20]). Their escape results from the non-uniformity of the confining field. With the loss of a large number of electrons the plasma ceases to be neutral and this, in turn, results in the excitation of plasma oscillations. Runaway electrons can form beams that also excite oscillations which lead to extremely high diffusion of particles across the magnetic field lines, thereby destroying the confining action of the magnetic fields. In some experiments γ-rays from runaway electrons, with energy up to some MeV, have been detected ([21]).

Almost in every case the production of neutrons is associated with the presence of a small number of deuterons, accelerated up to (10÷20) keV. In

([18]) V. D. KIRILLOV: *Žurn. Tekh. Fiz. Akad. Nauk USSR*, **30**, 320 (1960).

([19]) See, for instance, H. DREICER: *Proc. of the Second United Nations International Conference on the Peaceful Uses of Atomic Energy* (Geneva, 1958), vol. **31** p. 57; and J. A. WESSON: *Proc. of the Fourth International Conference on Ionization Phenomena in Gases* (Uppsala, 17-21 August 1956), (Amsterdam), vol. **2** p. 648.

([20]) Loc. cit.

([21]) V. S. STRELKOV: *Plasma Physics and the Problem of Controlled Thermonuclear Reactions*, edited by M. A. LEONTOVICH, English translation, (London and New York, 1959-1960), vol. **4** p. 161; R. BERNSTEIN *et al.*: *Proc. of the Second United Nations International Conference on the Peaceful Uses of Atomic Energy* (Geneva, 1958), vol. **32** p. 210.

unstabilized discharges they originate from local high-voltage gradients caused by « sausage » type of instabilities. The reason for deuterium acceleration in stabilized toroidal discharges is not quite clear, as runaway ions should not be expected at these energies. In some cases the mechanism of neutron production is also not clear ([22]) and might perhaps be of a nature different from those discussed above.

8. – Of particular interest is the so-called « θ-mode pinch », where the compression of the pre-ionized (and some time shock-heated) plasma takes place because of the fast build up of the axial magnetic field. In this way, azimuthal image currents centred at the axis of symmetry, are induced in the plasma. In order to prevent particle loss at the ends of the discharge tube, the magnetic field at the end is increased, *i.e.* magnetic mirrors are used ([23]).

If the plasma temperature is sufficiently high, *i.e.* if the conductivity is high, the plasma sheet at the fast implosion must trap the magnetic field existing in the volume occupied before the compression. Various experiments have shown that the plasma configuration is stable ([24]), provided the trapped and confining fields are directed in opposite directions.

In particular, in the Scylla experiment ([25]) neutrons have been observed. They have been supposed to be of thermonuclear origin, because no asymmetry has been found in their production. From X-ray measurements, the electron temperature has been estimated to be 200 eV. From spectroscopic measurements and from the energy spectrum of the d-d reaction products the ion temperature has been evaluated to be 1300 eV. It is not clear, however,

([22]) O. A. Anderson *et al.*: *Proc. of the Second United Nations International Conference on the Peaceful Uses of Atomic Energy* (Geneva, 1958), vol. **32** p. 150; W. R. Baker and S. A. Colgate: *Proc. of the Second United Nations International Conference on the Peaceful Uses of Atomic Energy* (Geneva, 1958), vol. **32** p. 125.

([23]) See, for instance, R. F. Post: *Proc. of the Fourth International Conference on Ionization Phenomena in Gases* (Uppsala, 17-21 August 1959), (Amsterdam), vol. **2** p. 987, and following articles.

([24]) S. A. Colgate: *Nucleonics*, **10**, 82 (1959); A. C. Kolb: *Proc. of the Fourth International Conference on Ionization Phenomena in Gases* (Uppsala, 17-21 August 1959), (Amsterdam), vol. **2** p. 1021; A. C. Kolb, H. R. Greim and W. R. Faust: *Proc. of the Fourth International Conference on Ionization Phenomena in Gases* (Uppsala, 17-21 August 1959), (Amsterdam), vol. **2** p. 1037; H. A. Bodin *et al.*: *Proc. of the Fourth International Conference on Ionisation Phenomena in Gases* (Uppsala, 17-21 August 1959), (Amsterdam), vol. **2** p. 1061; T. S. Green: *Phys. Rev. Lett*, **5**, 297 (1960).

([25]) W. F. Elmore *et al.*: *Proc. of the Second United Nations International Conference on the Peaceful Uses of Atomic Energy* (Geneva, 1958), vol. **32** p. 337; F. L. Ribe: *Proc. of the Fourth International Conference on Ionization Phenomena in Gases* (Uppsala, 17-21 August 1959), (Amsterdam), vol. **2** p. 1032; J. L. Tuck: *Proc. of the Fourth International Conference on Ionization Phenomena in Gases* (Uppsala, 17-21 August 1959), (Amsterdam), vol. **2** p. 923.

why the intensity of the X-rays in the Scylla experiments is approximately 400 times higher that would be expected from the plasma temperature and density, and from the duration of the stable state, which is about 10 μs. This fact might perhaps be explained if a large contribution to the X-rays came from impurities in the plasma.

In Kolb's experiment ([26]) the duration of the stable state is 10 μs. Radial oscillations do not disturb stability and therefore they do not lead to neutron production, but just modulate the neutron flux. The electron temperature has been estimated to be 800 eV, and the ion temperature about 2 keV. KOLB does not assert that the observed neutrons are of thermonuclear origin, because the reverse field diffusion through the plasma causes large electric fields that produce γ-rays with energies up to 2 MeV. However, he hopes to achieve plasma temperatures of 5 keV by increasing the length of the discharge tube from 30 cm to 3 m, and by increasing the power of the condenser bank.

III. – The stellarator ([27]).

9. – The models of stellarators existing at present are used to study non turbulent confined plasma (as opposite to plasma in pinch discharges). The confinement of individual particles in stellarators has proved to be quite satisfactory. Plasma confinement, however, has proved so far to be rather poor, although devices have been built where plasma shows good hydromagnetic stability. Electrons have been observed to escape across the magnetic lines of force, the diffusion coefficient being proportional to $H^{-\frac{1}{2}}$. Low frequency oscillations, limited to the cm region, have also been observed. All these processes take place during the plasma heating by electric currents. The electric field applied to the plasma produces a large number of runaway electrons. As it has already been mentioned, the presence of these electrons can give rise to instabilities of electrostatic nature and in stellarators this might lead to an abnormally high rate of particles loss from the plasma.

Techniques for achieving ultrahigh vacuum ($10^{-9} \div 10^{-10}$ mm Hg) have been developed in order to reduce impurities in the stellarator chamber. A special device, which reduces by a factor from 5 to 10 the number of impurity atoms ejected from the walls into the discharge has also been developed (divertor) ([28]).

([26]) A. O. KOLB: *Proc. of the Fourth International Conference on Ionization Phenomena in Gases* (Uppsala, 17-21 August 1959), (Amsterdam), vol. **2** p. 1037; R. A. ELLIS *et al.*: *Proc. of the Fourth International Conference on Ionization Phenomena in Gases* (Uppsala, 17-21 August 1959), (Amsterdam), vol. **2** p. 1129.

([27]) L. SPITZER jr.: *Proc. of the Second United Nations International Conference on the Peaceful Uses of Atomic Energy* (Geneva, 1958), vol. **32** p. 181.

([28]) C. R. BURNETT *et al.*: *Proc. of the Second United Nations International Conference on the Peaceful Uses of Atomic Energy* (Geneva, 1958), vol. **32**p. 225.

Recent experiments have shown that the best results can be obtained by vacuum training the chamber, *i.e.* by sharply increasing the pulse repetition frequency.

10. – As it has already been mentioned, ohmic heating does not achieve high temperatures. Methods of high frequency heating of the plasma in stellarators are now being developed ([29]). The plasma is alternatively compressed and expanded adiabatically, by means of a rapidly alternating magnetic field, as if by a sort of magnetic pumping action. To get the plasma heated by this method, the occurrence of irreversible processes is necessary, such as transfer of the energy of the particles from one degree of freedom to others, or escape of the particles from the region where the heating occurs within a time shorter than the period of the high frequency magnetic field.

It is possible to heat the ions only if the frequency of the field is close to the cyclotron frequency eH/Mc of rotation of the ions in the stellarator magnetic field. At present such research work is being carried out by T. H. Stix and his co-workers ([30]). Although all existing models are quasi-stationary, the stellarator might operate on a continuous basis, and could be a possible prototype of future thermonuclear reactors. To ensure good hydromagnetic stability, the values of β should be of the order of 0.1.

At present, the main task in this field seems to be the achievement of a steady hot plasma. This might require new ways of damping the oscillations, since they not only make the plasma escape to the walls, but do not allow the heating currents to be increased up to the theoretical Kruskal limit ([31]). If difficulties encountered in ohmic heating of the plasma are not overcome, it may be necessary to abandont his method altogether, and inject fast particles into the stellarator. In particular, it should be possible to use entropy trapping in the stellarator chambers.

IV. – The magnetic mirror approach.

11. – The confining action of magnetic mirrors is based on the conservation of the magnetic moment of charged particles in a magnetic field. Magnetic moment is only an approximate (adiabatic) invariant, and changes slowly if

---

([29]) L. Spitzer jr.: loc. cit.

([30]) T. H. Stix and R. W. Palladino: *Proc. of the Second United Nations International Conference on the Peaceful Uses of Atomic Energy* (Geneva, 1958), vol. **34** p. 282.

([31]) M. D. Kruskal *et al.*: *Proc. of the Second United Nations International Conference on the Peaceful Uses of Atomic Energy* (Geneva, 1958), vol. **32** p. 217; R. A. Ellis, L. P. Goldberg and J. G. Gormann: *Physics of Fluids*, **3**, 468 (1960).

the condition $\varrho/R \ll 1$ is not fulfilled (where ϱ is the Larmor radius of the particles and R the radius of curvature of the lines of force of the magnetic field). For magnetic mirrors this condition is usually not very strictly satisfied, and it can occur that during the time required for a thermonuclear reaction to take place, the magnetic moment changes, and particles escape from the trap before they have a chance to react. Experiments have been carried out with the purpose of investigating the behaviour of β-particles from tritium in magnetic mirrors ([32]). These experiments have shown that the magnetic moment does not change after 10^7 reflections at the mirrors, and that the life-time of electrons in the trap exceeds 100 μs. Similar results have been obtained from the experimental data of operation Argus ([33]) (high altitude nuclear explosions) as well as from experiments where positrons with some hundreds of keV have been confined in a trap (about 10^8 reflections have been detected: the life-time was approximately one second). S. N. Rodionov has performed experiments with tritium to investigate the dependence of the life-time of the particles in the trap on the magnetic field characteristics ([34]). The results are in good agreement with Budker's equation

$$t \sim \frac{m^{-\frac{1}{2}} T^{\frac{3}{2}}}{n Z^2 e^4 l p L} f(g) . \tag{4}$$

where $g = H_{\max}/H_{\min}$ is the mirror ratio and $f(g) \sim \ln g/2$ for large values of g. In these experiments information has been obtained on the behaviour of the individual particles rather than on the plasma as a whole.

As far as plasma confinement is concerned, the magnetic mirror configuration is exposed to different hydromagnetic instabilities, because of the shape of the lines of force (the Teller criterion), on the presence of collective oscillations of the electron and ion components, etc. Numerous experiments, however, performed by R. F. Post and co-workers ([35]) indicate that the trapped plasma remains stable for several μs. In these experiments, where adiabatic compression is used, electron temperatures of the order of 30 to 40 keV have been obtained, while the ion temperature has been considerably lower, of the order of 2 to 3 keV.

Interesting results have been obtained by M. S. Joffe ([36]) who has proved

([32]) See, for instance, ref. ([13]).

([33]) *Symposium on Scientific Effects of Artificially Introduced Radiations at High Altitudes. Journ. Geophys. Res.*, **64**, no. 8 (1959).

([34]) S. N. Rodionov: *Atomnaya Energya*, **6**, 623 (1959) and *Journ. Nucl. Energy*, part C, *Plasma Physics*, **1**, pp. to 247, 252 (1960).

([35]) Loc. cit.

([36]) M. S. Joffe *et al.*: *Proc. of the Fourth International Conference on Ionization Phenomena in Gases* (Uppsala, 17-21 August 1959), (Amsterdam), vol. **2** p. 1009.

that fast ions (*i.e.* with energies of about 3 to 5 keV) may escape from the trap because of a process that is different from Coulomb scattering or charge exchange and is connected to magnetic field characteristics. Thus, with $H_0 = 8\,000$ G, and $g = 1.57$, the life-time limited by this process has appeared to be 1.2 μs; with the same g-value and $H_0 = 5\,000$ G, the-life time is 200 μs; and with $g = 1.25$ and $H_0 = 8\,000$ G; it is 200 μs. This experiments have been carried out in the ion-magnetron type of trap ([37]).

12. – It is possible to get a net power gain in magnetic mirrors only if the temperature of the ions is high enough, *i.e.* about 1 to 2 MeV for pure deuterium and 100 keV for the d-t mixture ([38]). Therefore the problem of suppressing additional energy losses arising from instabilities has received particular attention ([39]). It can be seen, from eq. (4) that the life time of the impurities is very short compared with that of the plasma, because of their high Z and low temperature. The escape of fast particles as a result of charge exchange processes with the residual atoms of the gas can give rise to serious difficulties. Fast neutral particles produced in this way escape to the walls and possibly knock out atoms of adsorbed gases, or even atoms of the wall materials.

Hence, another stringent requirement for good operation of magnetic mirrors is that the gas should be completely ionized and the amount of adsorbed matter in the walls should be negligible.

It also follows from eq. (4) that the process cannot start with a cold plasma, since it cannot be confined by magnetic mirrors. One of the possible methods for injecting hot plasma into magnetic mirrors is the use of plasma guns with electromagnetic acceleration, which provide plasma bursts with energies of the order of a hundred eV. The trapping of plasma bursts is effected either by varying the magnetic field or by letting several plasma bursts collide, thus randomizing the initial velocities of the particles. Further increase of the temperature may be obtained by magnetic pumping or by multistage adiabatic compression. In experiments performed by R. F. Post and co-workers the magnetic field at the final stage of compression was about 200 000 G and the overall compression factor up to 1 000, while the plasma density increased up to 10^{14} cm^{-3}, with a β-value of 0.08.

([37]) B. B. Kadomtsev: *Plasma Physics and the Problem of Controlled Thermonuclear Reactions*, edited by M. A. Leontovich, English translation, (London and New York, 1959-1960), vol. **4** p. 431.

([38]) G. I. Budker: *Plasma Physics and the Problem of Controlled Thermonuclear Reactions*, edited by M. A. Leontovich, English translation, (London and New York, 1959-1960), vol. **3** p. 3.

([39]) N. I. Kurchatov: *Atomnaya Energya*, **5**, 105 (1958).

Another possible method of heating the plasma is the injection into the trap of particles with energies of some hundreds of keV. Their interaction with the gas or the plasma inside the trap causes a sudden change of the charges of the particles, and leads to trapping. In the DCX experiment ([40]) molecular ions of deuterium are injected. They pass through an intense carbon arc established near the axis of the magnetic mirror configuration, and become dissociated, producing deuterium ions and neutral deuterium atoms. In the Ogra machine ([41]) the dissociation of molecular ions would take place through collisions first with the residual gas and then with the built up plasma. The Alice device ([42]) now being developed by POST, is expected to make it possible to inject fast neutral deuterium atoms into a trap: their dissociation would be obtained by collisions first with the residual gas and then with the plasma. It is essential, for this type of installation, that the current of injected particles should exceed a certain minimum value, and that the initial gas pressure should be low enough to bring about the so-called neutral gas burn-out. In the Alice device the current of neutral particles should exceed 50 mA, at an energy of 50 keV and a pressure in the chamber of the order of 10^{-10} mm Hg.

Additional plasma confinement in magnetic mirrors can be obtained with the help of a radial electric field. This induces radial currents which, interacting with the main magnetic field, make the plasma rotate. As a result, the transverse component of the momentum of the particles increases and inhibits the escape of particles from the trap.

Such devices (ion magnetron, homopolar, ixion ([43])) can be considered as a kind of hydromagnetic condenser, with ε of the order of 10^6, the energy being stored as kinetic energy of the rotating plasma ([44]).

At present, it seems that magnetic mirrors could provide a practical method of building up a hot plasma and confining it for a long period in a trap, possibly providing a basis for a thermonuclear reactor.

13. – Before leaving this subject, let us consider other types of magnetic traps. From the point of view of magnetohydrodynamic stability, cusped geometry is preferable, because the energy lost by magnetic radiation is mini-

([40]) C. F. BARNETT *et al.*: *Proc. of the Second United Nations International Conference on the Peaceful Uses of Atomic Energy* (Geneva, 1958), vol. **31** p. 298; A. H. SNELL: *Proc. of the Fourth International Conference on Ionization Phenomena in Gases* (Uppsala, 17-21 August 1959), (Amsterdam), vol. **2** p. 997.

([41]) I. V. KURCHATOV: *Sourn. Nucl. Energy*, **8**, 168 (1958).

([42]) R. F. POST: *Proc. of the Fourth International Conference on Ionization Phenomena in Gases* (Uppsala, 17-21 August 1959), (Amsterdam), vol. **2** p. 988.

([43]) K. BOYER *et al.*: *Proc. of the Second United Nations International Conference on the Peaceful Uses of Atomic Energy* (Geneva, 1958), vol. **31** p. 319.

([44]) O. A. ANDERSON *et al.*: *Journ. Appl. Phys.*, **30**, 188 (1959).

mized. On the other hand, the existence of additional « escape cones » in velocity space and the greater chance of non-conservation of adiabatic invariance increases the number of particles escaping from this configuration. Numerous experiments using this approach are now being carried out.

It should also be pointed out that the escape of particles through a mirror is necessarily accompanied by the diffusion of particles across magnetic lines of force and, according to the classical theory, the diffusion coefficient is proportional to H^{-2}. Plasma oscillations have already been proved to increase the diffusion across the magnetic field. The study of the process of particle escape from the plasma across the magnetic field is obviously of great importance for the construction of future reactors of economic interest.

The ideal magnetic trap is formed by the magnetic lines of a ring current, but the necessity of some leads to the rings makes the confining action of such a trap much poorer. Recently LEHNERT has started experiments on this line ([45]). If the leads are connected to the ring from the inside, the system does not differ in principle from magnetic mirrors.

V. – Relativistic electron system.

14. – The possibility of obtaining a thermonuclear reaction in the potential well of a negative charge of stabilized beam of relativistic electrons has been pointed out by BUDKER ([46]). However, the energy radiated by the electrons happens to exceed that of thermonuclear reactions.

N. C. CHRISTOFILOS has used relativistic electrons as a means to confine and heat plasmas (the Astron) ([47]). The basic features of the concept can be illustrated as follows.

Electrons with energy $E = \gamma mc^2$ are injected into magnetic mirrors, with mirror ratio close to unity, and they form a cylindrical sheet (the so-called E-layer). When the electron current per unit length of the layer reaches high enough values, the direction of the magnetic field in the central region reverses and a pattern of closed lines of force is created. This pattern is similar to the lines of force produced by a ring current, and the whole system provides an effective method of confining the plasma, although particles can still escape from the system as a result of their diffusion across the magnetic field lines.

([45]) B. LEHNERT: *Ark. f. Phys.*, **15**, 579 (1959); R. BONNEVIER and B. LENHERT: *Ark. f. Phys.*, **16**, 231 (1959).

([46]) G. I. BUDKER: *Plasma Physics and the Problem of Controlled Thermonuclear Reactions*, edited by M. A. LEONTOVICH, English translation, vol. I (London and New York, 1959-1960), p. 295.

([47]) N. C. CHRISTOFILOS: *Proc. of the Second United Nations International Conference on the Peaceful Uses of Atomic Energy* (Geneva, 1958), vol. **32** p. 279.

In the Astron the magnetic field reverses its direction in the central region if the condition $\nu > \gamma$ is fulfilled, where $\nu = 1$ corresponds to 100 A/cm, if the radius of the sheet is 30 cm.

The formation of plasma results from the ionization of the residual gas by relativistic electrons. The heating is also due to the energy transfer from fast electrons to the plasma.

At present experiments are being carried out, with the aim of trapping the electrons in the magnetic field andt o determine whether it is possible to reverse the magnetic field in the central region ([48]). It has been shown that currents of some hundreds amperes have been accumulated, the electron energy being 700 keV and the life of the electrons sheet about 1 s. This value is determined only by Coulomb scattering on the residual gas. The trapping of electrons is performed by image currents induced in special rings around the tube. As a result of energy dissipation in the rings, the longitudinal component of the electron momentum decreases, and this prevents the electrons from hitting the injector after their reflection on the opposite mirror.

In order to excite currents satisfying the condition, high current injectors must be constructed. CHRISTOFILOS is now working on this problem ([49]).

The next step will be to test the ability of the *E*-layer to confine and heat the plasma, and to study the layer stability after the formation of the plasma.

([48]) N. C. CHRISTOFILOS *et al.*: *Bull. Amer. Phys. Soc.*, **5**, 80 (1960).
([49]) N. C. CHRISTOFILOS: *Bull. Amer. Phys. Soc.*, **5**, 354 (1960).

RIASSUNTO

Questo articolo è basato sulla seconda parte di una serie di lezioni tenute all'Università di Birmingham, e assume la conoscenza dei principi elementari della fisica del plasma. Esso ha lo scopo di fornire una descrizione dei progressi effettuati recentemente in questo campo, assieme ad una discussione critica dei principi che hanno ispirato il disegno di vari modelli di macchine termonucleari. I dettagli costruttivi delle macchine menzionate nel testo sono reperibili nella bibliografia.

SUPPLEMENTO AL VOLUME XIX, SERIE X
DEL NUOVO CIMENTO

N. 1, 1961
1° Trimestre

A Note on the Capture of Negative Mesons in Photographic Nuclear Emulsions.

R. D. Hill

Physics Department, University College - London (*)

(ricevuto il 1° Aprile 1961)

Summary. — The slowing down of extremely low energy negatively charged mesons has been discussed and range-energy curves have been obtained. Based on these curves, an evaluation has been made of the relative capture rates of negative mesons in light and heavy nuclei of photographic emulsions. These rates appear to be in very good agreement with experimental observations on the capture of negative μ-mesons in nuclear emulsions.

1. – Introduction.

Knowledge of the capture rates of negative mesons by different nuclear constituents of photographic emulsions is important in the investigation of interactions of low energy mesons with atoms and nuclei. One of these problems being currently investigated ([1,2]) is the multi-nucleon capture of K^--mesons. Another

(*) Fulbright scholar on leave from University of Illinois.

([1]) K^- Collaboration Paper, Part II: *Nuovo Cimento*, **14**, 315 (1959); B. D. Jones, B. Sanjeevaiah, J. Zakrzewski, P. G. Bizzeti, J. P. Lagnaux, M. René, M. J. Beniston, S. A. Brown, E. H. S. Burhop, D. H. Davis, D. Ferreira, E. Frota-Pessoa, W. B. Lasich, N. N. Raina, M. C. Amerighi, A. Bonetti, M. di Corato, C. C. Dilworth, C. A. Fedrighini, E. Quercigh, A. E. Sichirollo and G. Vegni: *Nuovo Cimento*, **19**, 1077 (1961); D. Evans, B. D. Jones, B. Sanjeevaiah, J. Zakrzewski, M. J. Beniston, V. A. Bull and D. H. Davis: *Proc. Roy. Soc.*, A **262**, 73 (1961).

([2]) M. Nikolić, Y. Eisenberg, W. Koch, M. Schneeberger and H. Winzeler: *Helv. Phys. Acta*, **33**, 221 (1959); Y. Eisenberg, M. Friedmann, G. Alexander and D. Kessler: *Nuovo Cimento* (in press).

problem of current interest ([3]) is the radiative and non-radiative capture of μ^- and π^--mesons in atoms.

In the capture of negatively charged mesons by homogeneous materials, either of a single element or chemical compound, there is still some discussion of whether the Fermi-Teller « Z-law » is valid ([4]). Latest experimental work ([5]) on this point appears to support the validity of the « Z-law ». In so far as nuclear emulsions are concerned, a direct applications of the « Z-law » to Ilford G-5 type would give the number of captures, n_H, in heavy nuclei (Ag, Br, I) as compared with the total number of captures, n, in both light (H, C, N, O, S) and heavy nuclei, the ratio: $q = n_H/n = 0.8$.

The nature of negative meson capture in photographic emulsions is, however, somewhat different from the capture process in a homogeneous material. Because of the granular nature of photographic emulsion, capture may occur either in a AgBr grain or a gelatin layer without any influence of the Z dependence. Capture will occur when the total energy of the meson is negative, and the problem of estimating the relative capture rates then becomes one of determining the probability of the negative meson stopping in a AgBr grain as compared with stopping in the surrounding gelatin layer.

2. – Capture and loss effects.

The range-energy relation for standard G-5 emulsion has been given by Barkas ([6]) for protons of energies down to 0.2 MeV, for which the range is 1.8 μm. Since the diameter of a AgBr grain is an order of magnitude smaller than this, range-energy relations for analysing the present problem are required down to energies of 10 keV and less.

For protons ranges of less than one micron, some experimental observations have been made on a few materials such as gold, aluminium and beryllium metal foils and on heavy (deuterium) ice ([7-10]) Although these data extend

([3]) A. Pevsner, R. Strand, L. Madansky and T. Toohig: *Nuovo Cimento*, **19**, 479 (1961).

([4]) J. F. Lathrop, R. A. Lundy, R. A. Swanson, V. L. Telegdi and D. D. Yovanovitch: *Nuovo Cimento*, **15**, 831 (1960).

([5]) A. Astbury, P. M. Hattersley, M. Hussain, M. A. R. Kemp and H. Muirhead: *Nuovo Cimento*, **18**, 1267 (1960).

([6]) W. H. Barkas: *Nuovo Cimento*, **8**, 201 (1958).

([7]) H. A. Wilcox: *Phys. Rev.*, **74**, 1743 (1948).

([8]) J. R. Young: *Journ. Appl. Phys.*, **27**, 1 (1956).

([9]) W. A. Wenzel and W. Whaling: *Phys. Rev.*, **87**, 499 (1952).

([10]) S. K. Allison and S. D. Warshaw: *Rev. Mod. Phys.*, **25**, 779 (1953).

the ranges down to values which approach significance in the meson capture problem, they are specifically only for positively charged protons and as such are affected strongly by the phenomenon of electron capture and loss.

No experimental or theoretical work on the ranges in condensed materials of very low energy particles of negative charge, other than electrons, appears to have been performed. It seems possible, however, that a fair approximation to a range-energy relation for negatively charged protons can be obtained by applying a correction to the ranges of positive protons. This correction, which is related to the fraction of time that a positive proton exists as a neutral system, owing to the capture of an electron, can be obtained from the experimental work of HALL [11] who measured the probability of charged protons emerging from various materials as a function of the energy of the protons.

The observed and extrapolated values of the Hall factor are given in Table I. HALL found the factor to be practically the same for all the materials studied. This factor has been used to correct the observed energy loss rates,

TABLE I. – *Estimated energy loss rates for negatively charged protons.*

E (keV)	Hall factor	$-dE/dx$ (keV/mg cm^{-2}) Gold	$-dE/dx$ (keV/mg cm^{-2}) Aluminium	$-dE/dx$ (keV/mg cm^{-2}) Heavy Ice
5	(0.39) (*)	49	585	—
10	(0.455)	66	650	—
15	(0.495)	77	665	—
20	(0.53)	80	670	1000
25	0.56	84	670	—
30	0.585	—	—	1050
40	0.64	—	—	1065
50	0.68	100	630	1040
75	0.75	105	580	—
100	0.82	105	560	870

(*) Values in parenthesis are extrapolated.

$-dE/dx$, from the combined data of references [7-10]. The modified data, which are given in Table I, are therefore the $-dE/dx$ values to be expected for negatively charged protons. The effect of the capture-loss correction is to increase significantly the energy-loss rates at low energies. Curves of $-dE/dx$ *vs.* E for negatively charged protons in heavy ice, aluminium and gold, are shown in Fig. 1.

[11] T. A. HALL: *Phys. Rev.*, **79**, 509 (1950).

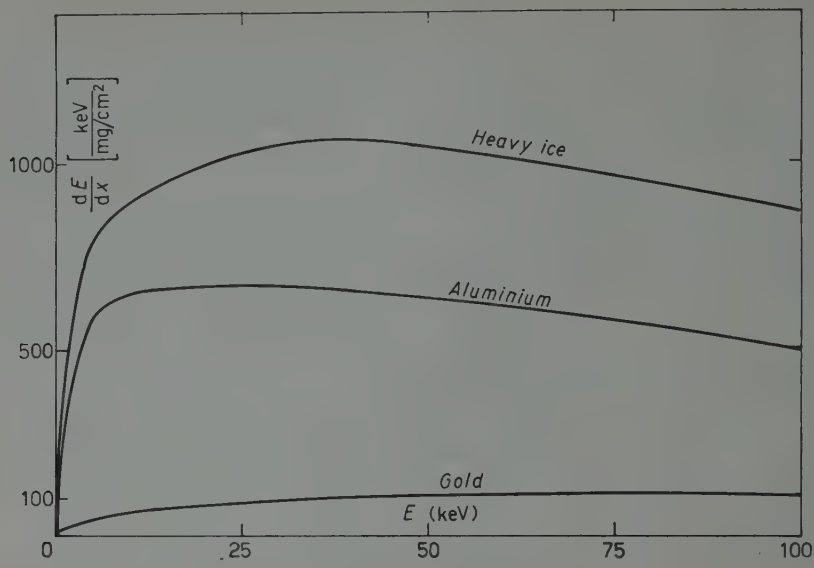

Fig. 1. – Estimated stopping powers of gold, aluminium and heavy ice for negatively charged protons.

3. – Energy losses to degenerate electron gas in solid.

For the investigation of the present problem, range-energy curves are actually required well below the region which has yet been experimentally observed in condensed materials. This problem, however, has been theoretically examined by FERMI and TELLER ([12]). They showed that when the negative particle velocity is below that of the valence electrons of the atoms of the stopping material, loss of energy from the negatively charged particle occurs to the collective assembly of electrons which may be regarded as a degenerate gas. This energy loss mechanism begins to be important for protons below 10 keV and for K-mesons below 5 keV. Evidence that the Fermi-Teller region has been reached in the neighbourhood of 10 keV appears to be indicated by the turning down of the dE/dx curves shown in Fig. 1.

FERMI and TELLER derived the following approximate formula for the rate of total energy loss, dW/dt, of a negatively charged particle to the electron gas of a solid:

$$-\frac{dW}{dt} \sim \frac{E}{t_0}, \tag{1}$$

([12]) E. FERMI and E. TELLER: *Phys. Rev.*, **72**, 399 (1947).

where E is the kinetic energy of the particle and $t_0 = M\hbar^3/m^2e^4 = 4.4 \cdot 10^{-14}$ s for a proton (M = mass of particle, m = mass of electron). For graphite and iron, FERMI and TELLER showed that the average kinetic energy, E, and the total energy, W, are essentially equal down to μ-meson energies as low as 0.05 keV. One might expect, therefore, for proton energies down to approximately 0.5 keV that W could be replaced approximately by E. With this approximation, it is readily shown that

$$-\frac{\mathrm{d}E}{\mathrm{d}x} = \frac{k\sqrt{2ME}}{t_0}, \tag{2}$$

where k is some constant determined by the nature of the stopping material. FERMI and TELLER expected that k would have approximately a constant value for all metals but might differ somewhat for insulators and other materials.

In extending the range-energy curves for negatively charged protons from 10 keV to zero energy it has been assumed, in conformity with the Fermi-Teller analysis, that the $\mathrm{d}E/\mathrm{d}x$ loss varies as $E^{\frac{1}{2}}$ and the curve joins as smoothly as possible on with the modified observed values of Table I and Fig. 1. In order to fit the modified values of $\mathrm{d}E/\mathrm{d}x$ on an absolute basis it has been found that the values of k in relation (2) are: 0.8 for gold, 1.2 for aluminium and 0.6 for heavy ice. These appear to be the first estimates of the constant k based on semi-experimental information. They are interesting because even for materials so dissimilar as gold, aluminium and ice, with such widely different stopping powers, they have a reasonably constant value which appears to be close to unity.

4. – Range-energy values in gelatin and AgBr.

Estimated energy losses for negatively charged protons in gelatin and AgBr were obtained from the curves for ice, Be, Al and Au by approximate interpolation in atomic number Z. An average Z for gelatin is 3.7 and for AgBr is 41. Estimated energy loss rates and ranges, the latter obtained from the rates by numerical integration, are given in Table II and plotted in Fig. 2. These values are again interesting because they reflect the fact, already pointed out by FERMI and TELLER, that the rate of loss of energy is rather independent of the nature of the stopping material.

Since the particle kinetic energies at these low values are given accurately by the non-relativistic formula, the range-energy relations for negative mesons

TABLE II. – *Estimated energy loss rates and ranges of very low energy and negatively charged protons in gelatin and* AgBr.

E (keV)	dE/dx (keV/mg cm^{-2}) Gelatin	x (μm) Gelatin	dE/dx (keV/mg cm^{-2}) AgBr	x (μm) AgBr
1.0	277	0.040	47	0.046
2.0	391	0.063	67	0.072
3.0	480	0.083	82	0.093
4.0	553	0.097	95	0.110
5.0	620	0.110	106	0.126
7.0	733	0.133	125	0.152
9.0	830	0.154	142	0.175
11.0	920	0.171	156	0.196

can be easily obtained from the proton curves. The curves for K- and μ-mesons are shown in Fig. 2.

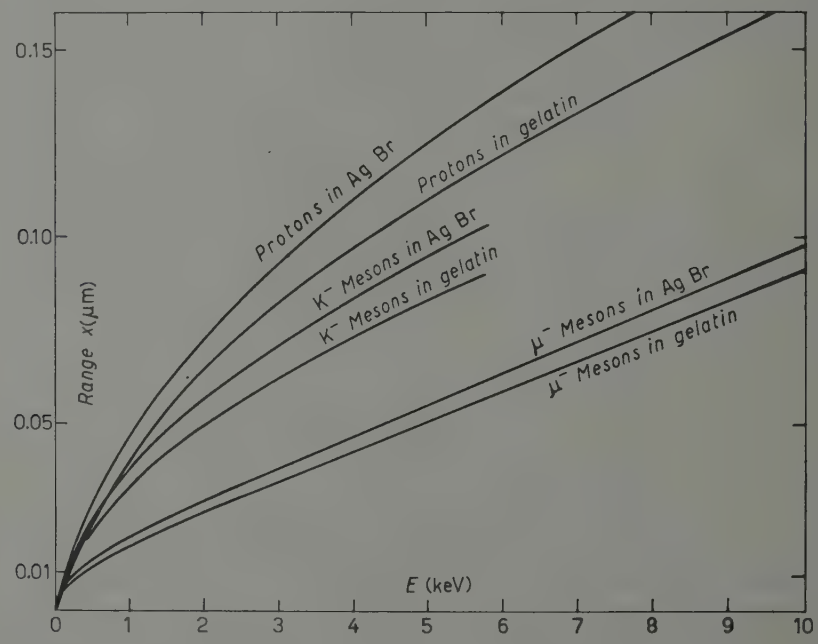

Fig. 2. – Estimated range-energy curves for low energy negatively charged particles.

5. – Capture rates in AgBr-gelatin emulsion.

A negatively charged meson will be captured by an atom when its total energy is less than zero. (As FERMI and TELLER showed, energy loss from

the charged particle to the degenerate electron gas will continue even as W approaches zero. This arises because a significant average kinetic energy of the particle is maintained from the contributions of the potential energies of the neighbouring atomic fields. In connection with the range-energy values at lowest energies already estimated, it was assumed that the average energy loss rate for protons in the interval $(0 \div 1)$ keV was 0.7 of the value at one keV. This is in reasonable accord with the Fermi-Teller calculation of the average kinetic energies of stopping particles in graphite and iron.)

Two types of nuclear photographic emulsion, Ilford G-5 and K-5, will be considered. In both types, the volume of AgBr is 0.486 cm^3 per cm^3 of emulsion, and the remaining 0.514 cm^3 is gelatin. The radii of the AgBr grains, assumed to be spherical, are given in Table III.

TABLE III. – *Estimated capture rates in* AgBr *and gelatin.*

Emulsion type	r_1 (μm)	AgBr Avg. path (μm)	Gelatin Avg. path (μm)	AgBr E_{max} (keV)	Gelatin E_{max} (keV)	$\frac{n_{AgBr}}{n_{Gelatin}}$
			K^--meson capture			
G-5	0.135	0.090	0.059	4.56	2.70	1.69
K-5	0.100	0.067	0.0435	2.72	1.63	1.67
			μ^--meson capture			
G-5	0.135	0.090	0.059	9.12	6.07	1.52
K-5	0.100	0.067	0.0435	6.35	4.13	1.54

A highly simplified model of the emulsion will be considered. It will be assumed that the uniform spherical grains of AgBr are surrounded by uniform thickness concentric spherical gelatin layers of the appropriate value to make up the gelatin volume. These spherical units will then be assumed packed on one another and the small interstices will be ignored.

The problem is then one of estimating the relative probabilities of a meson coming to rest in a AgBr grain as compared with in a gelatin layer. Considering a large number of stopping negative mesons, there will be particles of all energies incident on both AgBr grain surfaces and gelatin layer surfaces. On the average, only for energies less than certain maximum values will the mesons be brought to rest and captured within the particular grain or layer, on the surface of which the mesons are incident. If the numbers of mesons per unit energy interval are constant, in the rather small energy region from which the mesons may be captured, then the relative capture probabilities in AgBr

and gelatin will be proportional to the values of the maximum energies below which captures in AgBr and gelatin will take place.

For spherical grains, of radius r_1, it is readily shown that the average path length of a track traversing a grain without scattering is $2r_1/3$. For two spherical gelatin layers in contact, each of outer radii r_2 and inner radii r_1, the average path length of a track traversing the layers without scattering is $2r_2(1-r_1^3/r_2^3)/3$. For both types of emulsion, these estimated average path lengths are given in Table III.

The maximum energies of the particles which, being incident on a AgBr grain or gelatin layer, and on the average, will come to rest in these sections, can then be evaluated from the range-energy curves previously derived. These energy values for K- and μ-mesons are shown in columns 5 and 6 of Table III. If it is assumed that the numbers of mesons per unit energy interval are constant in these energy regions, it is then readily estimated that the value of q (*i.e.* $n_{AgBr}/(n_{AgBr}+n_{Gelatin})$) is 0.63 for K-mesons and 0.60 for μ-mesons.

This value of q for μ-meson capture is in excellent agreement with the latest experimental value of 0.58 observed by PEVSNER *et al.* [3], as well as with the earlier value of $0.6 \div 0.7$ derived from the collective work of PERKINS [13], COSYNS *et al.* [14] and FRY [15].

---

[13] D. H. PERKINS: *Phil. Mag.*, **40**, 601 (1949).

[14] M. G. E. COSYNS, C. C. DILWORTH, G. P. S. OCCHIALINI, M. SCHOENBERG and N. PAGE: *Proc. Phys. Soc. Lond.*, A **62**, 801 (1949).

[15] W. F. FRY: *Phys. Rev.*, **83**, 594 (1951).

RIASSUNTO (*)

Discuto il rallentamento di mesoni con carica negativa di energia estremamente bassa e ottengo le curve range-energia. Sulla base di queste curve, valuto le proporzioni relative di cattura dei mesoni negativi nei nuclei pesanti e leggeri delle emulsioni fotografiche. Risulta che queste proporzioni si accordano molto bene con le osservazioni sperimentali della cattura di mesoni μ negativi nelle emulsioni nucleari.

(*) *Traduzione a cura della Redazione.*

SUPPLEMENTO AL VOLUME XIX, SERIE X
DEL NUOVO CIMENTO

N. 1, 1961
1° Trimestre

Light-to-Light Discriminator Switch.

G. PALMIERI and R. SANNA

Istituto di Fisica dell'Università - Genova

(ricevuto il 19 Aprile 1961)

Summary. — Transducer yields calibrated light output when input is illuminated beyond a fixed treshold.

Light switching devices analogue to electronic multivibrators are obtained by combining photoresistors and electroluminors in positive-feedback circuits (1). Devices of this class can also be built using gas discharge light sources, where the abrupt breakdown characteristic is advantageous for obtaining quick, well defined switching over.

A light-to-light discriminator switch of this type is shown in Fig. 1. Photo-

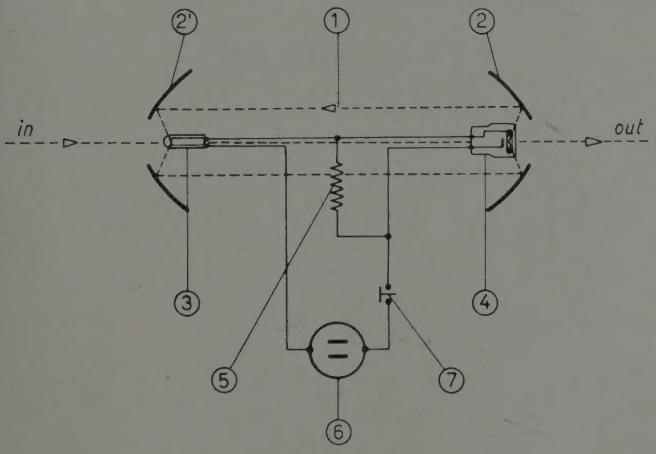

Fig. 1.

(1) See *e.g.* G. DIEMER and J. G VAN SANTEN: *Philips. Res. Rep.*, **15**, 368 (1960).

resistor 3 and neon lamp 4 are optically coupled through parabolic mirrors 2, 2′. Input light enters through a hole at top of reflector 2′ onto the photoresistor, whose resistence thus decreases. At a critical value of the incident flux the voltage drop across the photoresistor is low enough to enable neon bulb 4 to light on. A reinforcing action takes place between 4 and 3 through the optical path 1 until a stable state is reached, where 4 is fully on and the input loses control over the outgoing light from 4. Reset is accomplished by push-button switch 7; resistor 5 acts in conjunction with the photoresistor as a voltage divider, thus setting the input switch-over level.

The device is meant to be incorporated in our probabilistic automatic programmer and analyzer (PAPA) [2] for extracting data from a photographic register, the interrogation being made by modulated light pencils. Miniaturization of the units is accomplished substituting the mirrors with a fluid light pipe.

---

[2] G. PALMIERI and R. SANNA: *Methods* **48** (1961).

RIASSUNTO

Si descrive un trasduttore che fornisce un'uscita luminosa tarata quando l'illuminazione in ingresso supera una soglia fissa.

PROPRIETÀ LETTERARIA RISERVATA

Direttore responsabile: G. POLVANI Tipografia Compositori - Bologna
Questo fascicolo del *Supplemento* è stato licenziato dai torchi il 16-I-1961